This is to certify that the
thesis entitled

EXPERIMENTAL CHARACTERIZATION OF THE PULLOUT AND
GAP OPENING BEHAVIOR OF MISALIGNED DOWEL BARS
UNDER THERMAL EXPANSION

presented by

Deepa Thandaveswara

has been accepted towards fulfillment
of the requirements for the

Master of Science degree in Civil Engineering

Major Professor's Signature

09/06/05

Date

EXPERIMENTAL CHARACTERIZATION OF THE PULLOUT AND GAP OPENING BEHAVIOR OF MISALIGNED DOWEL BARS UNDER THERMAL EXPANSION

By

Deepa Thandaveswara

A THESIS

Submitted to
Michigan State University
in partial fulfillment of the requirements
for the degree of

MASTER OF SCIENCE

Department of Civil and Environmental Engineering

2005

ABSTRACT

EXPERIMENTAL CHARACTERIZATION OF THE PULLOUT AND GAP OPENING BEHAVIOR OF MISALIGNED DOWEL BARS UNDER THERMAL EXPANSION

By

Deepa Thandaveswara

This thesis focuses on studying experimentally the fundamental pullout behavior of misaligned dowel bars and gap-opening behavior of pavement joints with misaligned dowel bars in plain concrete slabs, under thermal expansion. The variables considered in the experimental plan include the number of dowel bars (1, 2, 3, and 5) and number misaligned (all or alternate), misalignment type (horizontal, vertical, and combined), orientation (uniform and non-uniform) and magnitude (0, ¼, ½ , ¾ , 1, and 2 in. over half-length (9 in.) of the dowel bar). The effects of these parameters on the bond stress between the dowel-concrete, load induced at different joint openings, and joint and slab distresses (spalling, cracking, non-uniform joint opening, and uplift) were studied.

The initial slip/debonding stress found to be in the range of 10-50 psi irrespective of the misalignment type and magnitude. Within a misalignment type, the load and intensity of distresses increases with an increase in the misalignment magnitude and number of dowels misaligned. Non-uniform orientation of misalignment of two dowel bars requires more load per dowel bar at a given joint opening as compared to the uniform orientation of dowels in the horizontal and combined misalignment types. For a given misalignment magnitude, the overall trend of load versus type of misalignment (horizontal, vertical and combined) is unclear. The load versus joint opening behaviors obtained through this study can be used for development of analytical models to obtain the stress states in dowel-concrete bond behavior subjected to pullout.

Dedicated to

My parents

ACKNOWLEDGEMENTS

I would first like to express my sincere gratitude to Dr.Neeraj Buch for his constant support, ideas, and guidance throughout this entire research study. I would also like to thank my committee members Dr.Karim Chatti and Dr.Gilbert Baladi for their support. I would like also to thank Dr.Amit Varma, co-principal investigator of the project for his guidance during this research study.

I would like to thank Mr.Michael Eacker, Mr.Doug Branch and other field engineers at the Michigan Department of Transportation for sharing their field experiences and facilitating field trips during different stages of the research. My appreciation is due to the Michigan DOT for sponsoring this research work.

I would like to thank Mr.Siavosh Ravanbakhsh, lab manager and Mr.J.C Brenton, lab technician for the help extended to me during the laboratory phase of my research. I would like to thank my fellow graduate student Milind Prabhu for the enormous help and assistance extended to me during the period of this research. I would also like to thank Alan Hahn and Vinay Singhal for their assistance.

Finally, I would like to appreciate the emotional support provided to me by my parents, Hyung Suk Lee, Golrokh Nossoni, Parama Sarkar, Swaroop Mannepalli, and Praveen Desaraju during this time.

TABLE OF CONTENTS

List of Tables

List of Figures

CHAPTER 1 INTRODUCTION

1.1 BACKGROUND

Jointed plain concrete pavements (JPCP) are commonly constructed with contraction joints to accommodate slab movements due to temperature and moisture variations. Because such discontinuities constitute intrinsic planes of weakness, it is also desirable to supply some means of transferring load across the discontinuity (Ioannides, 1990).

Aggregate interlock alone does not provide enough load transfer for good long-term performance for most highway pavements due to heavy truck traffic. The American Concrete Paving Association (ACPA) recommends that dowel bars should be used to provide added mechanical load transfer where truck traffic exceeds 120 per day or accumulated design traffic exceeds 4-5 million ESALs. Typically, this traffic will require at least an 8 in. thick slab. For most highway applications, dowels are recommended, for 8 in. slabs or greater (ACPA 2004).

Dowel bars are smooth round bars placed across joints to transfer loads without restricting horizontal joint movement. They also assist in maintaining the horizontal and vertical alignment of slabs. Since dowels span the joint, daily and seasonal joint opening does not affect load transfer across doweled joints as much as it does non-doweled joints.

Dowel bars have been used across transverse joints in PCC pavements at least since 1917 (Teller and Cashell 1958). Justification for their use is provided by the fact that edge-loading stresses and deflections are higher than the corresponding interior-loading responses. Thus, if a portion of the applied edge load is transferred to an adjacent slab, resulting stresses and deflections can be significantly reduced. Distresses commonly exhibited by PCC pavements are attributed to high levels of stress or deflection (Snyder

1989). For this reason, distresses tend to appear most often in the vicinity of slab edges and corners, the theoretically predicted locations of maximum system responses. Deflection related distresses include pumping (Packard and Tayabji 1983) and faulting (Darter et.al. 1985). High slab-bending stresses, on the other hand, may lead to premature cracking. Excessive dowel-concrete bearing stresses may also result in spalling and faulting (Ioannides 1990).

A non-doweled joint provides load transfer through shear forces developed at the rough joint interface due to aggregate interlock provided by the shape, size, and hardness of the coarse aggregate. As a result, joint opening highly affects load transfer efficiency (LTE) based on aggregate interlocking. That is why LTE of joints with aggregate interlock is highly dependent on temperature: it is only high during warm weather when the joint is tightly closed (small joint opening). In contrast, the load transfer mechanism of dowel bars does not rely on warm weather or closed joints to transfer load across the joint. As a result, dowels are effective throughout the year (Rufino et. al. 2005). Khazanovich and Gotlif (2003) performed a comprehensive analysis of LTE data from the Long-Term Pavement Performance (LTPP) program. They showed that doweled joints have much higher LTE than non-doweled joints.

Several field performance studies from the 1970's through 1990's, including Highway Research Board (1962), Darter et.al. (1985), Smith et.al. (1990), Darter (1977), FHWA (1989), and Khazanovich et.al. (1998), found that slabs without dowels at the joints showed substantially more faulting than doweled ones at the same location. In addition, some of these studies also concluded that dowels prevent corner breaks or diagonal cracks. Darter (1977) considered faulting "the most serious distress" because it had a significant effect on ride quality when it developed to a significant level requiring maintenance. The importance of dowel bars was further underscored at the AASHO Road test. An analysis was performed using NCHRP I-37A Mechanistic-empirical pavement design guide (ARA 2004), assuming the cross-sections, traffic, climate, and materials information from the AASHO Road Test. The analysis revealed that non-doweled joints could have had up to seven times more faulting than doweled ones. The most prominent advantage of using dowels is reduction in faulting, and consequently, maintaining smoothness (Rufino et.al. 2005).

Design factors to be considered include the diameter, embedment length, and spacing of dowels required to limit and control the magnitude of stresses developing in each bar and in the surrounding concrete matrix. From a construction viewpoint, it is important to install the dowels properly, i.e., in a horizontal plane, parallel to the pavement centerline. If they deviate from the desired position, they are said to be misaligned. Misalignment may result from either or both (a) misplacement (i.e. initially placing the dowels in an incorrect position), or (b) displacement (i.e. movement during the pavement operation). The amount of misalignment that can be tolerated is a matter of some disagreement in the literature (Ross 1989).

Misalignment during dowel installation restrains the ability of the bars to slip freely in the concrete, and may result in transverse slab cracking, corner breaks, and joint spalling around the dowel at the concrete face (Tayabji 1986). It is equally essential to provide dowel corrosion protection for the duration of the design life of the pavement (Schierer 1985).

Dowel bars lower edge and corner deflection and stress in the concrete slab and reduce the potential for faulting, pumping, and corner breaks. Performance evaluation of in-service concrete highway pavements show the use of dowels effectively reduces faulting. Dowels also increase pavement service life by reducing deflections and stresses in the slab by effectively transferring the load across the joint. Elongation of the dowel hole reduces load transfer capabilities (ACPA 2004).

In the current DOT practices of dowel and joint design (AASHTO 1993)., the design of dowels has been mostly based on experience, one rule of thumb being the diameter of the dowel should be equal to ⅛ th of the slab thickness. FHWA (1990) also recommends this guideline but limits the dowel diameter to a minimum of 1¼ in. for highways. ACPA (1991) recommends, for highway pavements less than 10 in. thick, 1¼ in. diameter dowels and for pavements 10 in. thick or greater, 1½ in. dowels. A minimum dowel diameter of 1¼ to 1½ in. is needed to control faulting on highway pavements. According to an ACPA survey (ACPA 2004a), the average dowel diameter used by state highway agencies is 1¼ in. Loads on smaller dowels induce higher bearing stresses and cause the concrete matrix around the dowel to deteriorate or elongate. Design methods are available that check the allowable bearing stress between dowel and concrete (Huang 1993). Because concrete is weaker than steel, the size and spacing of dowels required are governed by the bearing stress between the dowel and concrete, the allowable stress being given by equation (1):

$$f_b = \left(\frac{4-d}{3}\right) f_c' \qquad \ldots(1)$$

in which f_b is the allowable bearing stress in psi, d is the dowel diameter in inches and f_c' is the ultimate compressive strength of concrete in psi. The maximum bearing stress is determined theoretically by assuming the dowel to be a beam and the concrete to be a Winkler foundation based on the original solution by Timoshenko and Friberg (1940) (equation (2)).

$$\sigma_b = K y_0 = \frac{K P_t (2 + \beta z)}{4 \beta^3 E_d I_d} \qquad \text{...(2)}$$

where maximum deformation of concrete under the dowel y_o at the face of the joint is expressed as given in equation (3):

$$y_o = \frac{P_t (2 + \beta z)}{4 \beta^3 E_d I_d} \qquad \text{...(3)}$$

in which P_t is the load on the dowel, z is the joint width, E_d is the Young's modulus of the dowel, I_d is the moment of inertia of the dowel, and β is the relative stiffness of a dowel embedded in concrete given by equation (4):

$$I_d = \frac{1}{64} \pi d^4 \qquad \beta = \sqrt[4]{\frac{Kd}{4 E_d I_d}} \qquad \text{...(4)}$$

in which K is the modulus of dowel support, which ranges from 300 to 1500 kci and d is the diameter of the dowel. By limiting the bearing stress, the amount of faulting can be reduced to the allowable limit.

According to the formulation presented by Tabatabaie et. al. (1979), the ILLI-SLAB model considers the dowel bar as a thick-beam element whose shear stiffness (i.e., resistance to deformation in the vertical direction) is 12 C. This term expresses the shear force in the dowel per unit vertical deformation of the dowel. The support provided by the PCC matrix is modeled as a single spring that act as at the joint face and whose stiffness is dowel-concrete interaction (DCI) parameter. This is the shear force transferred by the dowel per unit deflection of the dowel with respect to the concrete matrix.

$$C = \frac{E_d I_d}{\omega^3 (1+\phi)} \qquad \ldots(5)$$

where ϕ is the parameter accounting for through-the-thickness shear deformations arising in deep beams and is expressed as $\phi = \dfrac{12 E_d I_d}{G_d A_z \omega^2}$ ...(6)

where ω = joint opening, A_z = cross-sectional area of dowel effective in shear = $0.9A_d$ for solid round bars. By reference to Friberg's analysis (1940), the expression for DCI is as given in equation (7):

$$DCI = \frac{P_i}{\Delta_{di}} = \frac{4\beta^3 E_d I_d}{(2+\beta\omega)} \qquad \ldots(7)$$

where P_i is the load transferred by any particular dowel, Δ_{di} is the deflection of any given dowel with respect to the concrete, and other parameters are as defined before.

The value of the critical dowel-concrete bearing stress, σ_{bc} is calculated using equation (8) (Ioannides 1990):

$$\sigma_{bc} = \frac{K}{DCI} P_c \qquad \ldots(8)$$

where P_c is the portion of the transferred load carried by the critical (design) dowel

As seen from the design methodology, the key parameter affecting the bearing stress is the dowel diameter. In the NCHRP I-37A design methodology (mechanistic-empirical design guide), bearing stresses have been linked to cumulative damage of the joint. Dowel misalignment contributes to the magnitude of bearing stresses at the dowel-concrete interface but to date, there is no structural model that accounts for the change in bearing stress due to dowel misalignment, hence necessitating the need to study the effect of dowel misalignment on pullout and joint opening behavior.

The research presented in this thesis is based on the laboratory phase of the MDOT sponsored project titled 'A laboratory evaluation of alignment tolerances for dowel bars and their effect on joint opening behavior'.

1.2 RESEARCH OBJECTIVES

The objectives of this thesis are:

- To investigate experimentally the fundamental pullout behavior of misaligned dowel bars in plain concrete pavements under thermal expansion.
- To investigate experimentally the gap-opening behavior of pavement joints with misaligned dowel bars under thermal expansion.

Its hypothesized that the misalignment type and magnitude would affect the following:

- Initial slip/debonding stress (bond stress at initial slip) (defined in chapter 4)
- Type of joint and slab distresses observed
- Post-slip behavior

1.3 LAYOUT OF THE THESIS

This thesis – 'Experimental characterization of the pullout and gap opening behavior of misaligned dowel bars under thermal expansion' is outlined as follows.

Chapter 2 contains a synopsis of the technical papers and reports on several topics related with this study. The topics of this chapter can be broadly classified into four groups: construction practices focusing on dowel bar placement methods, definition, factors and effects of misalignment, studies on misalignment - experimental as well as field, modern technologies of detection of dowel bar position in the field. Dowel baskets and dowel bar inserters are the two methods of dowel bar placement focused at during various stages of the chapter.

Chapter 3 provides a detailed description of the experimental plan and procedure. An experimental matrix, at the start of the chapter, addresses the different experimental variables – number of dowel bars and number misaligned, misalignment type, orientation, and magnitude, and sets out the plan for the testing. The various components of the experimental setup are described. The concrete mix and dowel bars are as per the Michigan DOT specifications. A detailed description of the material specifications and quality control tests of steel and concrete is provided. Details of the various instruments used in the tests, along with their calibration are presented thereafter. The instruments described include linear variable differential transducers (LVDT), spring return linear motion sensors (slider), pressure transducers, and hydraulic actuators. The chapter ends with a description of the events in a typical casting-testing cycle.

Chapter 4 discusses the results obtained during the different tests carried out, as per the experimental plan explained in chapter 3. A plot illustrating the typical bond stress vs joint opening behavior explains the concepts of initial slip/debonding stress and transverse contact. Distresses observed for different combinations of misalignment include spalling around the dowel-concrete interface, non-uniform joint opening, cracking, and vertical uplift. This chapter explains all observations – distresses and load vs joint opening in three subsections based on the misalignment types (horizontal, vertical, and combined). Each subsection starts with an overview of the distresses and load vs joint behavior, and then these details are substantiated with illustrations, provided for clarity and conciseness of data representation. The nomenclature (specimen ID) explained in chapter 3 is used while describing specifics of test results. Prediction of load vs joint opening behavior, for a given number of bars and misalignment magnitude within the gamut of the test matrix, is attempted.

Chapter 5 presents the conclusions of the research. This chapter also suggests scope of future research.

CHAPTER 2 LITERATURE REVIEW

This chapter summarizes the findings of the literature review conducted as a part of the research in five sections – dowel bar placement methods in field, construction practices of some state highway agencies, types of misalignment, measurement of dowel bar misalignment in the field, effects of misalignment, and field and experimental studies on the effects of dowel bar misalignment.

2.1 DOWEL BAR PLACEMENT METHODS

This section deals with practices in plain jointed concrete pavement construction, with a focus on dowel bar placement methods and possible causes of misalignment.

Pavements are constructed using fixed form paving and slipform paving. Fixed form paving is used generally for small jobs, complicated geometry pavements, or variable width pavements, while slipform paving is used for larger jobs that require high production rates. There are two main methods of dowel bar placement in the field: dowel basket assembly and dowel bar inserter (DBI). Slipform paving can accommodate both the methods of dowel bar placement while fixed form paving can accommodate dowel baskets only.

Due to the increased cost of approximately \$ 30,000/ interstate mile for basket-assembly compared with that of the implanting method, investigations are underway to check dowel alignment in existing pavements using both implanting schemes (Burati et.al. 1983). DBIs have been used in Europe for a quarter century. In 1996, the Federal Highway Administration (FHWA) officially encouraged the use of DBIs as an acceptable alternate means of dowel bar placement in jointed concrete construction (Donahue 2003).

2.1.1 Dowel Baskets

Dowel baskets are simple truss structures used to hold dowel bars at the appropriate height before PCC placement. Typically, dowel baskets span an entire lane width and are fabricated from thick gauge wire. They are left in place after the PCC is placed but do not contribute to the pavement structure.

When using dowel baskets, the dowels must be aligned and the dowel basket firmly anchored to the base course. The FHWA recommends that the dowel baskets be secured with steel stakes with a minimum diameter of 0.3 in. embedded at least 4 in. in stabilized bases, 6 in. in treated permeable bases and 10 in. in untreated bases or subgrade. Further, a minimum of 8 stakes per basket is recommended.

Figure 2.1 (a-d) illustrate a typical sequence of installation of dowel bars using dowel baskets at a construction site in Michigan. The dowels come precoated with lubricant from the manufacturer and are welded on alternate sides. Three nails each 12 in. long are driven into either sides of a basket covering one lane (Figure 2.1 (a)). Then the shipping/tie wires are cut (Figure 2.1 (b)). Figure 2.1 (c) illustrates the misalignment check that is performed to ensure the basket is leveled. Figure 2.1 (d) shows an installed basket.

2.1.2 Dowel Bar Inserter

The dowel bar inserter is a device which mounts behind the conforming pan of the slipform paver. The DBI can accommodate different dowel spacings, dowel depths, skewed or square contraction joints, and both crowned and flat pavements. Figure 2.2 (a-e) illustrate a typical dowel bar inserter and the sequence of operations in dowel bar insertion.

(a) Driving the nails into base course

(b) Cutting of tie wires

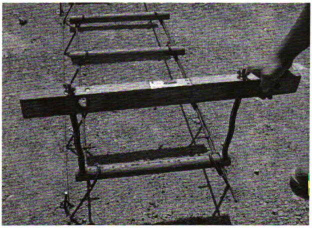

(c) Misalignment check

(d) Installed basket

Figure 2.1. Dowel Bar Installation sequence using basket assembly

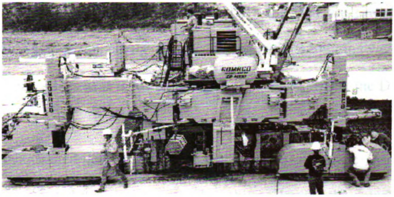

(a) Typical Slipform Paver with inbuilt Dowel Bar Inserter

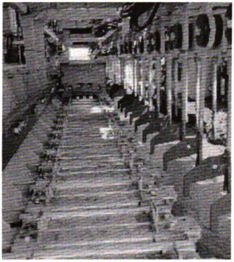

(b) Dowel Bar Magazine

(c) Forked Insertion Devices

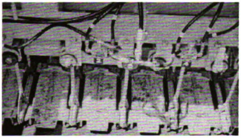

(d) Side and End Prongs

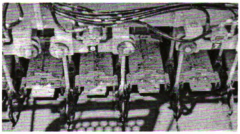

(e) Insertion into Plastic Concrete

Figure 2.2. Dowel Bar Insertion Sequence using Dowel Bar Inserter*

*Source: Gomaco Inc. Website www.gomaco.com

The DBI is supported by rollers and is suspended above the inserter pan. The pan confines the disturbance to the concrete surface where dowels are introduced into the fresh concrete. As the slipform advances, the DBI and pan are towed by hydraulic cylinders. Vertical guides connect the DBI and the pan without putting weight on the pan. Thus, when the pan glides as it is towed along the concrete surface, the DBI moves with it.

When the desired joint location is reached, the automatic insertion cycle is activated. A pan mounted dowel distributor then shifts allowing the dowels to drop from the magazine through the pan onto the fresh concrete. The vibration-isolated "inserting fork assemblies" then vibrate the bars until they have reached their proper depth in the concrete. Mounted on rubber-isolated beams, the vibrating forks reconsolidate the concrete as the forks are pulled out of the slab. Once the forks have cleared the concrete, the vibration is stopped and the roller-supported DBI and the pan are retracted. The oscillating correcting beam, which is required when using the DBI, then refinishes the concrete slab to a smooth concrete surface finish.

Because the dowels are being vibrated intensely and are inserted down to their final resting place under the weight of only the dowel inserter assembly and light hydraulic pressure, the concrete has enough time to flow around the bar rather than being displaced.

2.2 DOT CONSTRUCTION PRACTICES

An email survey was conducted amongst different state Departments of Transportation (DOTs) in August 2004 to find out key features in pavement design and dowel bar installation, with focus on:

- Dowel bar dimensions
- Methods used for dowel bar placement and preferred method, if any
- Tolerance in dowel bar placement
- Quality control/misalignment check method adopted during construction
- Initial bond stress specifications

The responses of the DOTs are summarized in Table 2.1 and a sample survey form is shown in Table 2.2. As seen from Table 2.1, there is no consensus on the preferred method of dowel bar installation. However, on an average, the states seem to prefer a higher % of dowels installed using dowel baskets.

Table 2.1. DOT preferred dowel placement methods*

DOT	Basket	DBI	% DBI	% Basket
Alabama	Yes	No	0	100
Colorado	Yes	Yes	75	25
Florida	Yes	No	0	100
Nevada	Yes	Yes	25	75
North Carolina	Yes	Yes	25	75
Ohio	Yes	Yes	25	75
Pennsylvania	Yes	Yes	75	25
Virginia	Yes	Yes	25	75
Washington	Yes	Yes	25	75
Wisconsin	Yes	Yes	50	50

*Based on survey conducted in August 2004

Table 2.2. Sample Survey Form

Use this form to participate in a survey of Dowel Bar Installation Practices currently used by State Highway Agencies in the United States.	
Participant Details	
Name	
Title	
Organization	
Phone Number	
Fax Number	
Email Address	
Pavement Design Practice	
What is the typical range of transverse joint spacing for each of the pavement type?	
What is the typical range of PCC slab thicknesses the network under DOT jurisdiction?	
What is the typical range of base thicknesses in the network under DOT jurisdiction?	
What % of the network in your state is JPCP and JRCP?	
What are the typical diameters for dowel bars used across transverse joints?	
What is the typical length of the dowel bar?	
What is the typical spacing between dowel bars?	
What are the typical paving mixture requirements?	Target compressive strength: Target flexural strength:
Dowel Bar Installation Practice	
How are dowel bars placed along the contraction joints?	☐ Dowel Bar Inserter ☐ Both ☐ Basket Assemblies
What are the allowable dowel alignment tolerances for	Vertical skew: Horizontal skew: Horizontal translation: Vertical translation: Longitudinal translation:
How does your agency ensure specification compliance with respect to dowel alignment tolerances?	
Have any studies on the effect of misalignment on joint performance been carried out by your DOT? If yes, please provide the reference	
General Comments	

As a part of the literature review, the detailed specifications of dowel bar placement of five state DOTs including Michigan were reviewed and the findings are summarized in Table 2.3.

As seen from Table 2.3, in general when using baskets, all DOTs (Michigan, Ohio, Iowa, California, and Illinois) recommend use of stakes or pins, or bearing plates to anchor the assembly. A minimum of 1 ft long nails are required to be driven into the unstabilized bases/subbases. In case of stabilized bases/subbases, concrete anchors or bearing plates are used.

The abovementioned DOTs require the following to be adopted while using dowel bar inserters:

- Concrete has to be placed and consolidated full-depth before insertion of the dowel bars.
- A light coating of oil or bond-breaking material has to be applied to the bars before loading the bars in the dowel magazine.
- The bars have to be inserted into the plastic concrete in front of the finishing beam or screed and it has to be ensured that there are no voids around the dowel bars.
- Concrete has to be reworked and refinished to ensure that there is no evidence on the surface of the completed pavement that there has been any insertion performed.

Table 2.3. DOT Construction Specifications for Basket Assemblies

State	Cutting of Tie Wires	Basket Installation Details
MI (2004)	Yes	• Stake shall engage bottom longitudinal spacer wire. • After staking, the bottom longitudinal spacer wire shall contact the base material (unless non-penetrable) along its entire length. • For non-penetrable bases, permanent concrete anchors and stacking clips shall be used to secure assembly to base.
OH (2005)	Yes	• At least eight ½-in. diameter steel pins a minimum of 18 in. long are driven at an angle to brace the assembly. • 2 of these pins are driven opposite each other at each end of the assembly, and the remaining pins are driven in staggered positions on each side of the assembly.
IA (2005)	Option of Contractor	• Securely staked or fastened to the base to line and grade. • Anchor pins should be 1 ft long.
CA (2002)	Yes	• A minimum of 8 alternating, equally spaced, concrete fasteners with clips are used to anchor each 3.6 m assembly (4 per lower runner wire). • At least 10 concrete fasteners are used for assembly sections greater than 3.6 m and less than or equal to 4.9 m.
IL (2002)	Yes	• Assembly is provided with two continuous bearing plates made of not less than 2 in. width and not less than 0.04 in. thick sheet steel. • The bearing plates are attached by welding to the subgrade members or by suitable clips and are punched to receive the protruding ends of the upright supports and stakes. • The stakes are driven parallel to and next to the upright supports. • Bearing plates are not required on stabilized subbases. • At least ten nails shall be used for each assembly. • Bearing plates are punched to receive the nails. • For soil or granular subbase, metal stakes shall be used instead of nails, and shall penetrate the subbase at least 12 in.

2.3 TYPES OF MISALIGNMENT

The basic types of dowel alignment errors that can occur in concrete pavements are horizontal translation, longitudinal translation, vertical translation, horizontal skew, and vertical skew. A combination of the above could also occur. Figure 2.3 shows a typical diagrammatic representation of the cross section and plan views of these errors. A shaded bar denotes the original position of the bar and the dotted view is the position after misalignment. Also shown in the table is a dowel bar with no misalignment.

2.4 CONSTRUCTION FACTORS AFFECTING MISALIGNMENT

With either method, care and attention to many details are required to achieve proper dowel bar alignment (Yu 2005). For dowel baskets, the most critical factor appears to be the manner in which the baskets are secured on the subbase or base prior to paving. If the baskets are not adequately pinned down, the baskets may be shoved, rotated, or pulled apart during paving, resulting in extreme dowel bar misalignments. The baskets may also get bent during handling or during concrete placement by being walked on. For DBI construction, the critical factors are the proper adjustment of the DBI and PCC mix design. When using a DBI, mix optimization is extremely important to ensure the dowel bars do not become displaced after insertion. The PCC mix for DBI construction must be stable enough to hold the bars in place without displacing them during paving.

Construction factors that may affect misalignment as identified by Tayabji (1986) have been summarized in Table 2.4. The following paragraphs discuss the possible effect of some construction factors when using dowel baskets (leaving the tie wires intact and the wall of concrete behind the basket) on dowel misalignment, if any.

Table 2.4. Construction Factors affecting Misalignment*

Dowel Baskets	Dowel Bar Inserter
• Basket rigidity • Quality control during basket fabrication • Care during basket transportation and placement • Fastening of basket to subbase • Location of saw-cut over basket • Paving operation • Field inspection during construction	• Implanting machine operation • Strike-off after dowel placement • Consolidation (vibration) after dowel placement • Location of saw-cut over implanted dowels • Field inspection during construction

*Ref: Tayabji (1986)

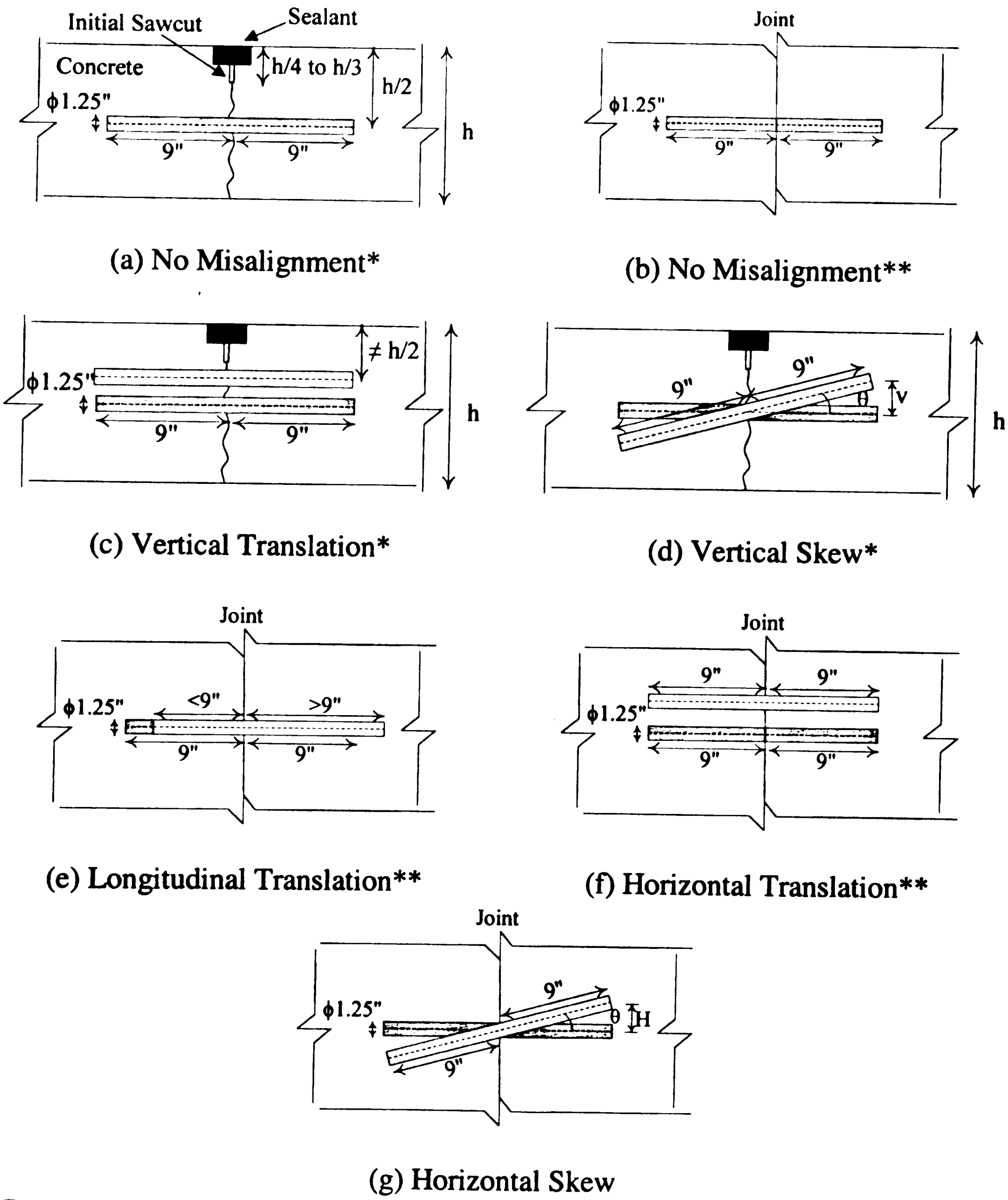

* Cross-sectional View
** Plan View

Figure 2.3. Basic Types of Dowel Alignment Errors

2.4.1 Cutting of Tie Wires

Most of the DOTs require the tie/spacer wires of the dowel basket assembly to be cut before concrete placement (substantiated through Table 2.3). Theoretical investigation (ACPA 2005) has indicated that leaving the tie wires intact has benefits and these have been described in the following paragraphs.

Leaving tie wires intact will strengthen the dowel basket, making it more resistant to movement and deflection while paving. This results in a smoother pavement, as well as dowels that are better aligned. The strengthening offered by uncut wires is more critical for taller dowel baskets used in thick pavements, such as heavy-use pavements. Dowel baskets that have the tie wires cut are more susceptible to spring-back problems, whereby the basket is compressed when the paver passes above it, then springs back up after the pressure is gone, resulting in a bump in the pavement.

Given the choice to cut the tie wires for purposes of location verification, or to leave the tie wires to enhance pavement quality, ACPA recommends leaving the wires intact. Since ACPA last conducted its review of state highway agencies practices in 1999, at least 3 states (Iowa, Washington, and Wisconsin) removed the requirement for cutting the tie wires (or spacer wires) in the dowel basket assemblies prior to paving. But around 20 state agencies still require concrete paving contractors to cut the tie wires prior to placing concrete. The intent of this requirement is to eliminate or reduce the apparent potential of the steel wires to lock the joint, or for the wires to cause micro-cracking in the early ages of the concrete. The underlying belief is that the three to five small-diameter wires, when crossing the joint, will restrict the shrinkage of the early-age concrete. In addition, the wires could reinforce and prevent movement of the transverse joint, and/or cause the concrete to crack.

These requirements are not well founded for a number of reasons. First, there are always stresses that build up in the concrete pavement due to early-age concrete shrinkage and temperature contraction. These are the same stresses that cause transverse saw cuts in jointed pavement to become working joints. The stresses have to build up to the point where they overcome the concrete strength, and then further build to overcome other restraining forces for the joints to open up. The restraining forces include friction provided by the subbase, and the amount of bonding between the concrete and the dowels themselves. Once these friction and restraint forces have been overcome, the stress would be transferred entirely to the tie wires.

For this mechanism to cause the concrete to crack, the tie wires must impart stress back to the concrete, and the total stress must be greater than the concrete strength at that point in time to cause a crack. But an analysis of the mechanics shows that the tie wires will fail one of two ways before they can cause damage to the concrete or lock the joint:

- The wires themselves will yield, or
- The welds holding the wires to the basket will fail.

2.4.2 Wall of Concrete behind Paver

Whether the wall of concrete ahead of the paver would create an overturning moment near the dowel baskets is a construction issue of key interest. Field visits to a mainline pavement construction site in Michigan and interaction with site inspectors eliminated this hypothesis. When using dowel baskets, the spreader places a significant amount of concrete on the dowel basket keeping it in place as shown in and when the paver follows the spreader it is ensured that consolidation is in the vertical direction and that the auger does not push or cause a moment on the basket in the horizontal direction. Also, since six pins are used on each basket, each driven at least a foot into the base, moment, if any, is resisted because of the firmness of the basket. Since the slump of concrete is also very low (about 2 in.), there is no flow induced when the spreader or the paver proceed towards the baskets.

Figure 2.4. Placement of Concrete while using Baskets

2.5 TOLERANCE ON MISALIGNMENT

The review of existing construction specifications indicate that there is no consensus on the practical limits placed on dowel misalignment tolerances (Table 2.5). The responses on tolerance specifications and on the misalignment check during construction, obtained through the previously mentioned survey, are summarized in Table 2.6. These tables indicate that there is no consensus among the DOTs on: (a) the techniques used for assessing dowel misalignment, and (b) the practical limits placed on dowel misalignment in jointed concrete pavements.

Table 2.5. DOT Tolerance Specifications

<table>
<tr><th rowspan="2">State</th><th colspan="2">Tolerance</th></tr>
<tr><th>Baskets</th><th>DBI</th></tr>
<tr><td>Michigan (2004)</td><td>Misalignment: Dowel bars shall remain aligned (parallel) with each other and ± 1/8 in. in both horizontal and vertical planes.
Transverse Location and Depth: Dowels shall be placed middepth ±1/2 in. Dowels shall be centered 1 ft ± ½ in.</td><td>Misalignment: ± ¼ in. over the length of the bar in the horizontal and vertical planes.
Longitudinal Location: ± 2 in. of planned longitudinal location.</td></tr>
<tr><td>Wisconsin (2004)</td><td>Hold dowel bars in the correct position and alignment using an engineer-approved device during construction</td><td>Misalignment: Parallel to the pavement surface and centerline ± ½ in. over 18 in.
Transverse Location and Depth: ± 1 in. of the planned transverse location and depth.
Longitudinal Location: ± 2 in. of planned longitudinal location.</td></tr>
<tr><td>Ohio (2005)</td><td colspan="2">Misalignment: ± ¼ in. per foot.
Transverse Location and Depth: Centerline of individual dowels shall be parallel to each other, the surface and the centerline of the slab. Dowels shall be ± ½ in. on centers. Dowels shall be placed mid-depth of the slab.</td></tr>
<tr><td>Iowa (2005)</td><td>Misalignment: ± 1/8 in. over 18 in.
Transverse Location and Depth: Centerline of individual dowels shall be parallel to the other dowels in the assembly ± 1/8 in. Spacing between dowels shall be 1 ft ± ¼ in. Each assembly shall be placed so that the bars are in a horizontal plane at T/2 ± 1/2 in.</td><td>N/A</td></tr>
<tr><td>California</td><td colspan="2">Misalignment: ± 0.354 in. over 18 in. in both horizontal and vertical directions.
Transverse Location and Depth: Parallel with the pavement lane centerline and surface of the pavement at mid-pavement depth.
Transverse location ± 1 in. from planned location.
Longitudinal Location: ± 2 in. of planned longitudinal location.</td></tr>
<tr><td>Illinois (2002)</td><td colspan="2">Misalignment: ± 1/8 in. over 1 ft. in the horizontal and vertical planes.
Transverse Location and Depth: Dowels, when used, shall be held in position parallel to the surface and centerline of the slab by metal devices.</td></tr>
</table>

Table 2.6. Survey Results for DOT Preferences of Dowel Bar Tolerance Checks

DOT	Bond Stress	Misalignment Tolerance		Quality Control of Misalignment
		DBI	Basket	
Alabama	No spec	None	¼ in. per 12 in.	Field inspection
Colorado	No spec	No spec		No requirement
Florida	No spec	None	½ in.	Contractor's responsibility
Nevada	No spec	½ in. over 18 in.		Coring. Also evaluating the the usefulness of MIT Scan-2
North Carolina	No spec	½ in.	¼ in., ¾ in. opposing skew	MIT Scan-2
Ohio	No spec	None	None	Pachometer or coring
Pennsylvania	2,200-4,400 lbs, depending on pavement width	¼ in. over the dowel length		Alignment verified prior to concrete placement. Baskets assumed to be rigid.
Virginia	No spec	No spec. Ensure that the dowels are parallel to the surface and the slab centerline. Parallel in the horizontal and vertical plane. ½ in. tolerance from the mid-depth of the slab		No requirement
Washington	No spec	½ in.		Developing specifications for MIT Scan-2
Wisconsin	No spec	½ in. over 18 in.		No spec

2.6 EFFECTS OF MISALIGNMENT

Various studies experimental as well as field have been carried out since 1930's to evaluate the effects of misalignment on pavement performance and this section has a compilation of these possible effects.

Segner and Cobb (1967) state that in general at least three types of failures, excluding bearing failures around the periphery of the dowels, in concrete pavements can be attributed to misaligned or locked dowel bars or other dowel bar defects. These failures may be described as follows:

- Cracks at or near the mid-span
- Local spalling at the contraction joint around the dowel bars
- Flexural cracks between the mid-span and the contraction joint, frequently near the ends of the dowel bars

Cracks near the mid-span are essentially tension failures caused by the lack of one or more contraction joints to function (open) properly. Contraction joints not opening properly causes two or more slabs to be "locked" or "tied" together and function as a unit rather than independently. This increased length under the action of initial shrinkage and contraction due to temperature changes causes the tensile strength of the concrete to be exceeded with cracks developing at more or less regular intervals. The failure of contraction joints to open properly may be caused by bonding between the dowel bars and the concrete due to deterioration of the dowel bar grease, misaligned dowels or a combination of both. When this "locking" of the joint occurs, the contraction joint (which is designed as a weakened plane in the slab) actually becomes a reinforced plane with the dowel bars functioning as reinforcing bars. Consequently, tension cracks develop in the slab some distance from the joint. Since concrete is inherently weak in tension, the critical period for this type of failure is the first few days after pouring, when the concrete is very green.

Local spalling around the dowel bars may be caused by dowel bar alignment errors in any plane, but are most likely to occur when the dowel bars are misaligned in the vertical plane. Flexural cracks between the mid-span and the contraction joint result from bending action in the pavement slabs caused by deflection of the slab ends. These deflections in the slab ends result from a combination of longitudinal slab movements due to shrinkage and temperature changes, and dowel bar alignment errors in the vertical or oblique planes. The deflections at the slab ends may actually force the end of each slab section to act as a very short cantilever beam; hence, flexural or bending failures may occur. It can be shown that deformations due to vertical alignment errors combined with sufficient joint movement may be critical.

Donahue (2003) states that translation, both horizontal and vertical, does not have as significant an impact as skew. He states that longitudinal translation is a measure of the bar's effective length on the approach and leave slabs. It is not realistic to expect every 18 in. bar to straddle a joint with 9 in. on either side, but it is expected that a bar have at least 6 in. on each side to ensure that it can adequately provide load transfer across the slabs. A study conducted in the late 1950's concluded that the dowel embedment length required to provide full load transfer is five or more times the bar diameter (Teller 1959).A recent study by Minnesota DOT (Burnham 1999) indicated that an embedment length of only 2.5 in. is sufficient to keep faulting at an acceptable level of ¼ in. and provide LTE with less variability.

Donahue (2003) states that horizontal translation has little impact on load transfer performance, unless grossly clustered enough to possibly create load transfer gaps and air pockets. He also states that since the baskets are designed for 12 in. spacing and the DBI slots are fixed for this spacing, there is virtually no chance of the abovementioned occurring. Dowel depth is not as critical as skew, but still must be monitored to ascertain that the bars are not being placed in higher stress zones where they could be deformed or cause debonding or bearing failures in the PCC.

Bock and Okamoto (1989) state that the dowels with excessive vertical translation from mid-depth can cause joints to spall. The capability of the dowel to transfer loads across the joint can also be reduced when dowels have large levels of vertical translation. Loss of load transfer can increase slab deflections under load causing pumping and loss of subbase support. This can cause premature joint and corner cracking. Resistance to movement is provided by subbase friction and locked joints. For slabs up to 20 ft, resistance due to subbase friction is not a major problem. The magnitude of restraint caused by locked joints depends on the degree of dowel misalignment, number of misaligned dowel bars, and degree of dowel corrosion. Locked joints may result in transverse cracking, corner breaks, and spalling at the concrete face around the dowel. Once a spall occurs around a dowel, load transfer effectiveness of the dowel may decrease.

The effects of these basic types of dowel misalignment on pavement performance have been summarized in Table 2.7 (after Tayabji 1987) in terms of the possible distresses including spalling, cracking, and loss of load transfer efficiency. As shown in Table 2.7, skew dowel misalignments are more detrimental and they can cause all three types of distresses at the pavement joints. In "in-service" pavements, the dowel misalignments are probably combinations of these basic types of misalignments and tentatively produce all three types of pavement distresses at the joint. The type and magnitude of skew will impact the concrete-dowel bearing stress which leads to higher cumulative damage at a joint.

The overall performance and distress of in-service concrete pavements are functions of: (a) the pavement design, (b) environmental conditions including thermal gradients, (c) joint spacing, (d) applied loads and number of passes, and (e) the dowel misalignments. The tolerance limits for dowel misalignment will depend on the other parameters (a - d mentioned here) and the required number of passes (design life) before pavement failure occurs in terms of the distress (spalling, cracking) or performance (load transfer efficiency < 70%).

Table 2.7. Possible Effects of Dowel Misalignment on Pavement Performance*

Type of Alignment Error	Effect on Spalling	Effect on Cracking	Effect on Load Transfer	Comment
Horizontal translation	-	-	Yes	Depends on the magnitude of translation
Longitudinal translation	-	-	Yes	
Vertical translation	Yes	-	Yes	
Horizontal skew	Yes	Yes	Yes	Horizontal rotation of the slabs is possible. If this rotation is restrained, cracking is possible.
Vertical skew	Yes	Yes	Yes	Vertical uplift of corners is possible, depending on the magnitude of the skew.
Combined skew	Yes	Yes	Yes	Both rotation and uplift are possible, depending on the magnitude of the skew.

*After Tayabji (1987)

2.7 EXPERIMENTAL STUDIES ON DOWEL MISALIGNMENT

This section discusses the findings of the different experimental studies on the effect of dowel misalignment.

Smith and Benham of Indiana (1938): They conducted tests on twenty specimens in four groups of five test specimens. The test specimens were 4 ft X 4 ft 8 in., cast on the ground, with a transverse contraction joint in the center (parallel to the 4 ft dimension), each containing four dowel bars. Two slab thicknesses were studied (5 and 6 in.). The dowel bars were ¾ in. in diameter, 24 in. long, and placed 12 in. on center. Dowel misalignments included in each group were 0, ¼, ½, 1, and 1.5 in. over 22 in. of the bar. The outer dowels were horizontally misaligned (in opposing/non-uniform orientations) while the inner two were vertically misaligned (in opposing/non-uniform orientations).

The contraction joints were filled with a piece of wood ¾ in. thick and having a vertical dimension equal to ⅓rd the slab thickness. A weakened plane was created by installing a piece of No.24 galvanized iron, extending from the wood strip downward to the subgrade. The dowel bars were passed through semi-circular openings, 3 in. diameter, in the sheet metal. At the age of 28 days, the joints were opened to a distance of ¾ in. using hydraulic jacks. After a few days, the process was reversed and the joints were closed till their original position. Ten such cycles of movement were performed within one year.

They found that for 6 in. thick slabs, misalignments in excess of 1 in. caused spalling when the joints were opened to ¾ in. while for the 5 in. thick slabs, ¼ in. misalignments resulted in minor distress. If the joint opening was limited to ½ in., misalignments up to 1.5 in. did not result in any observable distress when the slabs were pushed apart. Generally, the load required to open a contraction joint ½ in. did not exceed 3,000 lbs per dowel.

Segner and Cobb of the University of Alabama (1967): They conducted tests on 38 dog-bone shaped specimens that consisted of two slabs each 2 ft 9 in. long and 3 ft. wide at the joint. All slabs were 10 in. thick. Each specimen contained three dowels with the center dowel misaligned. The dowel bars were 1.25 in. in diameter, 16 in. long, and placed 12 in. on center. Dowel misalignments, defined over full length of the dowel bar, were 0, ½, ¾, 1, 1½, and 3 in. in the horizontal, ¼, ½, ¾, and 1 in. in the vertical, and ½ and 1 in. in the oblique planes.

Weakened planes were formed in the specimens by means of ¼ in. thick redwood strips held securely in place by slots cut in the side forms and a slotted 2 in. X 4 in. extending transversely across the top of the specimen forms. The slots were cut 2.5 in. deep and ¼ in. wide to assure the uniformity of the needed joint dimensions.

Generally 6 specimens were poured at a time with three different errors in alignment. After the concrete samples had reached their initial set, the top surface was cured with a liquid curing compound. One sample of each alignment error was tested at 2 and 7 days of age. Two 20-ton capacity hydraulic rams connected to a common pump were used to push the slabs apart. The specimens were loaded slowly (in approximately ten load intervals) until each failed at its weakened plane. The load was then reapplied to the specimens in approximately ten additional load intervals until the joint had opened 1 in.

They found that misalignments in the vertical plane are more critical than errors of equal magnitude in the horizontal plane with vertical alignment errors being the most severe. Loads required to produce a contraction joint opening of ½ and ¾ in. vary as a function of magnitude of misalignment. Misalignments in the horizontal plane can be as high as ¾ in. without causing any appreciable increase in load to produce joint openings of ½ and ¾ in. However, alignment errors of ¼ in. in the vertical plane require a significant increase in load to produce similar joint openings. Spalling was observed when the joint opening reached approximately 0.9 in., which could have been caused by the local crushing of the concrete around the periphery of the dowel bar. Load required in opening a joint ½ in. for a 1 in. vertical misalignment was about 4000 lbs, and for a 1 in. horizontal misalignment the load was about 2000 lbs.

Weaver and Clarke (1970): They conducted tests on specimens 10 in. thick slabs fitted with 1 in. diameter dowel bars, 18 in. long, spaced at 12 in. on center, with misalignments ranging from 4-16%. The variables considered were joint formation type (fractured and plain), concrete age (7 and 28), and joint width (0.025, 0.05, 0.125, 0.25, and 0.375 in.).

In the joints with fractured faces, crack inducers of brass sheet 2.5 in. deep and 0.015 in. thick were used to reduce the section at the top and bottom of each specimen at its midpoint; the joint was formed by cracking the specimen between the crack inducers. The plain joints were formed by completely separating the halves of the specimen with a ⅛ in. thick steel former; the former was fabricated in two parts, divided at the location of the dowel bar, facilitating easy removal from the joint. 100 kN capacity hydraulic jacks were used to load the specimens.

They observed that the rigidity of the dowels at the joint decreases with increasing joint openings. The rigidity of a dowel bar (load/unit deflection) in a joint decreases rapidly on initial application of load to a joint and then achieves a substantially constant value at an equivalent misalignment (deflection/unit of joint width) of about 3%. The measured rigidity of dowel bars increases up to an age of 7 days and little difference was detected between specimens of age 7 and 28 days. They also recommended that misalignments should not be greater than 4%.

Tayabji (1987): He conducted 16 tests on slabs that were 3 ft. wide by 3.5 ft. long containing a single dowel and 33 tests on slabs 3 ft wide by 2 ft long fitted with two dowel bars that were non-uniformly misaligned. Two slab thicknesses were studied (8 and 10 in.). The dowel bars were 18 in. long and placed 12 in. on center. Dowel misalignments, defined over full length of the dowel bar, were 0, ¼, ½, 1, 2, and 4 in. in the horizontal and the vertical planes. For each of the two dowel tests, both the dowels had the same misalignment.

A ⅛ in. thick steel plate was used to form the joint. Each specimen was cast on two layers of polyethylene sheets. The initial tests were conducted on single-dowel specimens and the pullout loads were low and hence the test procedure was modified and the 2-dowel series was tested. Specimens were tested at 1, 3, 7, and 28 days and the joint was opened to a maximum opening of ¼ in. One slab section was held firmly while the other slab section was pulled using a hydraulic jack. Pullout load was applied gradually and uniformly to produce a joint opening of ¼ in. in about 1 minute. For each test, the pullout test was performed three times. After each, the pulled slab was pushed back to close the joint and the pullout test was repeated. For the second and third tests, the maximum pullout load obtained was less than half that obtained for the first test.

From the single-dowel tests he found that a large portion of the pullout load was required to open the joint 0.01 in. After the joint was opened 0.05 in., there was no further increase in the pullout load. He did not find any significant difference in the pullout load for the different levels of misalignment in the single-dowel cases whereas in the 2-dowel cases although an increase in the pullout load was observed with increased level of dowel misalignment, the absolute magnitudes were relatively low for misalignment levels below 1 in. No spalling was seen around dowel bars at the joint face for specimens having misalignment levels of less than 1 in. at a maximum joint opening of ¼ in.

The most stringent specification requires vertical and horizontal alignment to be within ⅛ in. per foot of dowel bar length; the least stringent requires only ⅜ in. per foot (ACPA 2004). The current ACPA recommendation suggests a value of ⅜ in. per foot, or 3 %. There is, however, no consensus on the limit or tolerance of misalignment beyond which it is detrimental to slabs.

2.8 FIELD MEASUREMENT OF DOWEL BAR ALIGNMENT

There are four methods used for the detection and measurement of dowel bar placement in the field: coring, the pachometer and covermeter, the Ground Penetrating Radar (GPR), and the MIT Scan-2. Amongst these methods, coring is the only destructive method. By far, coring is the most accurate method but due to its destructive nature, its use is limited.

While the importance of achieving dowel alignment is widely recognized, the ability to monitor the placement accuracy of dowel bars effectively had been limited by the lack of practical means of measuring the position and orientation of dowel bars embedded in concrete (Yu 2005). The past difficulties in measuring dowel alignment had several important consequences on concrete pavement construction, including the following:

- *Limited validation testing for dowel alignment* – Most agencies conducted only a limited amount of coring to evaluate dowel alignment, leading to dowel alignment evaluation based on extremely small samples.
- *Possibility of extremely strict dowel placement tolerance* – Most agencies have fairly strict tolerances on dowel placement accuracy, but those standards are based on limited laboratory and field data. In some cases, the fabrication tolerances for

dowel baskets are adopted directly and used as the tolerance on dowel placement accuracy, which leaves no room for any placement error during construction. The actual dowel bar alignment needed to assure good pavement performance is largely unknown at this time.

- *Limited usage of DBI* - Because of the concern over the dowel alignment and the lack of practical means of verifying dowel alignment in the past, DBIs are not widely used in the US, and many highway agencies specifically prohibit the use of the DBI, although the DBI can offer significant advantage in construction cost and speed.

In this section, more focus has been given to the GPR and MIT Scan-2 methods as they are the most accurate methods, available to date. Details on the field studies that have used the above methods and any observations during the studies are described in this section.

2.8.1 Pachometer and Covermeter

Pachometer and covermeter are battery-operated magnetic detection devices, which are mainly intended to measure the depth of reinforcement in concrete, and to detect the position of rebars. Its use has been extended to pavements to detect the location of dowel bars. The device emits an electromagnetic field and detects disturbances in the field caused by embedded metals. Figure 2.5 illustrates a pachometer in use.

Field Experiences: Fowler (1983) and Burati (1983) used the same electronic detector model in Georgia and Alabama, respectively to measure misalignment. The detector was considered accurate for horizontal measurements, but vertical measurements could not be determined. Study by Fowler (1983) indicated that the accuracy obtained using the electronic metal detector was ⅓ in. on horizontal rotation. Donahue (2003) used a handheld pachometer or steel locator to measure actual dowel bar depths and used it as ground truth data for calibration of GPR. The latest versions of the covermeters have an accuracy of ± 0.04 in. and are used based on procedures similar to BS 1881-204:1988. Study at Minnesota indicated that while accurate results could be obtained using a covermeter, testing a large number of bars using this device is not practical (Yu and Khazanovich 2005).

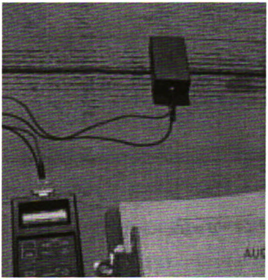

Figure 2.5. Typical Pachometer*
*Source: Donahue (2003)

2.8.2 Ground Penetrating Radar

The Ground Penetrating Radar (GPR) uses a radio wave source to transmit a pulse of electromagnetic energy into a subsurface (in this case, concrete pavement). The amplitude and arrival time of the reflected electromagnetic pulse (which originates from the top of the dowel) is recorded for analysis (determination of spatial location of the dowel). The GPR signal is characterized primarily by changes in reflection amplitude and changes in the arrival time of specific reflections. The GPR record consists of a continuous graphic display of reflected energy over a preset time interval. The depth to the dowel can then be determined if the propagation velocity, and electromagnetic energy through concrete are known or estimated. Figure 2.6 illustrates a typical GPR in use.

(a) Ground Penetrating Radar (GPR)

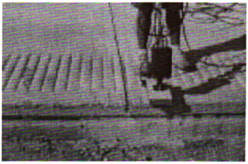

(b) GPR in use

Figure 2.6. Typical Ground Penetrating Radar in use*
*Source: Donahue (2003)

The resolution and depth penetration of the GPR tool is a function of the frequency of the antenna employed and the conductance of material imaged. Higher frequency antenna provide for better resolution, but less depth penetration. The GPR can penetrate resistive materials, but cannot be transmitted through highly conductive materials (such as dowel bars). When the GPR antenna crosses a dowel bar at right angles, the resulting GPR image looks (visually) like an inverted U (hyperbola). The apex of the hyperbola indicates the exact spatial location of the dowel bar.

Field Experiences-Advantages and Limitations: Study by Okamoto (1988) indicated that radar is an effective tool for evaluating dowel bar misalignment, but needs improvement with respect to horizontal misalignment and precision in this study was ~ ½ in. Study by Donahue (2003) used a 1.5 GHz GPR and use of a single dielectric constant while using GPR was attributed to lead to potential errors of ± ⅛ in. in dowel depth measurements (in an absolute sense). However, he states that depth estimates at any single joint study site would be accurate in a relative sense.

Interaction with pavement engineers at the Michigan Department of Transportation and University of Missouri-Rolla, who had used the GPR for similar studies, revealed that the speed of data collection is walking speed and takes no more than a few of minutes per joint. However, around 4 to 7 GPR profiles, perpendicular to the dowel bar, have to be obtained, in order to obtain complete information of the dowel bar location. The processing of data requires care and training in order to amass the different runs. Also, post-processing cannot be carried out on the field. The starting point of each GPR profile should be along the same horizontal line else it could lead to errors or mismatches in the processed data.

According to a Concrete Pavement Technology Program (CPTP) project (Task 7F) (ACPA 2004) study, with GPR, variations in material properties, which can be substantial along a project, can create random errors that significantly affect analysis results. Water on the pavement surface or in the pavement structure can also affect results.

2.8.3 MIT Scan-2

The MIT Scan-2 is a state-of-the-art device for measuring the position of metal bars embedded in concrete. Figure 2.7 shows a close up of the MIT Scan-2 and Figure 2.8 shows the operation of the MIT Scan-2.

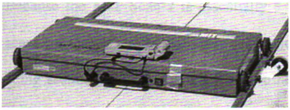

Figure 2.7. Close up of MIT Scan-2

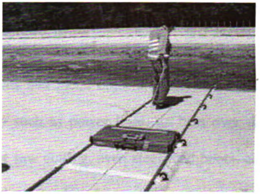

Figure 2.8. Typical Run of MIT Scan-2 in Field

The MIT Scan-2 utilizes an array of sensitive detectors and sophisticated data analysis algorithms to produce very accurate results. The device emits a weak, pulsating magnetic signal and detects the transient magnetic response signal induced in metal bars. The methods of magnetic tomography are then used to determine the position of the metal bars.

Unlike other devices that have been used in the past, which are general-purpose instruments adapted to the dowel bar detection application, the MIT Scan-2 was developed specifically for measuring dowel and tie bar alignments. As a result, the device is simple to operate, efficient, and provides real-time results in the field.

*Field Experiences-Advantages and Limitations:*The MIT Scan-2 tests the entire joint at once, providing results for all dowel bars placed in the joint in one shot. The testing takes about 1 minute per joint and up to three lanes can be tested together. In an 8-hr day, a 2-person crew can easily test 200 or more joints using the MIT Scan-2. It can be run continuously for 8 hours on one charge of the battery. The MIT Scan-2 is shown to provide very accurate results for dowel bars placed using a DBI. For DBI inserted bars, the magnetic technology may be more reliable because the results are based on direct measurements, rather than correlation to a calibration (Yu and Khazanovich 2005). Because the MIT Scan-2 is essentially a metal detector, its operators must choose a scanning location carefully, since magnetic fields and metal objects, close to the joint being scanned (within about 3 ft of the bars) - such as power lines, tie bars over the dowel, vehicles, marker nails in the concrete for saw cutting, even steel-toed boots, can interfere with the measurements. The dowel baskets also interfere with the measurement results; however, approximate results can be obtained if the following conditions are met:

- The dowel bars are epoxy coated
- The transport ties on the basket are either cut or removed

The accuracy of the MIT Scan-2 results depends on the position and the orientation of the dowel bars (Yu and Kim 2005). It produces the most accurate results when the bars meet the following typical placement tolerances:

- Mean dowel depth 4 to 7.5 in.
- Maximum vertical misalignment ± 0.8 in.
- Maximum horizontal misalignment ± 0.8 in.
- Maximum lateral position error (side shift) ≤ 2 in.

For bars meeting the limits of reliable results for MagnoNorm software (software used to analyze MIT Scan-2 results) listed above, the estimated overall standard deviation of measurement error is 0.12 in. in rotation, which means that the device can provide measurement accuracy of ± 0.2 in. with 95 % reliability. CPTP project (ACPA 2004) results reported that MIT Scan-2 was found to be reliable, efficient, and accurate within ± 0.08 in. when position errors are minimal. Accuracy depends on the degree of placement error. Within typical placement tolerances ± 0.38 in. for vertical and horizontal misalignment and 2 in. for side shift, the range of error is ±0.16 in. With gross misalignments, the error can be greater.

The California, Nevada, South Carolina, and Washington DOTs participated in the CPTP field trials that evaluated the MIT Scan-2. Apart from being impressed with its capabilities and practicality, they have provided the following suggestions/observations:

- South Carolina DOT: Sample of 10 to 20 joints from each day's production is adequate to monitor performance. Testing every joint can slow production.
- Washington DOT: 50 joints can be checked in 1 hr. Weston reported that minimal training would be needed to interpret the positional data.
- Nevada DOT: Sohila Bemanian commented that the trials were promising and is a very powerful tool to inspect 100 % of the work on the first day of production.

Because the MIT Scan-2 operates on electromagnetic field, presence or absence of non-conducting material does not affect the results. It is also not affected by changing moisture conditions in concrete, so, the testing can be conducted at any concrete age, including over fresh concrete. The test results are not affected by the presence of water on the pavement surface.

The CPTP study compared the performance of MIT Scan-2 and ground-penetrating radar (GPR) and found that both technologies can produce accurate results and both have limitations as listed previously.

2.9 FIELD STUDIES COMPARING BASKETS VS DBI

Table 2.8 summarizes the results of the field studies comparing the two dowel bar placement methods i.e. baskets and DBI in context of misalignment observed and distresses as a result of this, if any.

Some of the key observations include:

- No method is significantly superior over the other but the DBI in many cases has produced results comparable with the baskets and better with respect to average depth and vertical misalignment.
- Quality of dowel bar placement ultimately relies on quality of field inspection and contractor consistency.
- Occurrence of longitudinal translation is similar for both types of joints. Longitudinal displacement is affected at least as much by location of the sawed joint as it is by the actual dowel movement.
- Individual dowel position has no effect on the alignment achieved.
- Distribution of tilt is more symmetrical for basket joints than inserter joints indicating that vertical misalignment may not be independent of paving direction.

Also it has been emphasized that it is advisable to do a test stretch on the pavement using the DBI and a quick check on the placement in plastic concrete before proceeding with the rest of the project. Also the DBI's quality of placement depends on the manufacturer, and a study has to be carried out before using a DBI from a different manufacturer.

The reference used for vertical height in case of DBI is the concrete surface whereas for baskets, the reference is the base grade. The misalignment is measured with respect to the pavement surface and hence accuracy in depth of the dowel might be impacted by even a slight change in the thickness of the concrete slab and the comparisons might be misleading. The studies also recommend the use of a handheld pachometer or a magnetic rebar locator to be available on all doweled PCC construction projects, which would be useful in aligning sawn joints with the dowel bars and in identifying missing dowels.

In the field study by Yu et.al. (2003) comparing the baskets vs DBI, a joint score scheme was developed that takes into account both the number of misaligned bars in a joint and the severity of misalignment. A joint score greater 10 indicates a greater risk of joint problems, while joint score of 10 or less indicates relatively low risk of joint problems. The basket section had nearly twice as many joints in the >10 category, indicating a greater potential for joint problems.

Yu et. al. (2005) compared 5 DBI projects and 7 basket projects located in 6 states across the US, using the MIT Scan-2 and the results (Figure 2.9) indicate that both the methods are comparable. The last two categories have been termed as high risk zones by the authors.

In a dowel bar retrofit project in Washington, severe vertical misalignments of 1–2 in. were found in many dowel bars. However, from a visual standpoint, the pavement is performing well (ACPA 2004).

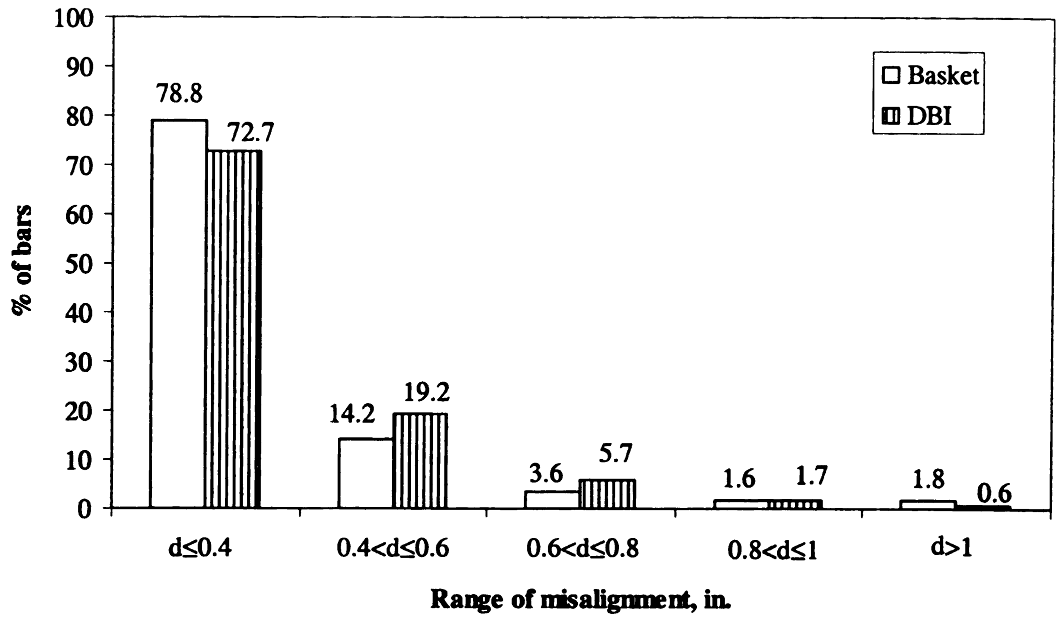

Figure 2.9. Comparison of Baskets vs DBI

Table 2.8. Summary of Field Study Results

Reference Study and Test Section	Specifications, Method of Measurement and Parameters Monitored	Findings/Conclusions
Georgia DOT (Gary Fowler, 1983) • M-5020 Richmond: Baskets • I-16 Bulloch paved in 1976: DBI • APD-056 Forsyth: DBI Contractor tried placing dowels after the paver had passed resulting in extra finishing, dowel depressions filled with grout, and poor riding surface. The implanter was positioned ahead of the paver after a short period. • Three interstate projects with dowels implanted and two projects with baskets	Dowels 1.25 in. diameter, 18 in. long, 15 in. c/c, joint spacing 20 ft ***Tolerance:*** H, V of ± 1 in. for translation Rotational misalignment was 1-1/8 in. H and 9/16 in. V **Method:** Coring, Electronic Metal Detector **Parameters:** • Depth • Longitudinal alignment • Vertical and horizontal rotation	• 1st project that used an implanter met the specifications in most cases and compared closely to the accuracy of one reference job that utilized baskets. • Utilization of baskets did not eliminate all problems of rotation and especially the problem of longitudinal alignment. • Longitudinal displacement is affected at least as much by location of the sawed joint as it is by actual dowel movement. • Most difficult factor to control with implanting seemed to be the vertical height of dowel. • No dowel related pavement distress occurred in either of the projects. • All dowels were working. The dowel bar paint is ineffective as a coating on the working end of the dowel. However, it does aid in breaking the concrete bond of the dowel.
Missouri DOT (John Donahue, May 2003) US 60 JPCP construction project near Van Buren (G&Z DBI, Baskets)	***Tolerance:*** Be parallel to the subgrade and parallel to the line of the joint Misalignment: ± ½ in. over 18 in. Transverse location: ± 1in. Longitudinal translation: ± 2 in. ***Method:*** Ground penetrating radar (GPR), handheld pachometer ***Parameters:*** • Dowel Skew • Dowel Translation • Dowel depth	• Both tend to have moderate horizontal skew tendencies with the DBI performing a little better. • Both have very good control of vertical skew with the baskets holding a slight edge in performance. • Both have few serious occurrences of high opposite skew between dowel bars in the same joint. • For depth, DBI was more consistent than baskets with respect to surface evaluation. • Average depth and average depth standard deviation was acceptable for both.
Burati et.al.,(1983) Alabama pavements	**Method:** Electronic Metal Detector **Parameters:** • Absolute horizontal rotation • Absolute longitudinal displacement	• No significant difference between DBI and basket projects with respect to joint-related distress. • No significant difference between DBI and basket projects with respect to joint-related distress.

Table 2.8. (contd.)

Reference Study and Test Section	Specifications, Method of Measurement and Parameters Monitored	Findings/Conclusions
Burati et.al.,(1983) Alabama pavements	• Absolute horizontal displacement	• Overall results indicated that the dowels in the implanted projects, on the average, were better aligned than were the dowels in the basket projects. But contractor difference and inconsistency might have contributed to the difference. • Overall results indicated that the dowels in the implanted projects, on the average, were better aligned than were the dowels in the basket projects. But contractor difference and inconsistency might have contributed to the difference. • Individual dowel position had no effect on the alignment achieved. • No effect from pavement grade on dowel alignment or distress was found. • No correlation between misalignment types and distress was found. • Absolute horizontal rotation values were virtually the same for both implanted and basket projects. • Absolute longitudinal and horizontal displacements were noticeably better in implanted projects.
James Parry (Wisconsin DOT) (1987) Three projects each using DBI and baskets on I-90 at Janesville in 1987	***Tolerance:*** Depth of dowel: ½ in. above the mid-depth Vertical/Rotation: ± ½ in. over full length Longitudinal translation: ± 3 in. in either direction **Method:** Coring **Parameters:** • Average depth • Vertical rotation • Horizontal rotation • Ride quality • Voids • Missing dowels	• DBI is capable of consistent satisfactory placement of dowel bars with respect to average depth, vertical and horizontal rotation. • Initial setup of the DBI with respect to depth of dowel placement is critical at the start of each project, and dowel depths should be verified by probing through the fresh concrete. • Accurate marking for sawing joints is important. • Having a magnetic rebar locator available on all doweled PCC construction projects would be useful in aligning sawn joints with the dowel bars and in identifying missing dowels. • Ride quality of 4.6 can be achieved on DBI projects with minimum grinding. • Improved consolidation is required on both projects. • Problems with missing dowels on existing DBI projects appear to be infrequent and isolated, but this problem should be monitored on future projects.

Table 2.8 (contd.)

Reference Study and Test Section	Specifications, Method of Measurement and Parameters Monitored	Findings/Conclusions
Bock, Okamoto (1988) I-86, Idaho (Gomaca DBI) I-45, Texas (Baskets, DBI) I-90, Wisconsin (Baskets, DBI)	**ID**-1.25 in., 18 in. long @ 12 in. c/c. 10 in. PCC, random joint spacing **Tolerance:** ± ¼ in. per 12 in. **TX**-1.25 in., 22 in. long @ 12 in. c/c. 10 in. PCC, 15 ft. joint spacing **WI**-1.25 in., 18 in. long @ 12 in. c/c. 10 in. PCC, random joint spacing **Tolerance:** Dowel depth: mid-depth ± 1 in. Misalignment: ± ½ in. per 18 in. Horizontal Translation: ± 1 in. ***Parameters:*** • Average depth • Vertical Misalignment • Horizontal Misalignment • Longitudinal Displacement (qualitative)	• DBI performed well compared to baskets. • Based on dowel depth, longitudinal displacement, vertical tilt, and horizontal skew, there is no significant difference between DBI and baskets. • Distribution of tilt is more symmetrical for basket joints than inserter joints, indicating that vertical misalignment may not be independent of paving direction. • Horizontal misalignment seems to be independent of paving direction. • Occurrence of longitudinal translation is similar for both types of joints.
Okamato (1987) I-45, South of Dallas, Texas	***Method:*** Ground penetrating radar, Coring ***Parameters:*** • Average depth • Vertical Misalignment • Horizontal Misalignment • Longitudinal Displacement (qualitative)	• Overall, the dowels in the inserter sections tended to be misaligned slightly downward in the leave direction. • Displacement can be introduced if the joint location is not marked correctly for sawing, or if the saw cut does not follow the marked joint location. • Average dowel depths appear to be uniform for both methods. • DBI performance is better than basket in terms of both degree of vertical misalignment and variability of vertical misalignment with each joint. • If other sources of variability, such as accuracy of joint locating and sawing are assumed to be constant, it appears that more longitudinal displacement was detected in the DBI sections than basket sections. Number of occurrences was, however, small in comparison to the number of dowels evaluated.

Table 2.8 (contd.)

Reference Study and Test Section	Specifications, Method of Measurement and Parameters Monitored	Findings/Conclusions
Yu, Khazanovich (2003) One section each using DBI and baskets, totaling 100 joints each, on I-15 reconstruction project near Victorville, California	***Tolerance:*** Horizontal and vertical misalignment: $\pm \frac{1}{4}$ in. per 1 ft Lateral dowel position: ± 1 in. ***Method:*** MIT Scan-2 ***Parameters:*** Horizontal and vertical misalignment	• Dowel alignment in the DBI section is no worse than that in the basket section. • In terms of number of bars misaligned, the basket section performed better (15.2 % vs 19.1 %) • In terms of the risk of the improper dowel alignment causing joint problems, the DBI section may be better because the greater percentage of the out-of-spec bars in the DBI section was due entirely to the higher percentage of misaligned bars in the 0.35 to 0.6 in. range. • In both of the more severe misalignment categories (0.6 to 0.8 in.; and >0.8 in.), the basket section had a higher percentage of misaligned bars than the DBI section.

CHAPTER 3 EXPERIMENTAL PLAN AND PROCEDURE

This chapter describes the experimental setup and plan, instrumentation and material testing details, and typical preparation steps in a casting-testing cycle.

3.1 EXPERIMENTAL SETUP

The experimental investigations were conducted on laboratory-scale pavement specimens with doweled contraction joints. Each pavement specimen consisted of two 48 x 24 x 10 in. concrete slabs connected at the joint using steel dowel bars. Steel dowel bars that are 1.25 in. in diameter and 18 in. long are placed at the mid-depth at the joint, with equal lengths (9 in.) embedded in each concrete slab, and are placed 12 in. on center. The number of dowel bars at the joint and their misalignment type, magnitude, and uniformity varied from specimen to specimen, according to the test matrix presented in the next section. Figure 3.1 shows the overall dimensions (plan view) of the concrete after demolding (for a 1-dowel test). Figure 3.2 (a-c) illustrates the different parts of the experimental setup and details of the components. Each concrete slab is supported on smoothened rollers placed on hardened steel plates. There is an ⅛ in. gap between the concrete slabs that serves as a full-depth contraction joint. The pavement specimen is tested by pushing apart the two concrete slabs using hydraulic actuators simulating thermal expansion.

Essential parts of the molds are made from steel sections. The concrete slabs are cast in-place directly in the molds and are ready to test after the concrete sets. The joint between the concrete slabs was formed using a ⅛ in. thick aluminum plate with circular holes of appropriate diameter to pass the dowel bars through it. This aluminum plate is left in place after casting the concrete, and it does not hinder the experiment or the separation of the slabs in any way.

In all, three molds were fabricated for specimens accommodating one and two dowels and one mold for three and five dowel specimens. The mold consists of the following, starting from the ground up: base rails, solid rollers, base plate, and channels. The channel sections are held in place with the help of bolts located at maximum spacing as per the AISC Steel Manual. The key mold details (cross sectional and plan view) are illustrated in figures A-1 through A-4 in Appendix A.

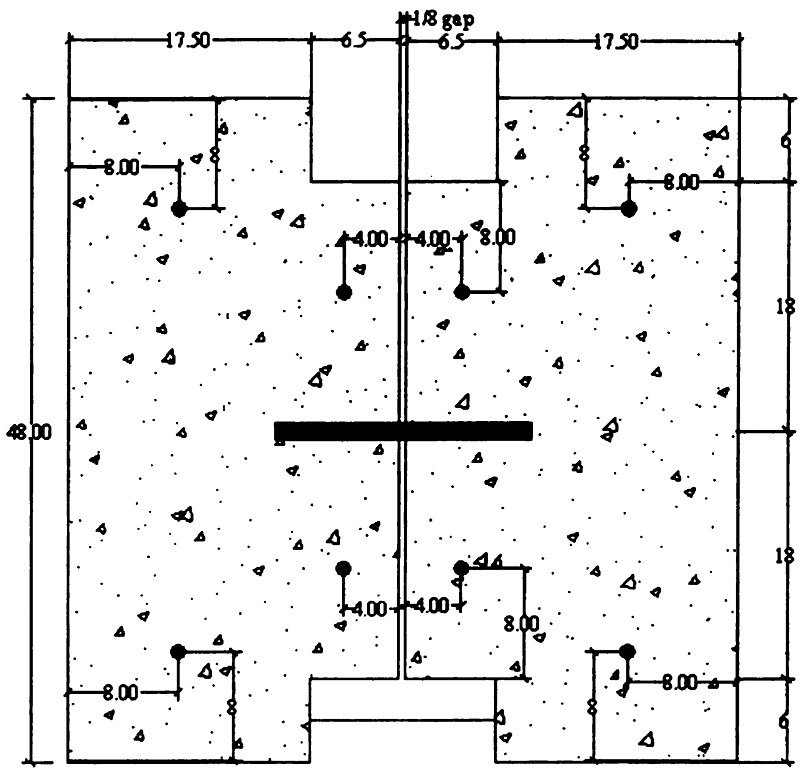

Figure 3.1. Plan – Section view of the overall mold for 10 in. slab (All dimensions are in in. unless specified otherwise)

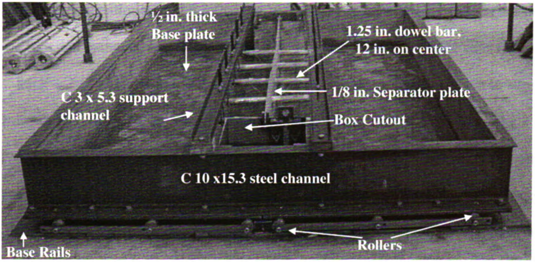

(a) Experimental Setup

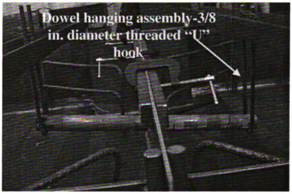

(b) U-hook Assembly

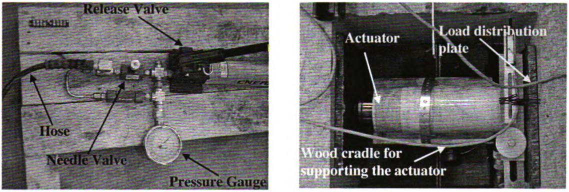

(c) Hydraulics

Figure 3.2. Experimental Setup and Components

The dimensions mentioned in the following paragraphs are in context of the small mold but the function is the same in both the small and the big molds. The base rails (54 x 6 x ½ in. thick – 2 in number and 54 x 10 x ½ in. thick) have a polished surface to support the solid rollers of 2 in. diameter and 54 in. long. The base rails help in providing a flat surface. The base plates (53 in. x 27 in. x ½ in. thick – 2 in number), with the bottom surface smoothened are placed on the solid polished smooth rollers. This smoothness is required to ensure that when the pullout load is applied using the actuators, the base rails, solid rollers, and base plate move with minimal frictional resistance relative to each other.

The east and west channels are structural steel sections C10x15.3 attached with a removable steel box cutout (13 x 6 x ½ in. thick) with the corners having fillets. The north and south sides are similar to the east and west channels but do not have the box cutout. The north and south channels including box cutouts are removed during demolding. The steel box cutout joins the two base plates together thereby providing height and rigidity to the mold. The purpose of the box cutout is to provide space for placing the actuators and the steel spreader plates during the pullout of the slabs.

The permanent section of C10x 15.3 (48 in. long) stays bolted to the base plate throughout the duration of the experiment. The structural steel section used for hanging the dowel bar assembly is illustrated in Figure 3.2 (a-b). A slot of 5¼ x ⅜ in. on the channel section provides the ⅜ in. finely threaded mild steel bar enough room to move in a horizontal direction. The dowel hanging assembly shown consists of threaded U-hooks that are bolted to supporting channels. This specially designed assembly allowed fine adjustments to the dowel position in the vertical and horizontal directions.

A new test setup was added, with the size of the specimen, nearly double of the previous test setup for the one and two dowel bars, to accommodate three to five dowel bars. These specimens consisted of 2 concrete slabs, each 96 x 36 x 10 in.

The specimens were tested by pushing apart the concrete slabs, using hydraulic actuators, shown in Figure 3.2 (c). The hydraulics and the testing procedure are described later in the chapter.

3.2 EXPERIMENTAL PLAN

The following variables were taken into account while designing the experimental matrix:

- Number of dowels and number misaligned
- Misalignment type
- Misalignment magnitude
- Orientation

The experimental design matrix is shown in Table 3.1 and is explained in the following paragraphs.

Number of dowels: Tests were carried out on two slab sizes – the smaller slabs (2' X 4') accommodating either one or two dowel bars and big slabs (3' X 8') accommodating three or five dowels. On the 2-dowel systems, tests with either one or both misaligned were performed. On the 5-dowel systems, tests with all dowels misaligned, and alternate dowels misaligned (outer and center dowels misaligned) were performed. A total of 51 unique misalignment combinations have been tested (15 one-dowel, 25 two-dowel, 3 three-dowel, and 8 five-dowel, respectively).

Table 3.1. Experimental Design Matrix

Slab Dimensions	Number of Dowels	ID	Misalignment	Magnitude, in.
2 slabs each (48 X 24 X 10 in.)	1	1A	Aligned	0
		1H14	Horizontal	¼
		1H12		½
		1H34		¾
		1H1		1
		1H2		2
		1V14	Vertical	¼
		1V12		½
		1V34		¾
		1V1		1
		1V2		2
		1C14	Combined	¼
		1C12		½
		1C34		¾
		1C1		1
	2	2A	Aligned	0
	2 (Uniform)	2H12U	Horizontal	+ ½, + ½
		2H1U		+ 1, + 1
		2V12U	Vertical	+ ½, + ½
		2V1U		+ 1, + 1
		2C12U	Combined	+ ½, + ½
		2C1U		+ 1, + 1
	2 (Non-uniform)	2H14NU	Horizontal	+ ¼, - ¼
		2H12NU		+ ½, - ½
		2H34NU		+ ¾, - ¾
		2H1NU		+1, -1
		2V14NU	Vertical	+ ¼, - ¼
		2V12NU		+ ½, - ½
		2V34NU		+ ¾, - ¾
		2V1NU		+1, -1
		2C14NU	Combined	+ ¼, - ¼
		2C12NU		+ ½, - ½
		2C34NU		+ ¾, - ¾
		2C1NU		+1, -1
	2 (One bar misaligned)	2H12AM	Horizontal	+ ½, 0
		2H34AM		+ ¾, 0
		2V12AM	Vertical	+ ½, 0
		2V34AM		+ ¾, 0
		2C12AM	Combined	+ ½, 0
		2C34AM		+ ¾, 0

Table 3.1 (contd.)

Slab Dimensions	Number of Dowels	ID	Misalignment	Magnitude, in.
2 slabs each (96 X 36 X 10 in.)	3 (Non-uniform)	3H12NU	Horizontal	+ ½, - ½, + ½
		3V12NU	Vertical	
		3C12NU	Combined	
	5 (Non-uniform)	5H12NU	Horizontal	+ ½,- ½, + ½, - ½, + ½
		5V12NU	Vertical	
		5C12NU	Combined	
	5 (Outer and Center dowel misaligned)	5H14AM	Horizontal	+ ¼, 0, - ¼, 0, + ¼
		5V14AM	Vertical	
		5H12AM	Horizontal	+ ½, 0, - ½, 0, + ½
		5V12AM	Vertical	
		5C12AM	Combined	

Misalignment Type: Three types of misalignment have been focused on – horizontal, vertical, and combined misalignment. Combined misalignment refers to equal magnitude of misalignment in the vertical and horizontal directions. A total of 16 cases of vertical and horizontal misalignment each, and 14 cases of combined misalignment have been tested.

Misalignment Orientation: In cases of multiple bars, the effect of two orientations was studied – uniform and non-uniform misalignment. Uniform misalignment has been termed for cases where the consecutively misaligned dowel bars are parallel to each other in the direction of misalignment. In non-uniform misalignment, the misalignment of consecutive dowels is opposite to each other. Uniform and non-uniform misalignments are illustrated in Figure 3.3. A total of 6 uniform and 20 non-uniform misalignment cases were tested.

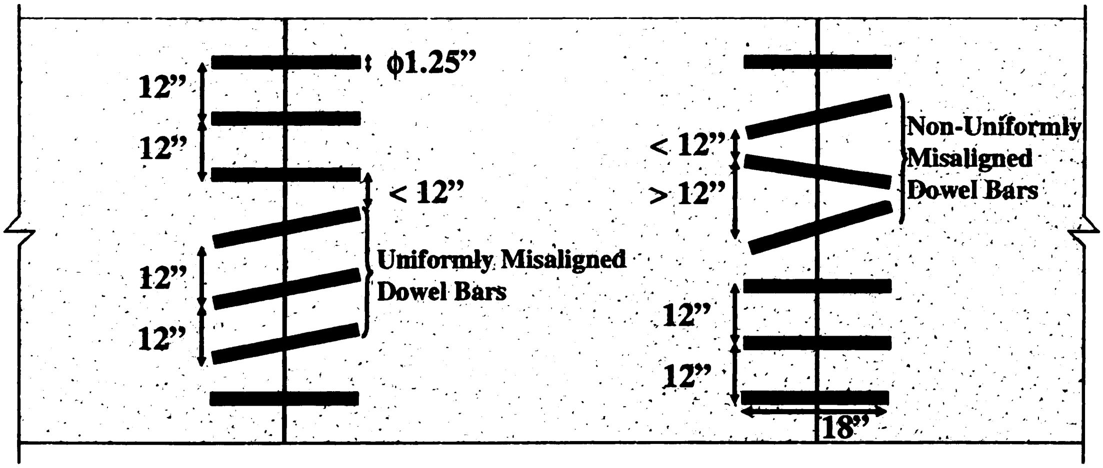

Figure 3.3. Plan view of Uniform and Non-uniform Misalignment

Misalignment Magnitude: Tests with misalignment magnitudes of 0, ¼, ½, ¾, and 1 in. over half-length of the bar (9 in.) have been carried out. The choice of these magnitudes were based on three factors – maximum accuracy, maximum probable limit of misalignment in the field, and limit at which distresses develop. The aligned one and two dowel specimens are treated as the control specimens.

Nomenclature of test ID: Each test is identified with an ID and the nomenclature is based on the various variables discussed above. The first number is the number(s) of dowel bars in the specimen. The second letter is the misalignment type, A for aligned (or straight), H for horizontal, V for vertical, and C for combined. The number(s) following the misalignment type is the misalignment magnitude in inches per half length. An ¼ in. misalignment is denoted as 14, ½ in. as 12, ¾ in. as 34, and 1 as 1 in. If there is more than one dowel bar in the test specimen, then the alphabets following the misalignment magnitude is the relative orientation of the dowels. Non-uniform misalignment is denoted as NU, uniform as U, and alternate bars misaligned as AM. Clockwise (CW) is considered positive and is used to define the orientation of the misalignment. A plan view and section view of a dowel bar with clockwise combined misalignment is shown in Figure 3.4. The transverse joint runs in the North-South direction. Clockwise direction is defined with reference to the East side for horizontal and the North side for vertical misalignment. The north most dowel has a clockwise orientation in all cases and the orientation of the following dowels depends on the orientation type.

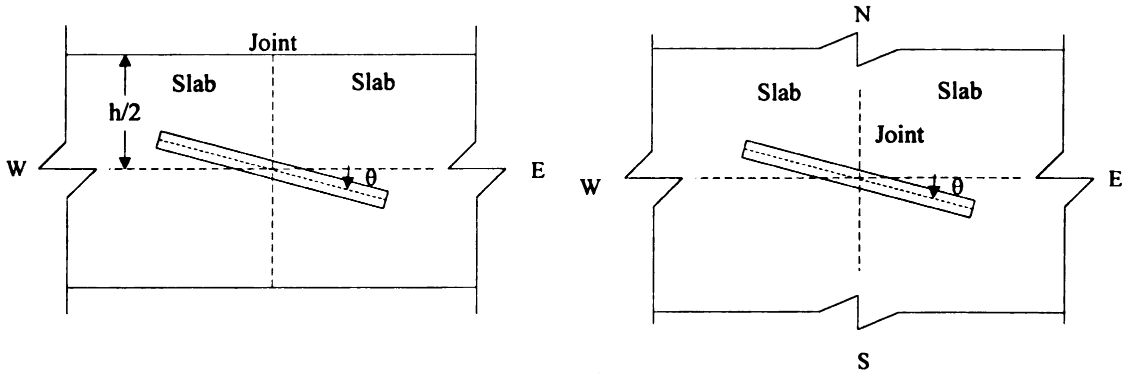

(a) Cross-sectional View (b) Plan View

Figure 3.4. Clockwise orientation of the dowel

3.3 MATERIAL SPECIFICATIONS

The MDOT specifications require the dowel bars to be made of billet steel grade 40 as per AASHTO specification M31, and to have minimum yield strength of 40,000 psi and a minimum ultimate strength of 70,000 psi. The dowel bars are epoxy coated as per AASHTO M254. Most of the steel dowel bars were obtained from the same heat and batch as far as possible. The concrete mixture is the MDOT pavement mix grade P1 the mix design of which is summarized in Table 3.2. The detailed mix design specifications are shown in Table A-1 of Appendix A.

Table 3.2. Mix Design of Concrete

Source of Concrete: Plant 14-East Lansing

Material	Class: Source	SSD Weight (lb/yd^3)	Yield, ft^3
Cement	ASTM C-150 Type I: Essroc	564	2.87
Fine Aggregate	2NS: Builders Aggregates (#34-86)	1275	7.65
Coarse Aggregate	6AA: MLO LS(#71-3)	1720	10.81
Water		256	4.1
Air Content		6.5 %	1.77
		Total	27.2

Admixtures added:

ASTM C-494A Water Reducer Type A	MB 200 N	3.0 oz/c
ASTM C-260 Air Entrainer	MB Microair	1.2 oz/c

Desired Plastic Concrete Properties

Slump	3 in.
Concrete Unit Weight	142 pcf
Air Content	6.5 %

3.3.1 Steel Coupon Testing

Nine test coupons were obtained from 3 dowels bars. The specimen size and testing was in accordance with ASTM E8-99 as shown in Figure 3.5. Figure 3.6 (a-c) illustrate the different stages in coupon testing.

A typical stress-strain curve is shown in Figure 3.7. The properties derived from each of the curves include (i) yield strength, (ii) ultimate strength, and (iii) the elastic modulus of steel. Figure 3.8 (a-c) summarize these properties for all the coupons tested. The horizontal line in each plot indicates the minimum required value of the corresponding parameter as specified by ASTM A615. The averages of the yield strength, ultimate strength, and elastic modulus of steel obtained are 69 ksi, 95 ksi, and 30,270 ksi, respectively.

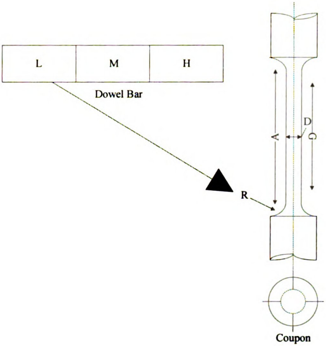

D= nominal diameter = 0.500 in.

A= length of reduced section = 2¼ in.

G = gage length = 2.000 ± 0.005 in.

R = radius of fillet = ⅜ in.

L= left, M=middle, R=right

Figure 3.5 . Standard ½ in. Round Tension Test specimen with 2 in. gage length (ASTM E8-99)

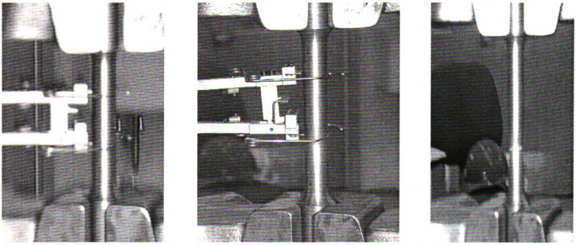

(a) Coupon before testing (b) Coupon at the Initiation of Necking (c) Coupon at Failure

Figure 3.6. Stages of Coupon Testing

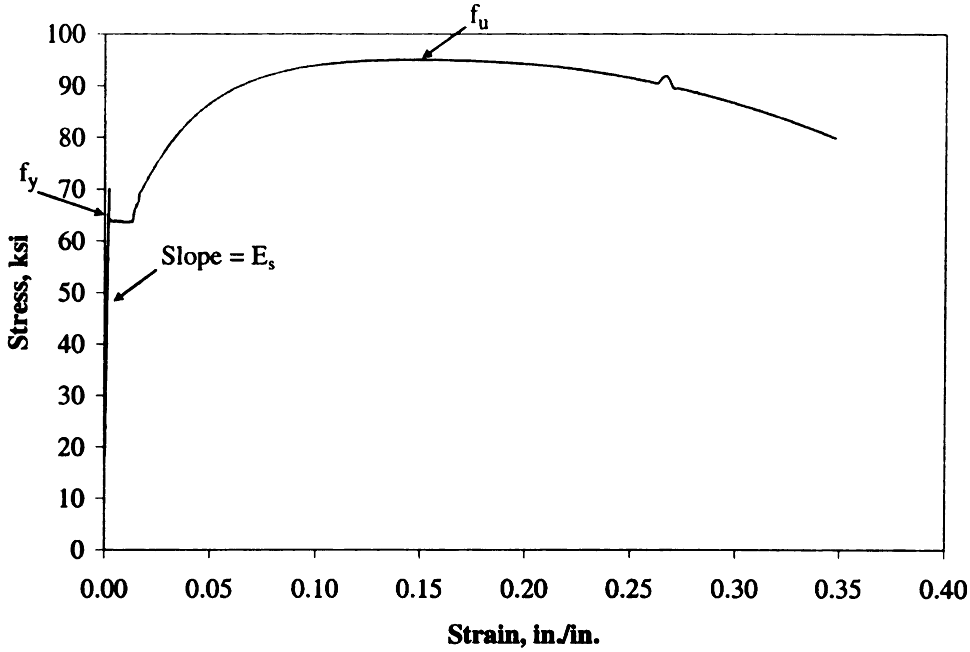

Figure 3.7. Typical Stress-Strain Curve for a coupon

3.3.2 Concrete Testing

The fresh and hardened concrete properties measured and their corresponding ASTM standards are listed in Table 3.3. Concrete cylinders (4 X 8 in.) were cast at the same time as the pavement specimens. The hardened concrete properties were measured at three specimen ages -3-day, 7-day, and 28-day. 3-day and 7-day correspond to the days of demolding and slab testing, respectively.

Table 3.3. Concrete Properties

Type of Test	Property Measured	ASTM Standard
Fresh Concrete	Slump (in.)	ASTM C143
	Unit Weight (pcf)	ASTM C138
	Air Content (%)	ASTM C138
	Temperature (°F)	ASTM C1064
Hardened Concrete	Compressive Strength (psi)	ASTM C39
	Split Tensile Strength (psi)	ASTM C496
	Flexural Strength (psi)	ASTM C78

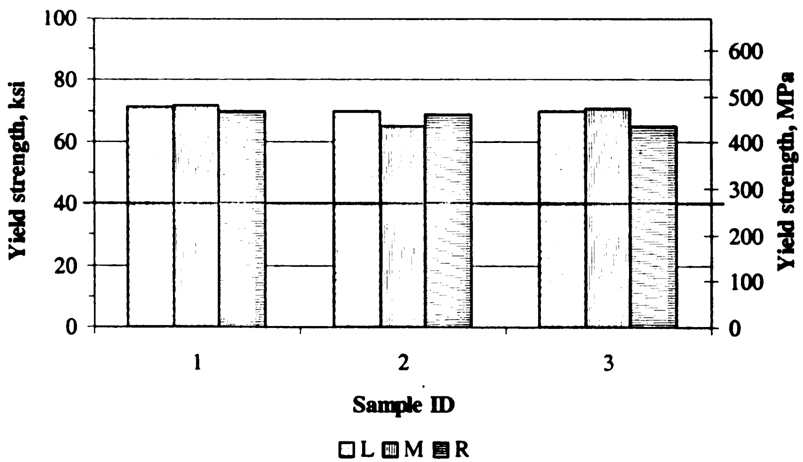

(a) Yield Strength

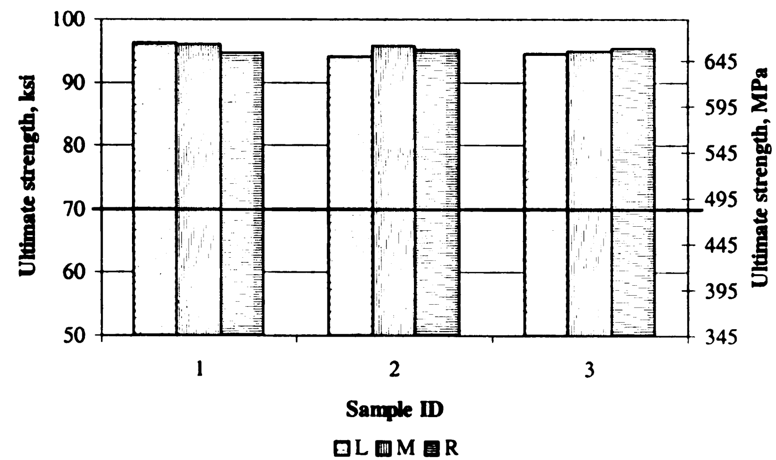

(b) Ultimate Strength

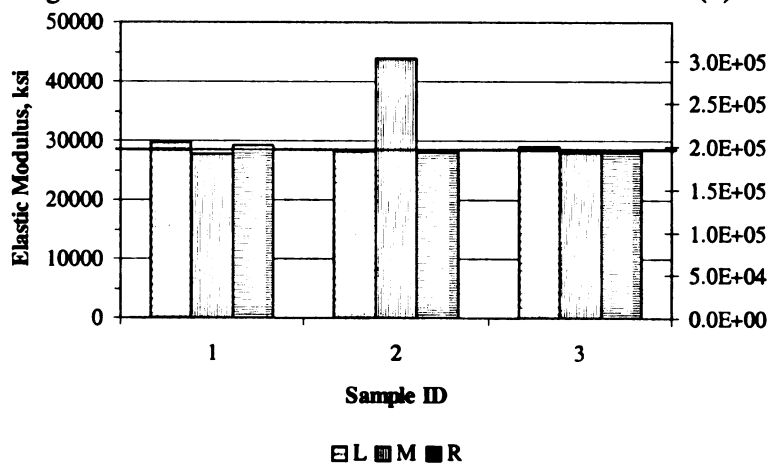

(c) Elastic Modulus

Figure 3.8. Coupon Tests Strength Results

Fresh properties were tested on only one sample per test and the averages over all the batches tested are:

- Temperature: 70.8 °F
- Slump: 3.6 in.
- Unit Weight: 144.5 pcf
- Air Content: 6.1 %

The number of samples used for the hardened concrete tests consisted of 3 cylinders for compression and 2 cylinders for spilt tension on each of the three days of testing. 1, 2, and 3 beams, respectively, were tested on the 3rd, 7th, and 28th day. The averages of all the strengths at 28 days and the sample sizes associated with their calculation are presented in Table 3.4.

Table 3.4. Statistical Parameters for Raw Strengths

Property	Average, psi
Compressive Strength (45)*	4991
Split Tensile Strength (32)*	392
Flexural Strength (39)*	609

*The number in braces is the number of samples tested.

The variation across batches was very high but the variation within a batch was not as high, which is as expected. Also, the compressive strength exhibited less variance than the flexural and split tensile strengths.

3.4 INSTRUMENTATION

This section describes the instrumentation used in the measurement of the slab responses and the calibration of the instruments. Table 3.5 describes the location of the various instruments and the response measured. After vertical uplift was observed in the two dowel non-uniform vertical misalignment cases, sliders were used at the slab corners where vertical uplift was expected, i.e. in vertical and combined misalignment cases.

Figure 3.9 (a-d) show stand alone pictures of the instruments while Figure 3.10 (a-b) show a close up of the same in use.

Figure 3.11 shows a diagrammatic representation of LVDT and slider locations in a 5-dowel test. Figures 3.12 and 3.13 illustrate the instrumentation setup in a two dowel test with expected vertical uplift and a five dowel test.

Table 3.5. Instrumentation Location and Purpose

Instrument	Response Measured	Location
Spring Return Linear Motion Sensor (Slider)	Measure Joint Opening	Placed perpendicular to the joint at dowel bar locations and at 4 or 8 in. from the longitudinal edges depending on the slab size.
Linear Variable Differential Transducer (LVDT)	Measure Joint Opening	Placed perpendicular to the joint at dowel bar locations.
Pressure Transducer	Measure pressure applied to the actuators	Placed in the box cutouts.

(a) Linear Variable Differential Transducer

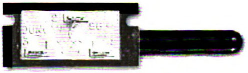
(b) 9610 Linear Motion Position Sensor (1.0 in. stroke)


(c) PX303-015G5V Pressure Transducer

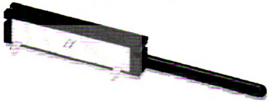
(d) 9615 Linear Motion Position Sensor (1.5 in. stroke)

Figure 3.9. Closeup of Instruments*

*Source: www.omega.com (a,c), www.beiduncan.com (b,d)

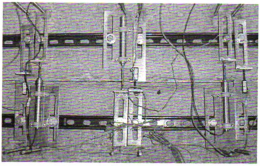

(a) LVDTs and Sliders

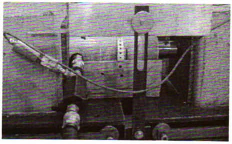

(b) Pressure Transducer and Hydraulic Jack

Figure 3.10. Instruments

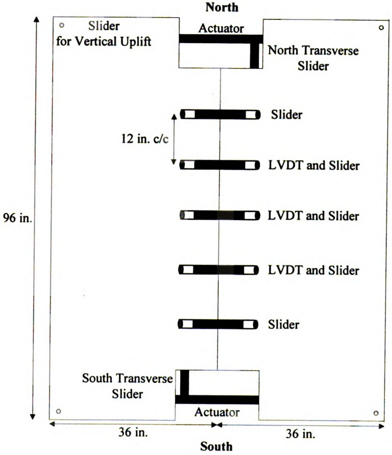

Figure 3.11 . Plan of Instrumentation Setup for 5-dowel test

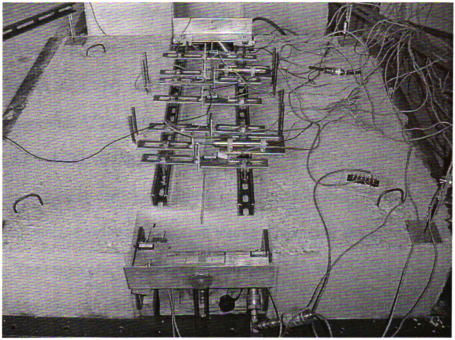

Figure 3.12. Instrumentation Setup for Typical 2-dowel setup with Instrumentation for Vertical Response

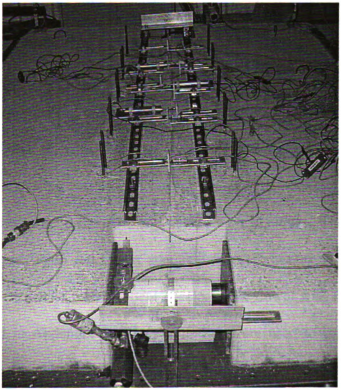

Figure 3.13. 5-dowel Instrumentation Setup

The pullout load for the experiments was provided by the hydraulic actuators and hand-pumps. Each hand pump can be connected to either a RC 156 or a RC 256 actuator. The specifications for the LVDT and the pressure transducer are summarized in Tables A-2 and A-3 of Appendix A. The calibration of the instruments is described in Appendix A.

3.5 TYPICAL CASTING-TESTING CYCLE

The steps in a typical casting-testing cycle are mold assembly, rough misalignment, misalignment check, casting and material testing, demolding and instrumentation setup, and testing. The length of a typical casting-testing cycle is 14 days (2 weeks).

Rough Misalignment: After the mold has been assembled, the dowels are placed in the U-hook hanging assembly and are misaligned as per the desired combination. As per MDOT construction specifications R-40-E, the spacing of the dowels is 12 in. c/c for no misalignment and the dowels are suspended at mid-depth of the slab i.e. 5 in. for a 10 in. slab. After rough misalignment using a tape measure, each dowel is welded on one side and greased on the other half as per R-40-E. Alternate dowel bars are welded on the same side. The greasing is, however, done just before casting.

Surveying: The dowel misalignments are adjusted and measured accurately (before placing the concrete), using two total electronic stations (theodolites), a reference point (base plate), trigonometric principles, and surveying techniques. The accuracy of the measurement system (0.005 rad.), was adequate for determining dowel misalignment angles with confidence. The misalignment checks in the dowel with respect to the base plate are described in Appendix B. The theodolites were used to measure the various angles between the dowel bar, base plate, and the horizontal and vertical planes. For each of the misalignments in the test setups shown in Table 3.1, the calculation of misalignment using the theodolite was compared to misalignment obtained using the tape measure. The maximum error tolerated is ± ⅛ in.

A typical surveying setup is shown in Figure 3.14. Details on the calculations for typical cases of surveying for horizontal and vertical misalignment are given in Appendix B. Tables B-1 through B-8 provide a summary of the surveying of the various cases. Tables B-1 through B-4 summarize the comparison of height checks and tables B-5 through B-8 summarize the horizontal misalignment checks.

The average error was found to be 0.093 in. and 0.028 in. in vertical and horizontal measurement, respectively.

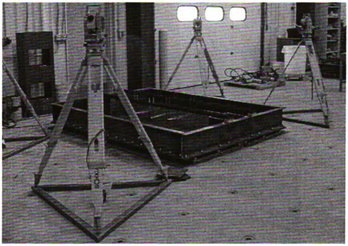

Figure 3.14. Typical Misalignment Check Setup (Surveying)

Casting: The concrete slabs are cast in-place directly in the molds placed and are ready to test 7-days after the concrete sets. The aluminum separator plate is left in place after casting the concrete, and it does not hinder the experiment or the separation of the slabs in any way. The test specimens along with beams and cylinders for quality control are cast using the MDOT approved paving mix delivered by ready mix concrete suppliers.

Figure 3.15 shows casting of a 5-dowel test setup. Figure 3.16 shows the fresh concrete properties apparatus and molds for hardened concrete properties specimens. Before casting the main specimens, quality control tests are performed on a sample of concrete to ensure it meets the specifications for slump and air content, else the concrete is rejected. Figure 3.17 (a-c) show typical hardened concrete properties test setups.

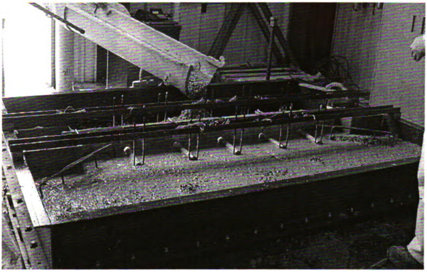

Figure 3.15. Casting

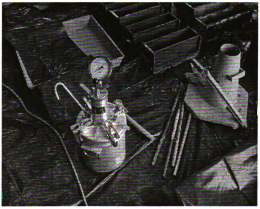

Figure 3.16. Fresh and Hardened Concrete Test Apparatus

Demolding and Instrumentation Setup: A typical specimen containing one dowel is shown in Figure 3.18. The test specimens are demolded typically three days after casting, after it had been ensured that the concrete had achieved at least 50 % of the target 28-day compressive strength (3500 psi). The instrumentation is setup as described in section 3.4.

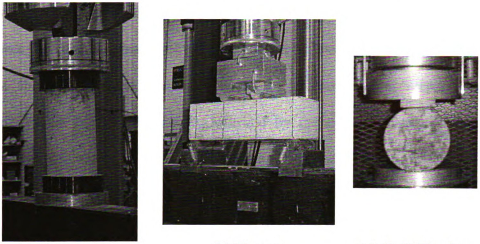

(a) Compression (b) Flexure (c) Split Tension

Figure 3.17. Concrete Hardened Properties Test Setup

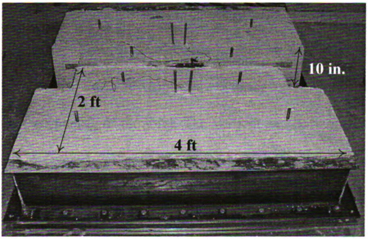

Figure 3.18. Cast Specimen

Testing: Pullout tests on the slabs under thermal expansion are conducted 7 days after casting. The protocol maintained during the entire testing regime was to continuously measure the induced load in the dowel bar due to joint opening of up to 1 in. The total load measured as the joint opened was divided by the number of dowels in the test specimen.

The specimens are tested by pushing apart the concrete slabs using hydraulic actuators, which are of 15-kip capacity for the small slabs and of 25-kip capacity for the big slabs, each having a stroke of 6 in. The actuators were used to apply controlled monotonic longitudinal loading. The hydraulic pressures in the actuators were synchronized using split flow and needle valves. The concrete slabs were pushed apart very slowly at the approximate load rate of 20 lbs/min. followed by the opening displacement rate of approximately 0.02 in./min.

Pressure transducers were used to measure the hydraulic pressures in the actuators. The loads applied by the actuators were estimated using the measured hydraulic pressures and the calibrated actuator piston areas. This procedure for determining the applied loads using the measured hydraulic pressures was calibrated and validated prior to testing. Several instruments including spring-return linear motion sensors (sliders) and linear variable displacement transducers (LVDTs) were used to measure the transverse opening of the joint. The vertical and horizontal displacements of the slabs were also measured using sliders and LVDTs. The sliders had measurement ranges of either 0-1 in. or 0-1.5 in. with accuracies of 0.02 in. and 0.03 in., respectively and the LVDT had a measurement range of 0-1.5 in. with accuracy of 4.5×10^{-3} in. All the instruments were calibrated prior to conducting the experimental investigations, details of which are provided in Appendix A.

The data from the different instrumentation was collected at the rate of 6 scans per second, using a data acquisition system, the details of which is given in Appendix A. The data acquisition system is capable of handling all the different instruments – sliders, LVDTs, and pressure transducers. The software interface used to collect and process data is Little General Version 6.1. The calibration files, obtained as described in earlier sections are input into the software and, the data is acquired in the desired units of measurement. As mentioned earlier, quality control tests on concrete were conducted in parallel on the 7th day also.

3.6 COMPARISON OF THE EXPERIMENTAL SETUP AND PLAN WITH PREVIOUS STUDIES

In this section, the different features of the experimental setup and plan, described in the previous sections of this chapter, are compared with that of the previous experimental studies. Different features of the experimental setup were based on lessons learnt from previous experimental studies described in the literature review (chapter 2).

Experimental Setup: Specimen configuration is similar to the dog-bone shaped specimens used by Segner and Cobb (1967) to facilitate the placement of the hydraulic jacks during the pullout test. The plain transverse joint between the concrete slabs was formed using a ⅛ in. thick aluminum plate with circular holes of appropriate diameter to pass the dowel bars. This concept was derived from Tayabji (1987). In the present research, each concrete slab is supported on smoothened rollers placed on hardened steel plates. Smoothness was to ensure that when the pullout load is applied using the actuators, the base rails, solid rollers, and base plate move with minimal frictional resistance relative to each other and the pullout load acts perpendicular to the joint face. The method for misalignment check is unclear in the literature available. In the present research, surveying principles were applied using total electronic stations that had an accuracy of 0.005 radians and the maximum error tolerated in this study was ± ⅛ in. Dowel hanging assembly consisting of ⅜ in. finely threaded mild steel U-hooks that are bolted to supporting channels were used to support the dowel bar, on the lines of the assembly used by Segner and Cobb (1967). This specially designed assembly allowed fine adjustments to the dowel position in the vertical and horizontal directions. Corner reinforcements near the box cutouts were used to prevent excessive build up of stresses at the box cutouts corners. Segner and Cobb (1967) had used shoulder reinforcement near the axes of application of the load.

Experimental Plan: One of the main limitations of previous pullout studies includes the low rate of data collection accompanied by a high rate of loading. The limitations of the previous laboratory studies have been addressed in the following manner:

- Bond stress behavior has been studied.
- In this research study, the data was collected at the rate of 6 data points per second and the displacement rate of approximately 0.02 in./min, which is approximately 1600 data points collected for each 0.1 in. joint opening increment. This rate of data collection helps in the understanding of the dowel-concrete bond behavior, especially at smaller joint openings where debonding takes place and the slope of the load vs joint opening curve is very high.
- Study of the relative effect of the misalignment orientation on load vs joint opening behavior has been conducted.
- Tests on specimens accommodating up to five dowels have been carried out which is close to simulating half a lane.

CHAPTER 4 DISCUSSION OF RESULTS

This chapter deals with the discussion of the results obtained from the various pullout experiments conducted. The discussion presented includes typical bond stress versus joint opening behavior (hypothesized and observed), overview of the results that includes distress observations, and the load vs joint behavior results for the different tests and load zone prediction given misalignment magnitude and number of dowels.

4.1 TYPICAL BOND STRESS VERSUS JOINT OPENING BEHAVIOR

As mentioned earlier in chapter 3, the load induced per dowel bar is calculated by multiplying the pressure by the corresponding calibrated piston area and dividing by the total number of dowel bars. The bond stress τ, is then calculated by dividing the load by the circumferential area of the greased side of the dowel bar (π*1.25*9). It is hypothesized that the bond stress versus joint opening curve has two distinct regions: (a) fully bonded region (OA) and (b) post-slip/debonded region (BC) as shown in Figure 4.1.

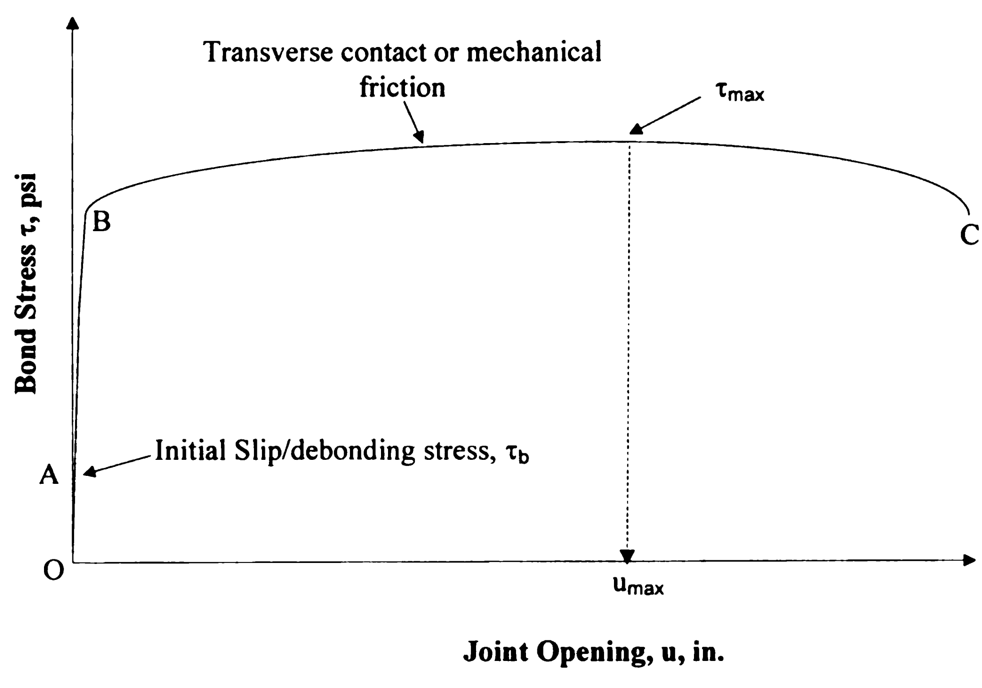

Figure 4.1. Typical Bond Stress versus Joint Opening curve

The first region is the high initial slope region where there is bond between the dowel bar and concrete. The applied pullout force which can be resolved in the axial and normal directions of the dowel bar is opposed only by the dowel-concrete bond force in this region as illustrated in Figure 4.2 (a). Slip occurs after the bond stress per dowel increases beyond a certain threshold value. The magnitude of the bond stress at the point of debonding or initial slip is denoted as the initial slip/debonding stress (τ_b), and is calculated using equation 4.1:

$$\tau_b = \frac{F_b}{\pi DL} \qquad ..(4.1)$$

where F_b is the force at initial slip/debonding in lbs, D is the dowel bar diameter in inches and L is the embedment length of the dowel bar (9 in.). Section 914.07 of MDOT (2003) requires this stress not to exceed 60 psi. PENNDOT requires the force at initial slip to be in the range of 2,200-4,400 lbs, depending on the pavement width (based on survey conducted in August 2004).

As further thermal expansion is induced, the forces induced in the dowel bar increase and depending on the misalignment, the induced force could form a plateau or increase causing failure of the test specimen. It should be noted that only the forces induced due to joint opening were measured in the lab and not the stress states at the interface of the dowel and concrete. Each of the misalignment type, magnitude, and orientation would cause a specific certain stress state zone at the interface along the length of the bar and at the joint, which cannot be studied directly through lab observations/tests. Due to the presence of misalignment and joint opening, normal bearing stress in concrete is introduced and due to the frictional effect across the interface, shear stresses are developed as shown in Figure 4.2 (b).The effects of these parameters on the post-slip joint opening behavior are presented later in the chapter.

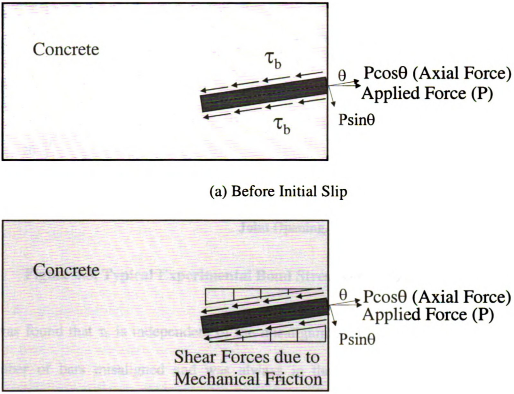

(a) Before Initial Slip

(b) Post-slip

Figure 4.2. Forces on a Misaligned dowel

After the experimental plan was completed it was found that for any specimen tested, the bond stress vs joint opening behavior always showed an initial bond behavior between the dowel and concrete at less than 0.01 in. joint opening. The experimental curves closely followed the regions or shape of the curve proposed in Figure 4.1. A typical experimental curve obtained is shown in Figure 4.3 .

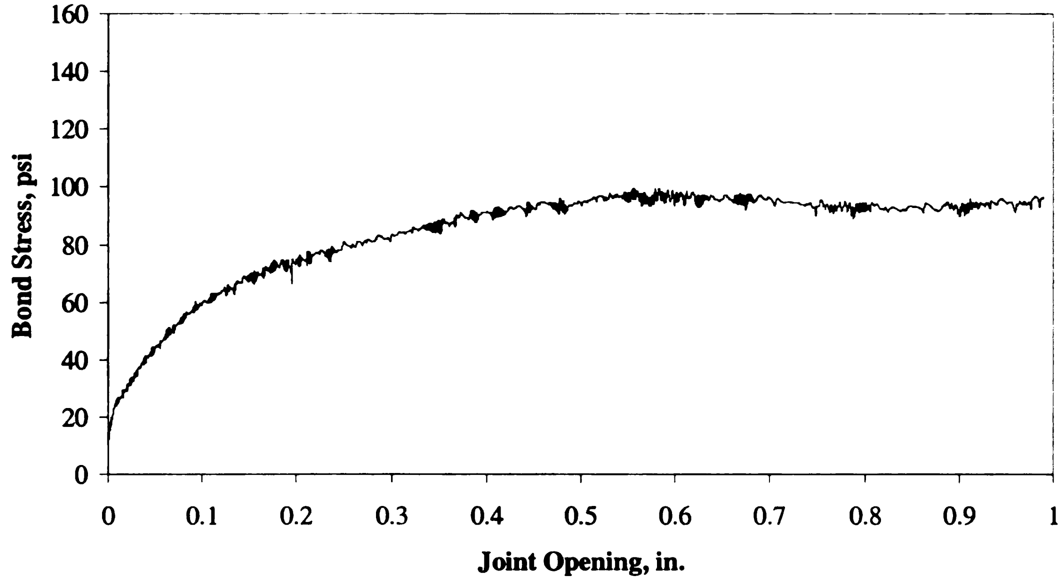

Figure 4.3. Typical Experimental Bond Stress versus Opening Behavior

It was found that τ_b is independent of the misalignment magnitude, orientation, and the number of bars misaligned and was always in the range of 10-50 psi. Figure C-1 illustrates the τ_b for all the gamut of tests conducted. The bond stress vs joint opening graphs substantiating these results are presented in Appendix C.

The slip strain can be estimated as the joint opening divided by the embedded length (9 in.) of the greased side of the dowel. The bond shear stress-slip strain responses for the 1-bar straight specimens (with zero misalignment) provide information regarding the overall longitudinal bond interaction between straight (aligned) dowels and the surrounding concrete and are critical in the analytical modeling of the dowel-concrete behavior. The bond shear stress-slip strain responses for the remaining 1-bar specimens provide information regarding the longitudinal bond between the misaligned dowel and the surrounding concrete, while including the effects of friction and bearing stresses (from dowel misalignment).

4.2 OVERVIEW OF THE RESULTS

The discussion focuses on two main aspects:

- Overview of the type of joint and slab distresses observed; and
- Effect of misalignment type and magnitude on load vs joint opening behavior (post-slip behavior)

The results are grouped as per the misalignment types– horizontal, vertical, and combined misalignment. Overall, the following distresses were observed during the tests:

- Bearing failure/Spalling of concrete near the dowel-concrete interface
- Cracking
- Non-uniform joint opening
- Vertical uplift

The first three distresses are destructive even without traffic and/or restraints from the adjacent slabs and base while non-uniform joint opening and vertical uplift in the current setup of just thermal expansion are not destructive. The significance of the different distresses is described in section 4.5.

During the pullout test, the slab that opens or pulls out is the slab that contains the greased side of the dowel. Because of the restraint due to welding on the other side it is the greased side that slips out after debonding during the pullout test. Hence in all cases where spalling was observed, spalling was found to occur at the dowel-concrete interface at the joint face near the greased end of the dowel.

4.2.1 Horizontal Misalignment Tests

This section discusses the key visual observations in the horizontal misalignment tests. In the single dowel tests, spalling at the dowel-concrete interface was observed in the 2 in.

test only. In the 2, 3, and 5-dowel tests, different combinations resulted in different distresses: spalling at the dowel-concrete interface, non-uniform joint opening, and cracking. Spalling was the predominant distress in these tests. The spalls ranged from 2 in. by 2 in. to more than half-depth of the slab. Table 4.1 summarizes the visual observations for the different horizontal misalignment tests.

Typical illustrations of spalling and non-uniform joint opening observed in the 2H1U test are shown in figures 4.4 and 4.5, respectively. Illustrations of other horizontal misalignment tests where spalling and non-uniform joint opening occurred are shown in figures D-1 (a-d) and figure D-2 of Appendix D.

Table 4.1. Summary of Visual Observations in the Horizontal Misalignment tests*

Specimen ID	Visual Observations
1A, 1H14, 1H12, 1H34, 1H1	None
1H2	Spalling on the West joint face (3 in. X 3¼ in.)
2A, 2H14U, 2H12U, 2H34U	None
2H1U	• Spalling on the East joint face (3.5 in. 7 in.) • Non-uniform joint opening (At the end of test, south edge at about ¼ in. higher opening than north edge)
2H14NU	Spalling
2H12NU	Spalling on the East joint face (2 in. X 2 in.)
2H34NU	• Spalling on the west joint face • Cracking at 0.72 in. joint opening
2H1NU	• Spalling on the west joint face • Cracking at 0.67 in. joint opening
2H12AM, 2H34AM	None
3H12NU	Spalling
5H12NU	• Spalling near the outer and center dowels • Non-uniform joint opening (At the end of test, north edge at about ¼ in. higher opening than south edge)
5H12AM	Spalling near the outer and center dowels
5H14AM	None

*Spalling dimensions should be viewed in conjunction with the corresponding photograph

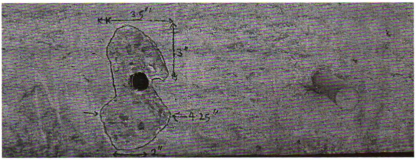

Figure 4.4. Spalling in the 2H1U test

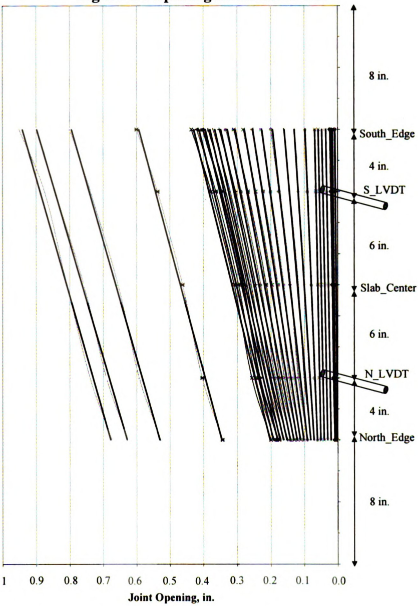

Figure 4.5. Joint opening as a function of distance along the joint (2H1U)

Cracking of slabs in later stages of the tests (at joint openings higher than ½ in.) were observed in the 2H34NU and 2H1NU tests are described below.

Cracking in the 2H34NU test: At a joint opening of 0.716 in., cracking occurred in the west slab, which resulted in a sudden drop of load from 4198 to 515 lbs, resulting in a joint movement of 0.065 in. in about ½ a second. One full depth crack appeared instantaneously and it split the west slab into two halves at the position of the dowel bar on the north side. The dimensions and position of the crack are shown in Figure 4.6 (a). The crack at its point of initiation and at the end of the test is shown in Figure 4.6 (b) and (c), respectively. The sudden drop in pressure is captured in the load versus joint opening curve shown in Figure 4.7. As further load was applied, the crack continued to open, pushing the two halves of the slab apart rather than opening the joint. Thus the test was stopped at a joint opening of 0.87 in.

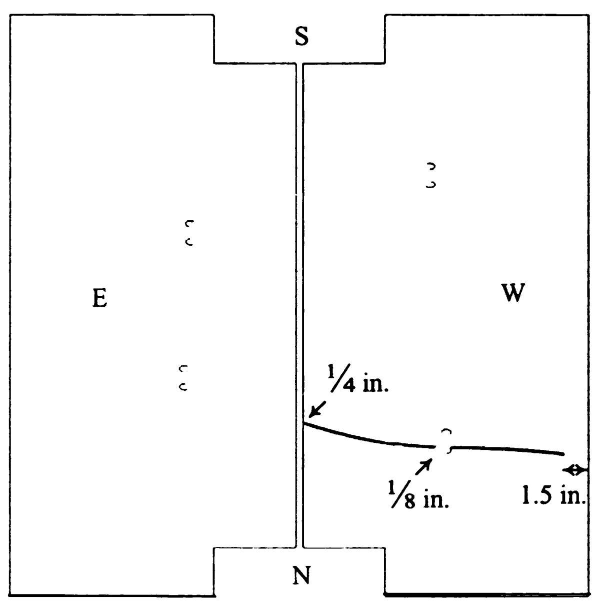

(a) Crack Pattern and Initial dimensions

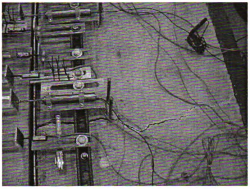

(b) Crack initiation

(c) Crack at end of test

Figure 4.6. Cracking in 2H34NU

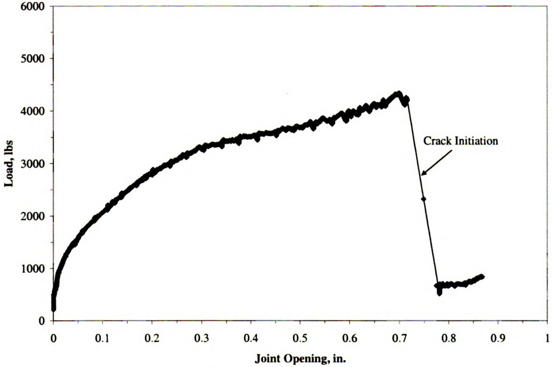

Figure 4.7. Load vs joint opening curve (2H34NU)

Cracking in the 2H1NU test: At a joint opening of 0.668 in., cracking occurred in the west slab, which resulted in a sudden drop in load from 4891 to 1476 lbs. One full depth crack appeared instantaneously and it split the west slab into two parts at the position of the dowel bar on the north side. The dimensions and position of the crack are shown in

Figure 4.8. Since the pattern is to the similar to the 2H34NU test, the photographs have not been provided here.

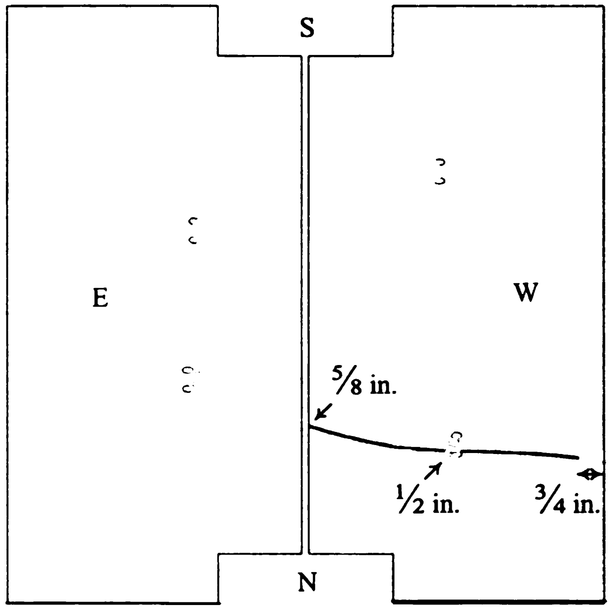

Figure 4.8. Crack pattern and Initial dimensions in 2H1NU

The sudden drop in pressure is captured in the load versus joint opening curve as seen in Figure 4.9. As further load was applied, the crack continued to open, pushing the concrete pieces apart rather than opening the joint. Thus the test was stopped at a joint opening of 0.857 in. and the crack width at the joint at the end of the test was ¾ in.

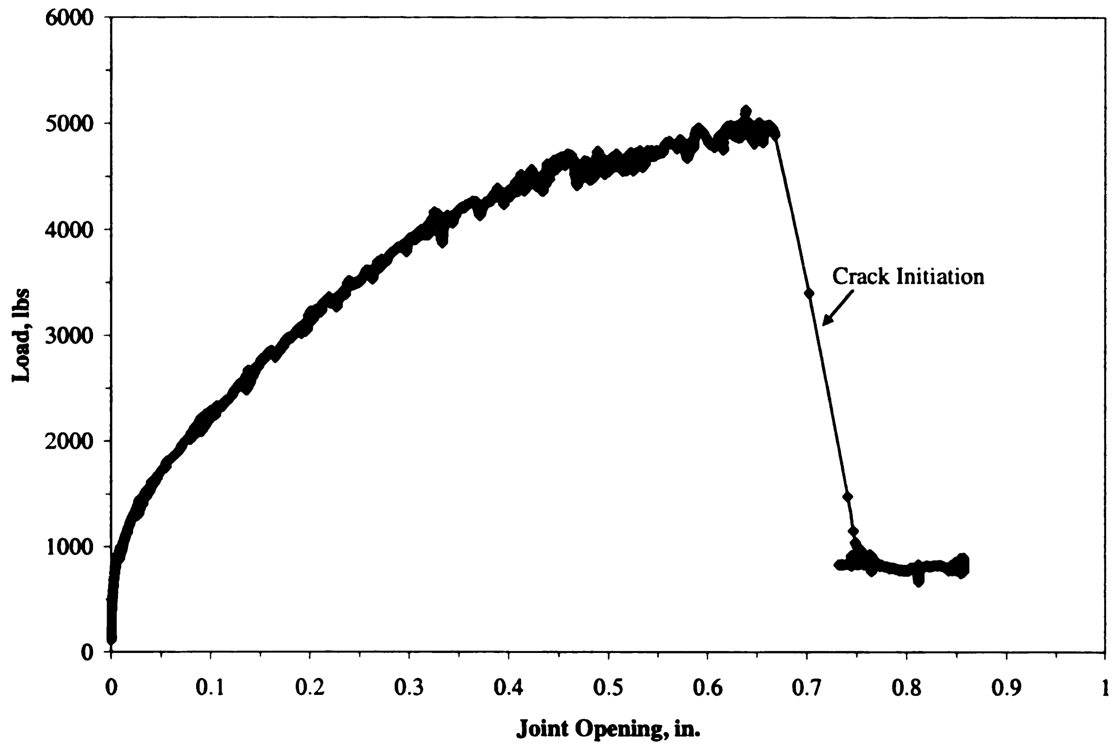

Figure 4.9. Load vs joint opening (2H1NU)

4.2.2 Vertical Misalignment Tests

This section discusses the key visual observations in the vertical misalignment tests. In the 1-dowel tests, there were no distresses observed. In the 2, 3, and 5-dowel tests, different combinations resulted in different distresses: spalling at the dowel-concrete interface, non-uniform joint opening, vertical uplift, and cracking. Table 4.2 summarizes the visual observations for the different vertical misalignment tests.

Illustrations of spalling and non-uniform joint opening in the vertical misalignment tests are shown in figures D-3 (a-d) and figure D-4 of Appendix D. In the 2V1NU test, in addition to surface spalling and non-uniform joint opening, the northwest and southeast ends of the slabs lifted up (the welded sides of the two dowel bars). Figure 4.10 (a) gives a diagrammatic representation of the uplift and Figure 4.10 (b) and (c) show the vertical uplift at the NW and SE faces, respectively. The vertical uplift of the slabs in the 2V12NU and 2V34NU tests is similar to that observed in the 2V1NU test and have not been shown. The magnitude of the uplift was not recorded.

Table 4.2. Summary of Visual Observations in the Vertical Misalignment tests*

Specimen ID	Visual Observations
1A, 1V14, 1V12, 1V34, 1V1, 1V2	None
2A, 2V14U, 2V12U, 2V34U	None
2V1U	• Spalling on the West joint face (4.5 in. X 2¾ in.) • Spalling on the East joint face (2 in. X 1¾ in.)
2V14NU	None
2V12NU, 2V34NU	Spalling and vertical uplift
2V1NU	• Spalling on the West joint face (5 in. X 3¼ in.) • Spalling on the East joint face (3⅝ in. X 2⅝ in.) • Non-uniform joint opening (At the end of test, south edge was at about 0.13 in. higher opening than north edge) • Vertical uplift
2V12AM, 2V34AM	None
3V12NU	Spalling
5V12NU	• Spalling near the outer and center dowels • Cracking at a joint opening of 0.862 in. • Non-uniform joint opening (At the end of test, north edge at about ¼ in. higher opening than south edge)
5V14AM	None
5V12AM	Spalling near the outer and center dowels

*Spalling dimensions should be viewed in conjunction with the corresponding photograph

Cracking of the slab in later stages of the test (at joint openings higher than ½ in.) was observed in the 5V12NU test. At a joint opening of 0.862 in., the pressure started dropping drastically Figure 4.11 and after about 2.5 seconds, a hairline crack was observed in the east slab, near the center dowel bar, diagrammatically shown in Figure 4.11. This crack resulted in a drop of load from 3902 to 2832 lbs, in one second. The sudden drop in pressure is captured in the load versus joint opening curve shown in Figure 4.12. As further load was applied, the crack continued to open, pushing the two halves of the slab apart rather than opening the joint. Thus the test was stopped at a joint opening of 0.93 in.

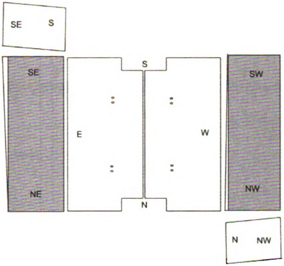

(a) Diagrammatic representation

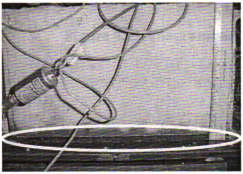

(b) NW side

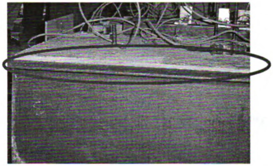

(c) SE side

Figure 4.10. Vertical Uplift (2V1NU)

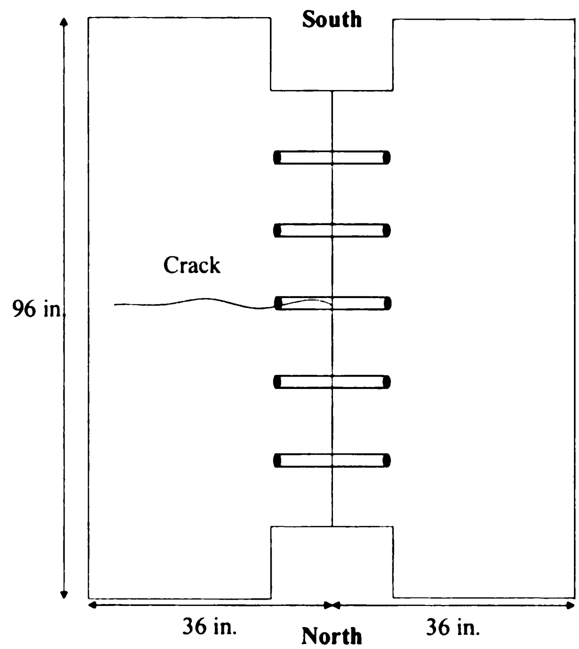

Figure 4.11. Diagrammatic representation of Crack in 5V12NU

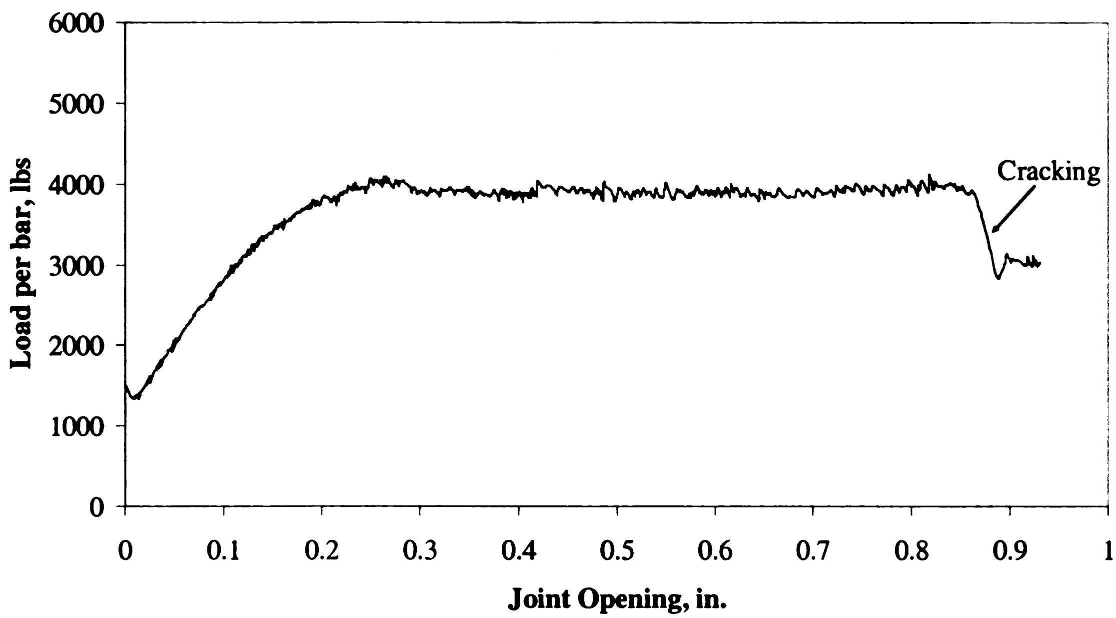

Figure 4.12. Load vs joint opening curve (5V12NU)

4.2.3 Combined Misalignment Tests

This section discusses the key visual observations in the combined misalignment tests. In the 1-dowel tests, the only distress observed was spalling at the dowel-concrete interface in the 1 in. test. In the 2, 3, and 5-dowel tests, different combinations resulted in different distresses: spalling at the dowel-concrete interface, non-uniform joint opening, and cracking. Spalling was the predominant distress in these tests. The spalls ranged from 2 in. by 2 in. to more than half-depth of the slab. Table 4.3 summarizes the visual observations for the different combined misalignment tests. Illustrations of spalling and non-uniform joint opening in the combined misalignment tests are shown in figures D-5 (a-f) and figure D-6 of Appendix D.

Table 4.3. Summary of Visual Observations in the Combined Misalignment tests*

Specimen ID	Visual Observations
1A, 1C14, 1C12, 1C34	None
1C1	Spalling on the West joint face (2¼ in. X 1¾ in.)
2A, 2C14U, 2C12U, 2C34U	None
2C1U	• Spalling on the East joint face (3 in. X 2¼ in.) • Spalling on the West joint face (2¼ in. X 3⅞ in.) • Non-uniform joint opening (At the end of test, south edge was at about ¼ in. higher opening than north edge)
2C14NU	Spalling
2C12NU	Spalling on the East joint face (5 in. X 4 in.)
2C34NU	• Spalling on the west joint face • Cracking at 0.95 in. joint opening
2C1NU	• Spalling on the east joint face (3.67 in. X 2¼ in.) • Cracking at 0.45 in. joint opening
2C12AM, 2C34AM	None
3C12NU	Spalling
5C12NU	• Spalling near the outer and center dowels at 0.58 in. • Cracking at 0.824 in. joint opening
5C12AM	Spalling near the outer and center dowels
5C14AM	None

*Spalling dimensions should be viewed in conjunction with the corresponding photograph

Cracking of slabs observed in the 2C34NU and 2C1NU tests are described below.

Cracking in the 2C34NU test: At a joint opening of 0.949 in., cracking occurred in the west slab, which resulted in a sudden drop of load from 4060 to 1124 lbs, resulting in a joint movement of 0.032 in. in about ⅓rd a second. Two cracks formed on the concrete above the north dowel bar, the positions of which are diagrammatically shown in Figure 4.13 (a). One of the cracks was a full-depth crack appeared instantaneously and split the west slab into two halves at the position of the dowel bar on the north side. The cracks at their point of initiation are shown in Figure 4.13 (b). The sudden drop in pressure is captured in the load versus joint opening curve shown in Figure 4.14.

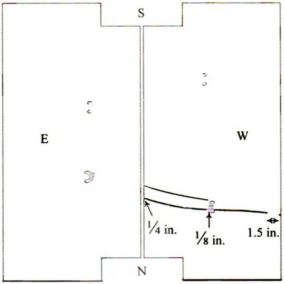

(a) Crack Pattern and Initial dimensions

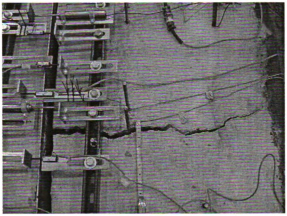

(b) Crack initiation on top of the north dowel

Figure 4.13. Cracking in 2C34NU

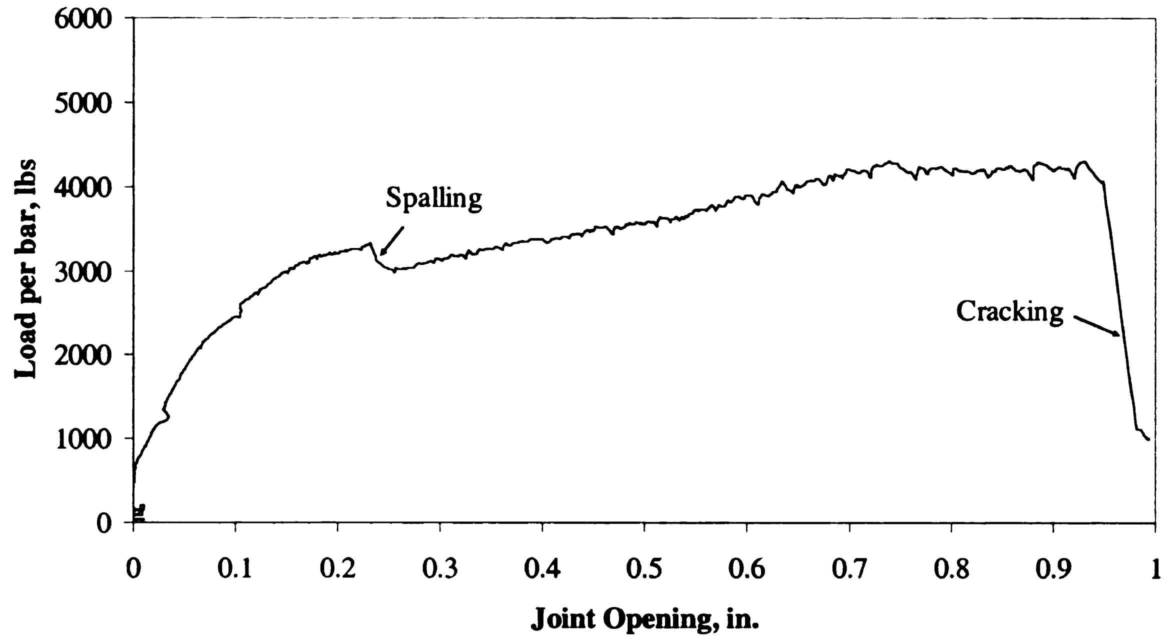

Figure 4.14. Load vs joint opening curve (2C34NU)

Cracking in the 2C1NU test: At a joint opening of 0.447 in., two closely spaced cracks formed in the west slab near the south box cutout, which resulted in a sudden drop of load from 5550 to 4691 lbs. On further separation of the slabs, it was seen that the crack observed at the surface was a result of the crack that was initiated near the south dowel bar. At the surface, the cracks did not open significantly, but at the west joint face, the crack propagated from one dowel bar to the other. No further cracks were formed. The position of the cracks is shown in Figure 4.15 (a). The slabs were pushed further apart after the test and the southwest box cutout corner separated eventually (Figure 4.15 (c)). The sudden drop in pressure is captured in the load versus joint opening curve shown in Figure 4.16.

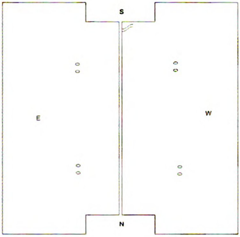

(a) Crack pattern

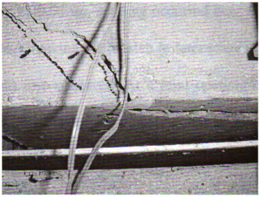

(b) Cracks at end of test

(c) Stages of separation of the slabs

Figure 4.15. Cracking in 2C1NU

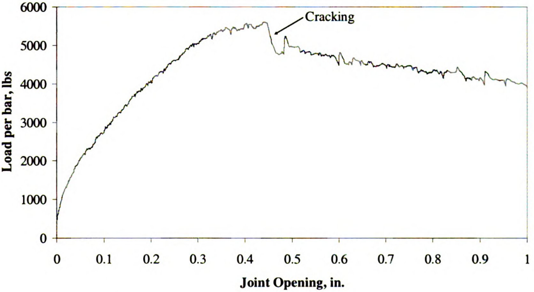

Figure 4.16. Load vs joint opening curve (2C1NU)

Cracking in the 5C12NU test: At a joint opening of 0.58 in., spalling occurred near the outer dowels which resulted in a drop in pressure. Cracking of the slab in later stages of the test (at joint openings higher than ½ in.) was also observed. At a joint opening of 0.824 in., a hairline crack occurred in the east slab, near the center dowel bar, the location similar to the location in the 5V12NU test. This crack resulted in a drop in load from 4108 to 1568 lbs, resulting in a joint movement of 0.046 in. in about ⅔rd a second. The sudden drop in pressure is captured in the load versus joint opening curve shown in Figure 4.17.

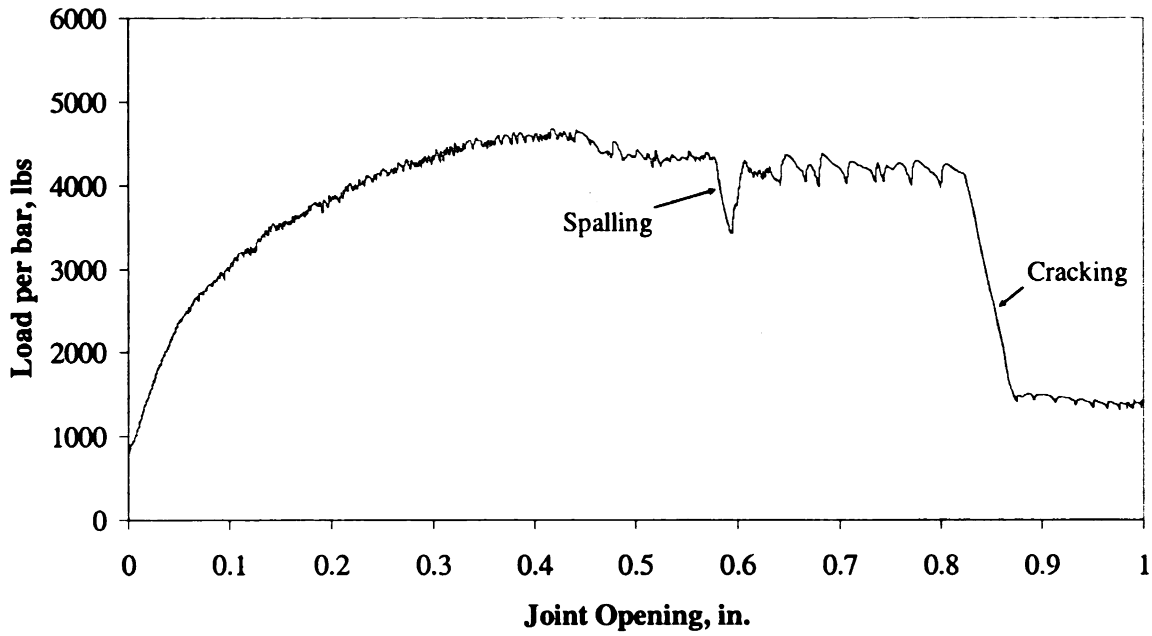

Figure 4.17. Load vs joint opening curve (5C12NU)

4.3 COMPARISONS OF LOAD VS JOINT BEHAVIOR

The key conclusions that are also substantiated by the plots in this section can be summarized as below:

- Within a misalignment type, the load increases with an increase in the misalignment magnitude.

- Non-uniform orientation of misalignment of two dowel bars requires more load per dowel bar at a given joint opening as compared to the uniform orientation of dowels in the horizontal and combined misalignment types and it is vice versa for vertical misalignment.
- Degree of locking is higher in the non-uniform orientation of dowel bars. Non-uniform orientation of misalignment of dowels is more destructive.
- For a given misalignment magnitude, the load required per bar increases as the number of dowels misaligned increases.
- For a given misalignment magnitude, the trend of load versus misalignment type (horizontal, vertical and combined) is inconclusive. However, some trends were observed within specific tests and are listed later.

The discussion is divided into two main subsections (x = H, V, or C):

- Comparisons within same number of dowels tests (within 1x, 2xU, and 2xNU series)
- Comparisons across different number of dowels tests (2xAM vs 2xNU/U and 5xAM vs 5xNU;1x vs 2xNU/U and 3xNU vs 5xNU)

4.3.1 One and Two Dowel tests

The plots in this section (figures 4.18 through 4.38) collectively illustrate the comparisons of load versus joint opening behavior for different misalignment magnitudes within a given misalignment type (horizontal, vertical, or combined). In general, the load per dowel increases with an increase in the misalignment magnitude. This trend is more evident in the 2-dowel tests (non-uniform and uniform orientations). However, there are some exceptions due to experimental variability. Since there are overlaps in the curves corresponding to different misalignment magnitudes at smaller joint openings, bar graphs of loads at ¼ and ½ in. joint openings have been plotted for better representation in the area of interest (joint opening up to ½ in.).

4.3.1.1 Horizontal Misalignment

Figures 4.18, 4.19, 4.20, and 4.21 illustrate the comparisons of load vs joint behavior in the 1-dowel, 2-dowel (non-uniform and uniform orientations), and 2-dowel setup with one dowel misaligned tests, respectively.

Table 4.4 summarizes the comparisons of loads at a ¼ in. joint opening derived from the bar graphs (Figures 4.23 and 4.24). Similar trends hold good for the loads at a ½ in. joint opening. The last column indicates either a percent increase or decrease of load at a ¼ in. joint opening as we move from test 1 to test 2. '+' indicates an increase in the load and '–' indicates a decrease in the load. For example, when the horizontal misalignment is increased from ½ in. to 1 in. in a 1-dowel setup, this is accompanied by a 43 % increase in the load at a ¼ in. joint opening (first row of Table 4.4).

Table 4.4. Pair wise comparison of loads at ¼ in. joint opening (Horizontal misalignment)

Test 1 – load	Test 2 – load	% change from Test 1 to Test 2
1H12 – 2100 lbs	1H1 – 3000 lbs	+43 %
2H12NU – 2600 lbs	2H1NU – 3500 lbs	+35 %
2H12U – 1400 lbs	2H1U – 2900 lbs	+107 %
2H12U – 1400 lbs	2H12NU – 2600 lbs	+86 %

For a given misalignment type and magnitude, the non-uniform orientation of misalignment in the 2-dowel tests has higher loads at a given joint opening as compared with the uniform orientation tests (figures 4.22 through 4.24).

Cracking, as in the 2H34NU and 2H1NU tests, is captured on the load versus joint opening curve by an instantaneous drop in pressure at the time when the crack occurs, which was approximately at 0.67 and 0.72 in. joint openings, respectively (Figure 4.19). Spalling also leads to a drop of pressure, but in most of the tests where spalling occurred, the drop has been observed to have occurred over a significant time and cannot be captured by mere inspection of the load versus joint opening curve. Non-uniform joint opening, as in the 2H1U and the 5H12NU tests, is captured by observing the variation of the joint opening magnitudes along the joint through plots similar to Figure 4.5.

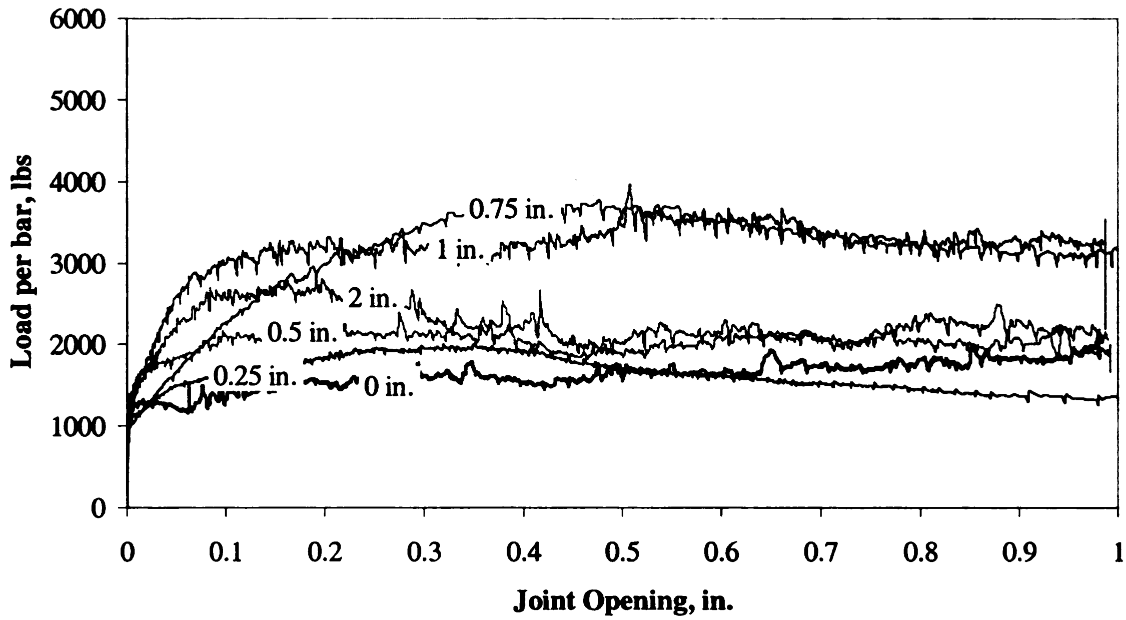

Figure 4.18. Comparison of load vs joint opening curves for 1-dowel Horizontal Misalignment tests

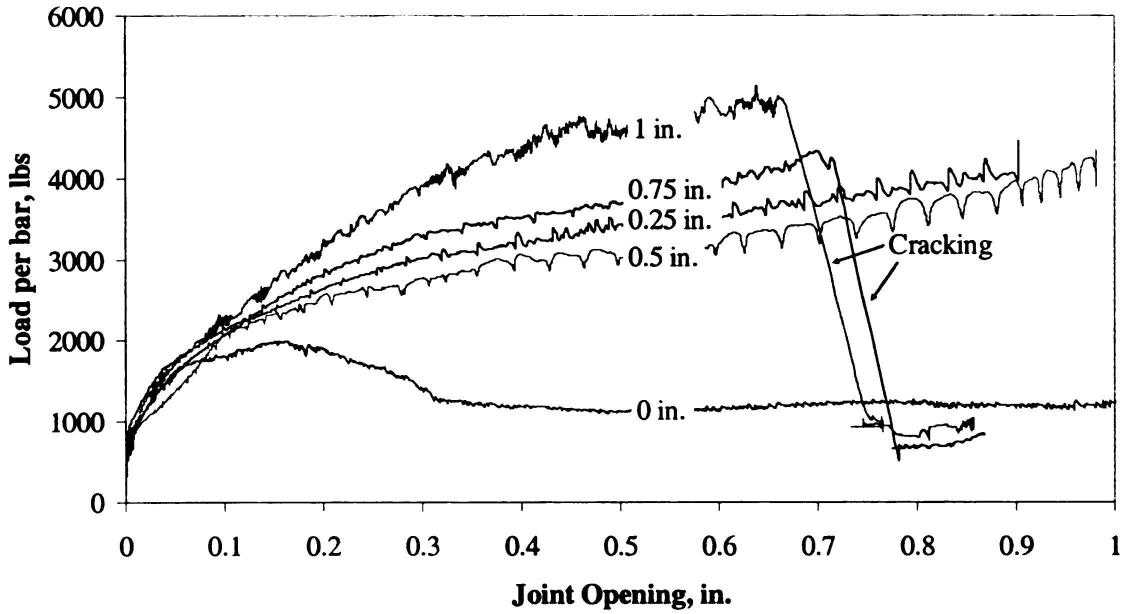

Figure 4.19. Comparison of load vs joint opening curves for 2-dowel Non-uniform Horizontal Misalignment tests

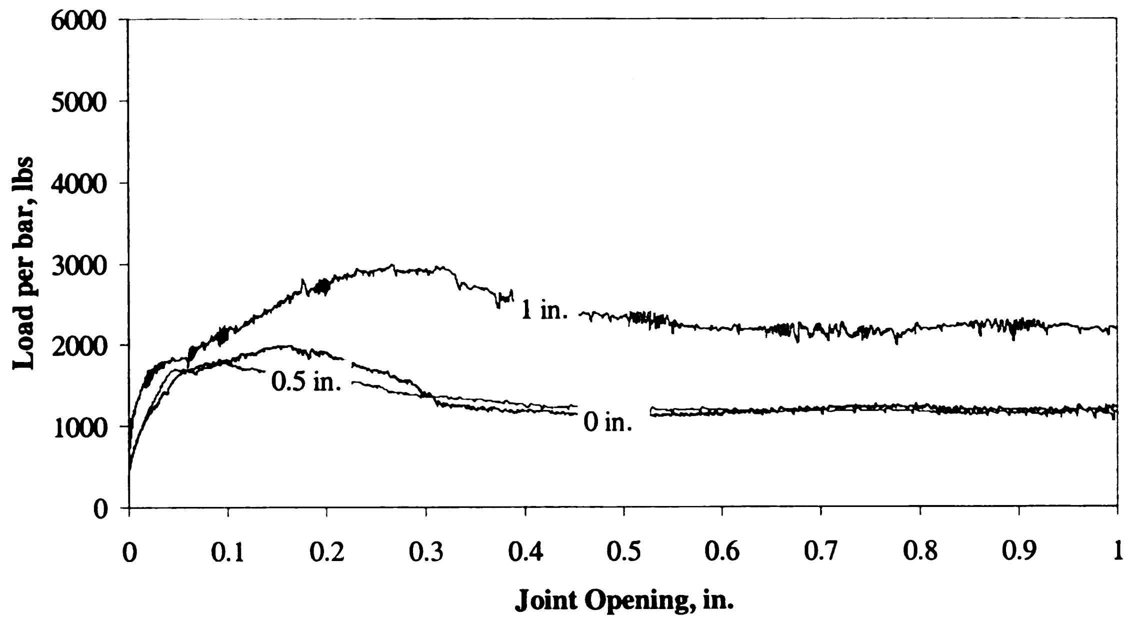

Figure 4.20. Comparison of load vs joint opening curves for 2-dowel Uniform Horizontal Misalignment tests

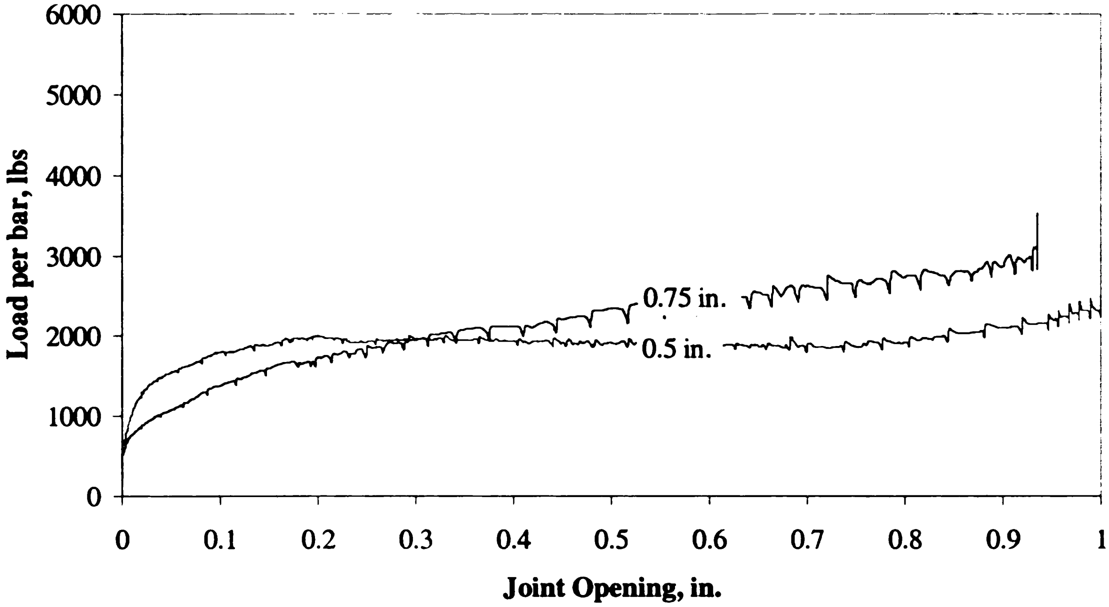

Figure 4.21. Comparison of load vs joint opening curves for 2-dowel Horizontal Misalignment tests (One dowel misaligned)

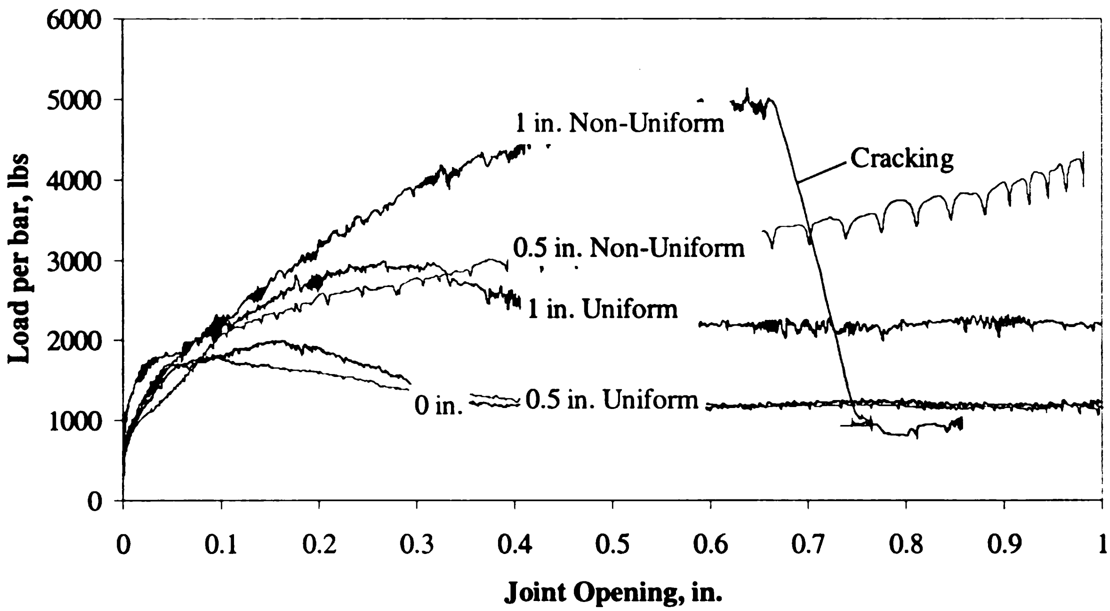

Figure 4.22. Comparison of load vs joint opening curves for 2-dowel Horizontal Misalignment tests (Non-uniform vs Uniform)

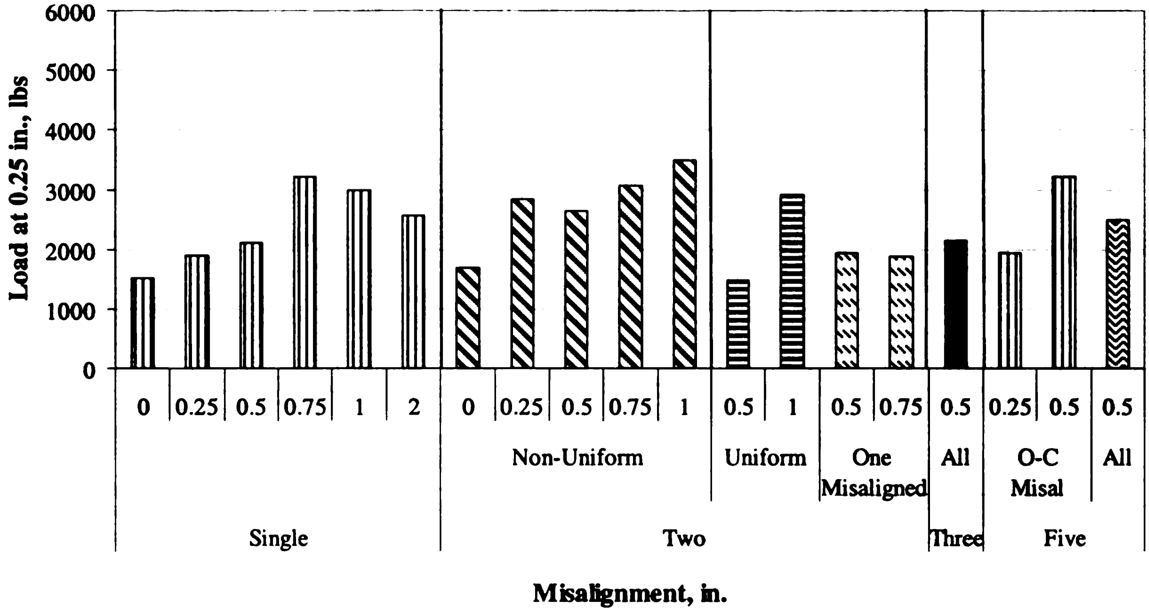

Figure 4.23. Comparison of loads at ¼ in. joint opening (Horizontal Misalignment)

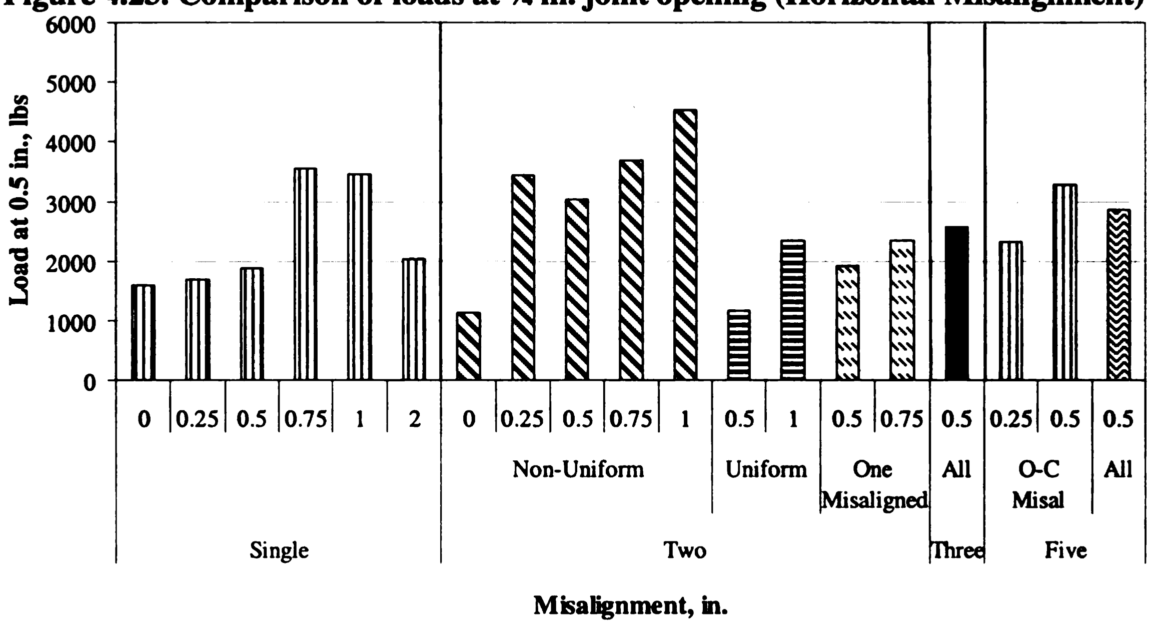

Figure 4.24. Comparison of loads at ½ in. joint opening (Horizontal Misalignment)

4.3.1.2 Vertical Misalignment

Figures 4.25, 4.26, 4.27, and 4.28 illustrate the comparisons of load vs joint behavior in the 1-dowel, 2-dowel (non-uniform and uniform orientations), and 2-dowel setup with one dowel misaligned tests, respectively. As seen from the plots, in general, the load per dowel increases with an increase in the misalignment magnitude, but the magnitude of the increase is lesser than in the horizontal tests.

Table 4.5 summarizes the comparisons of loads at a ¼ in. joint opening derived from the bar graphs (Figures 4.30 and 4.31). Similar trends hold good for the loads at a ½ in. joint opening. The format of Table 4.5 is similar to Table 4.4.

Table 4.5. Pair wise comparison of loads at ¼ in. joint opening (Vertical Misalignment)

Test 1 – load	Test 2 - load	% change from Test 1 to Test 2
1V12 – 2700 lbs	1V1 – 3100 lbs	+15 %
2V12NU – 2300 lbs	2V1NU – 2900 lbs	+26 %
2V12U – 2500 lbs	2V1U – 3980 lbs	+59 %
2V12U – 2500 lbs	2V12NU – 2300 lbs	-8 %

For a given misalignment type and magnitude, the uniform orientation of misalignment in the 2-dowel tests exhibit higher loads than the non-uniform counterparts, with some experimental variability. At a ¼ in. joint opening, the trend is valid for both the ½ and 1 in. misalignment series, while at a ½ in. joint opening, the trend reversed in the ½ in. misalignment test and remained the same in the 1 in. misalignment test (Figures 4.29 through 4.31). The reason why uniform orientation tests exhibit a higher behavior is due to the physical restraints preventing uplift in the direction of pullout of the slabs, indirectly leading to a higher locking effect.

Non-uniform joint opening, as in the 2V1NU test, is captured by observing the variation of the joint opening magnitudes along the joint through plots similar to Figure 4.5. Vertical uplift, however, was not captured through measurement and was visually observed during the tests (2V12NU, 2V34NU, and 2V1NU tests).

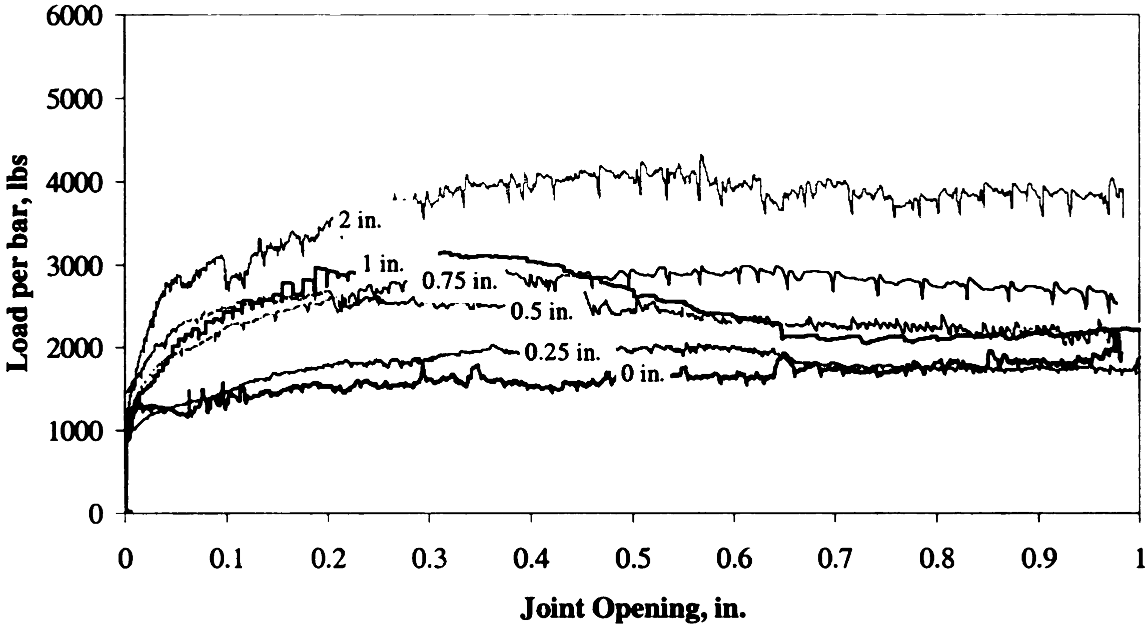

Figure 4.25. Comparison of load vs joint opening curves for 1-dowel Vertical Misalignment tests

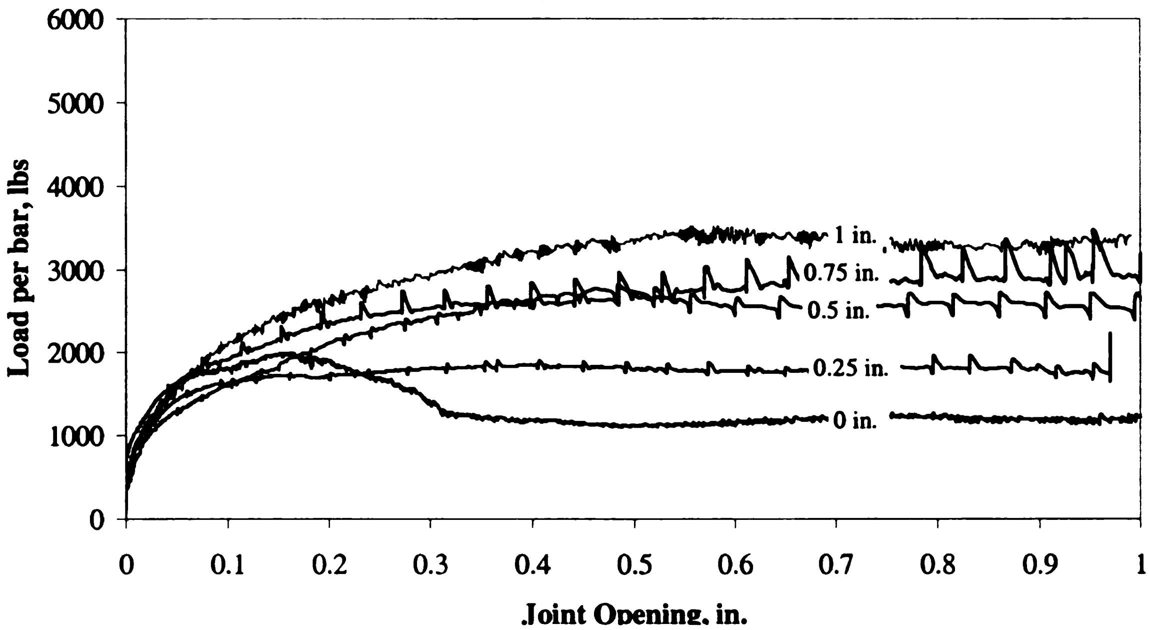

Figure 4.26. Comparison of load vs joint opening curves for 2-dowel Non-uniform misalignment tests

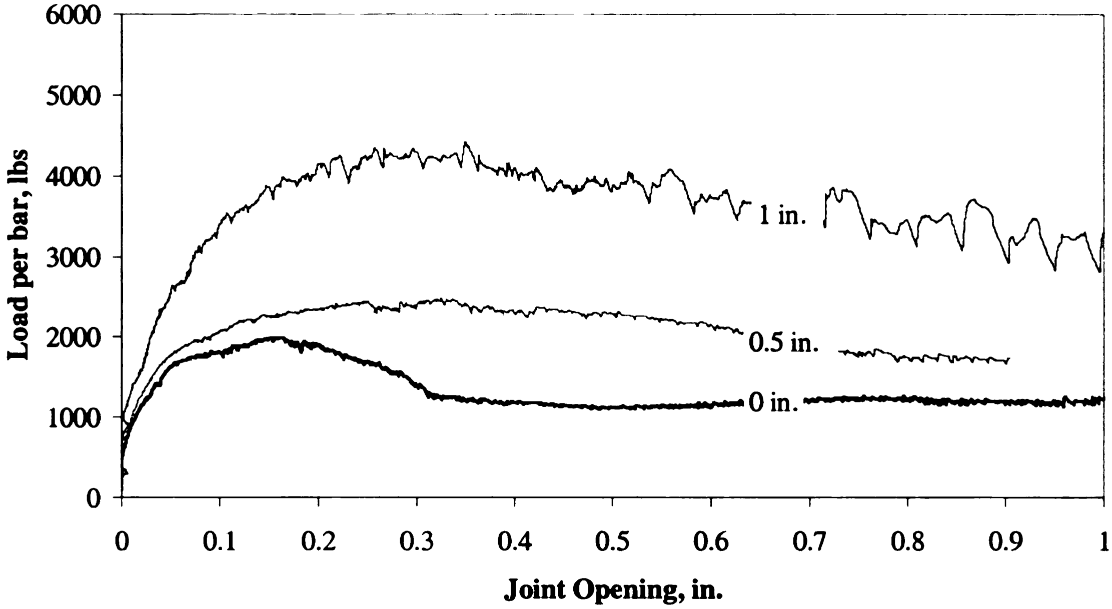

Figure 4.27. Comparison of load vs joint opening curves for 2-dowel Uniform Vertical Misalignment tests

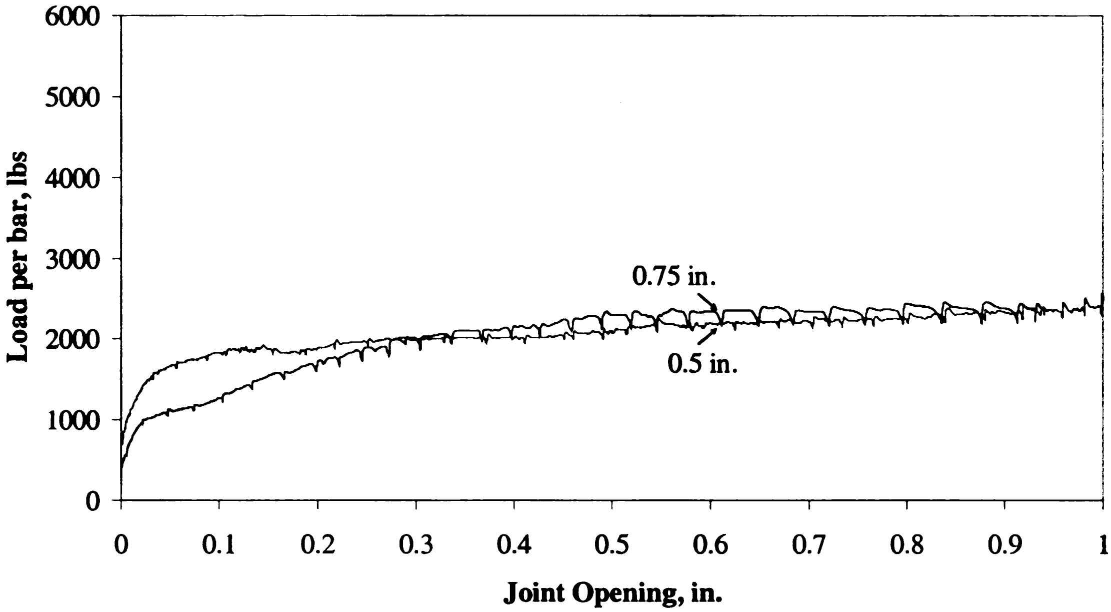

Figure 4.28. Comparison of load vs joint opening curves for 2-dowel Vertical Misalignment Tests (One dowel misaligned)

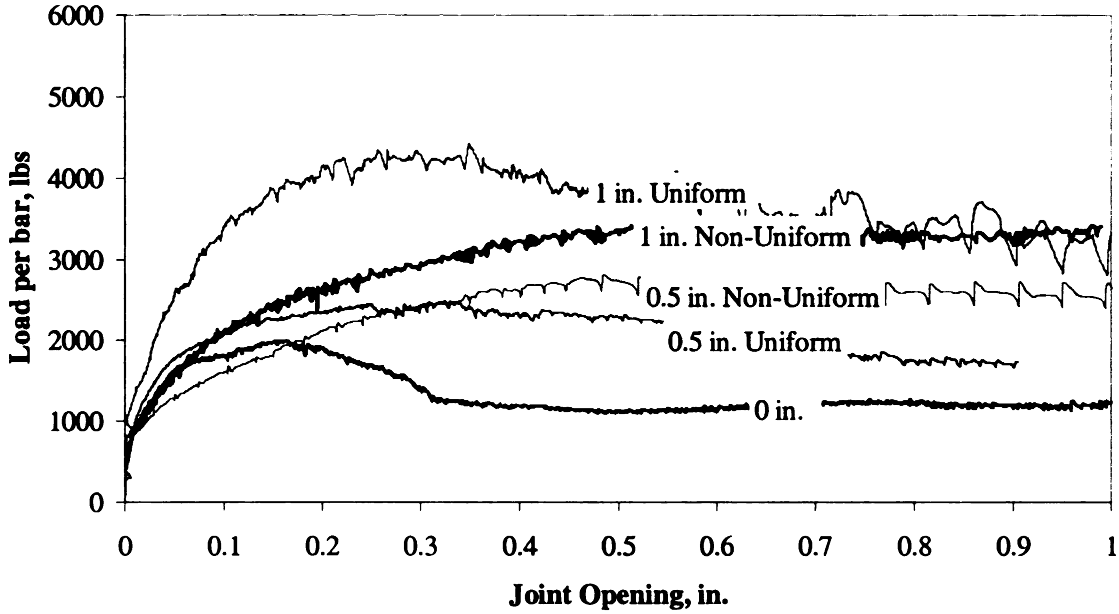

Figure 4.29. Comparison of load vs joint opening curves for 2-dowel Vertical Misalignment Tests (Non-uniform vs Uniform)

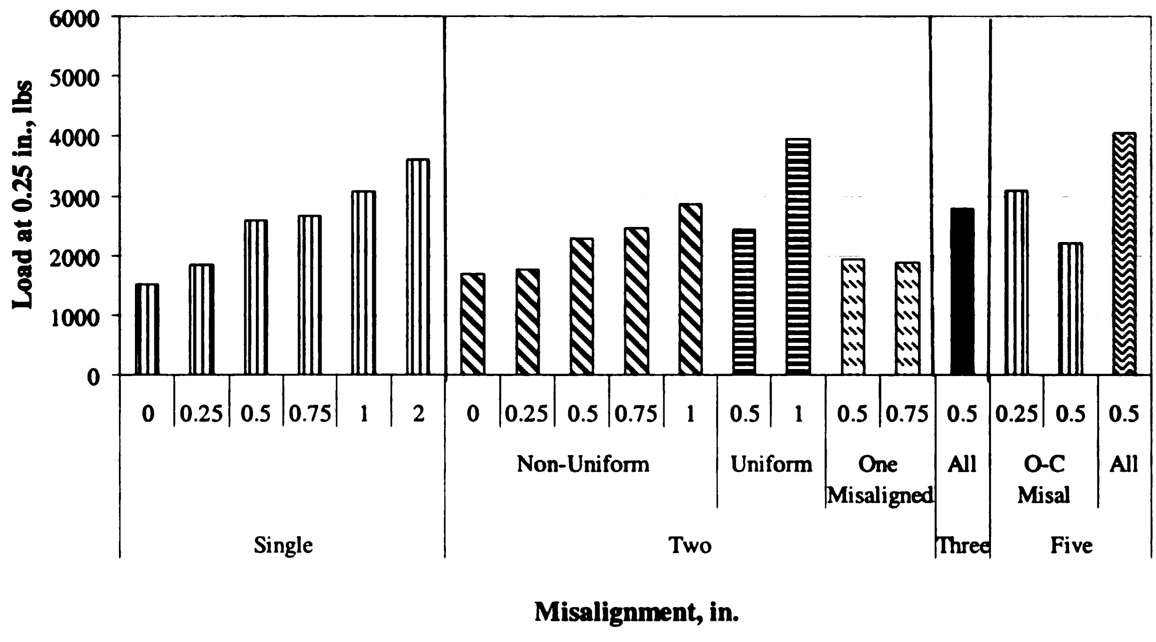

Figure 4.30. Comparison of loads at ¼ in. joint opening (Vertical Misalignment)

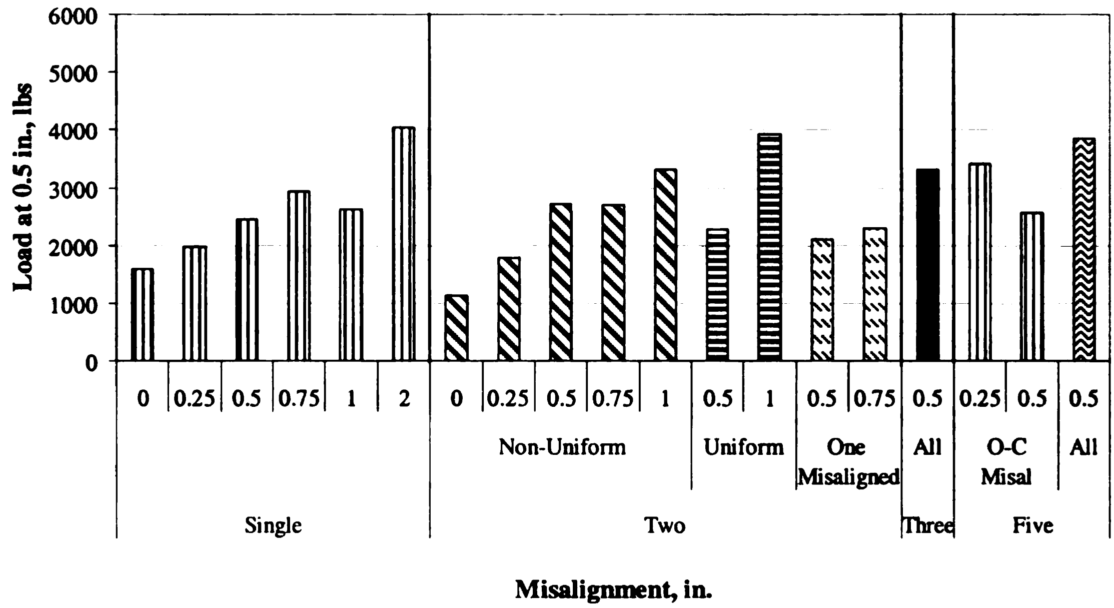

Figure 4.31. Comparison of loads at ½ in. joint opening (Vertical Misalignment)

4.3.1.3 Combined Misalignment

Figures 4.32, 4.33, 4.34, and 4.35 illustrate the comparisons of load vs joint behavior in the 1-dowel, 2-dowel (non-uniform and uniform orientations), and 2-dowel setup with one dowel misaligned tests, respectively. Since combined misalignment constitutes horizontal as well as vertical misalignment, the load versus joint opening behavior is a hybrid of the behavior exhibited in the horizontal and vertical tests.

Table 4.6 summarizes the comparisons of loads at a ¼ in. joint opening derived from the bar graphs (figures 4.37 and 4.38). Similar trends hold good for the loads at a ½ in. joint opening. The format of Table 4.6 is similar to Table 4.4.

Table 4.6. Pairwise comparison of loads at ¼ in. joint opening (Combined misalignment)

Test 1 – load	Test 2 - load	% change from Test 1 to Test 2
1C12 – 1900 lbs	1C1 – 3300 lbs	+74 %
2C12NU – 2900 lbs	2C1NU – 4600 lbs	+59 %
2C12U – 1800 lbs	2C1U – 3700 lbs	+105 %
2C12U – 1800 lbs	2C12NU – 2900 lbs	+61 %

For a given misalignment type and magnitude, the non-uniform orientation of misalignment in the 2-dowel tests has higher loads at a given joint opening as compared with the uniform orientation tests (figures 4.36 through 4.38).

Cracking, as in the tests of 2C34NU and 2C1NU is captured on the load versus joint opening curve by an instantaneous drop in pressure at the time when the crack occurs, which was approximately at 0.45, 0.95, and 0.82 in. joint openings, respectively (Figure 4.33). Spalling also leads to a drop of pressure, but in most of the tests where spalling occurred, the drop has been observed to have occurred over a significant time and cannot be captured by mere inspection of the load versus joint opening curve. However, in the 2C34NU test, spalling induced the occurrence of cracking, and this is captured by the drop in the pressure at about 0.22 in. joint opening. Non-uniform joint opening, as in the 2C1U test, is captured by observing the variation of the joint opening magnitudes along the joint through plots similar to Figure 4.5.

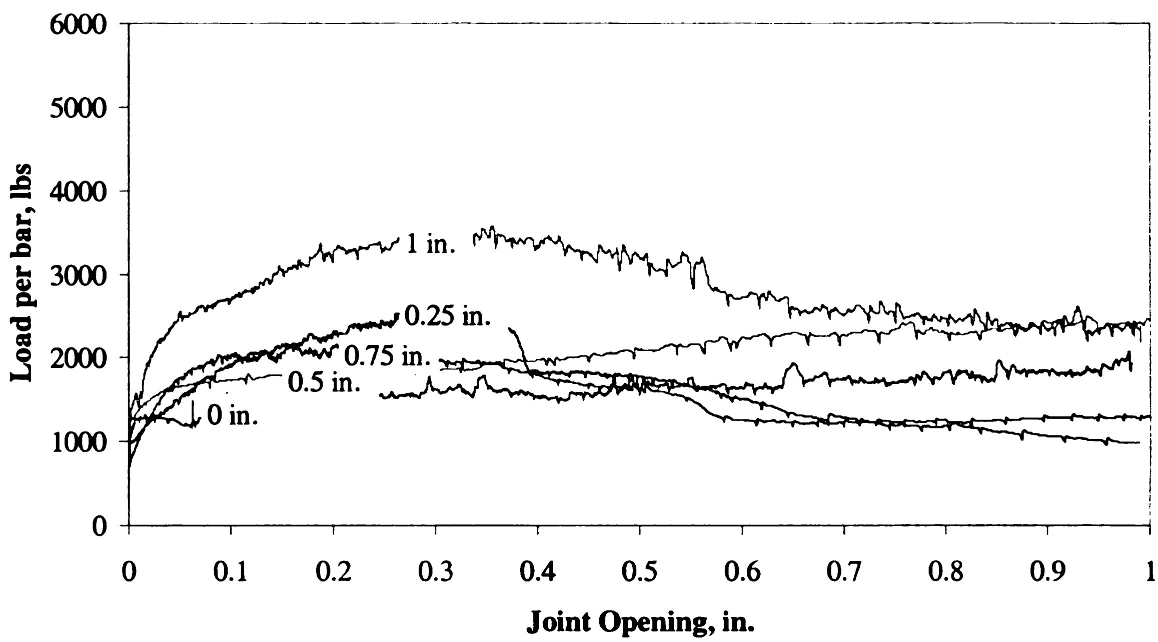

Figure 4.32. Comparison of load vs joint opening curves for 1-dowel Combined Misalignment tests

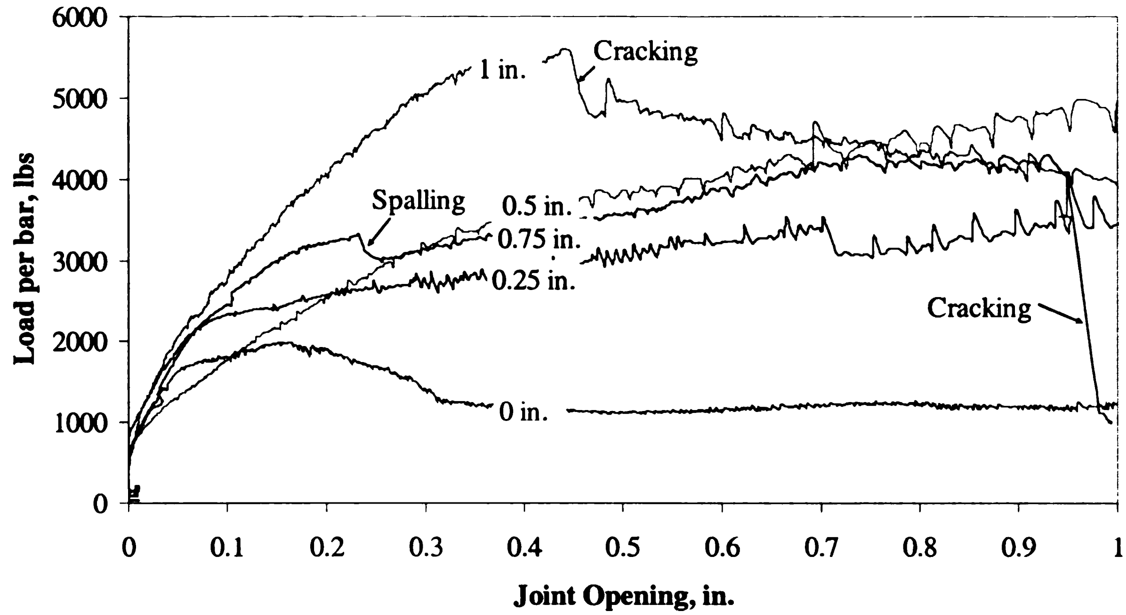

Figure 4.33. Comparison of load vs joint opening curves for 2-dowel Non-uniform Combined Misalignment tests

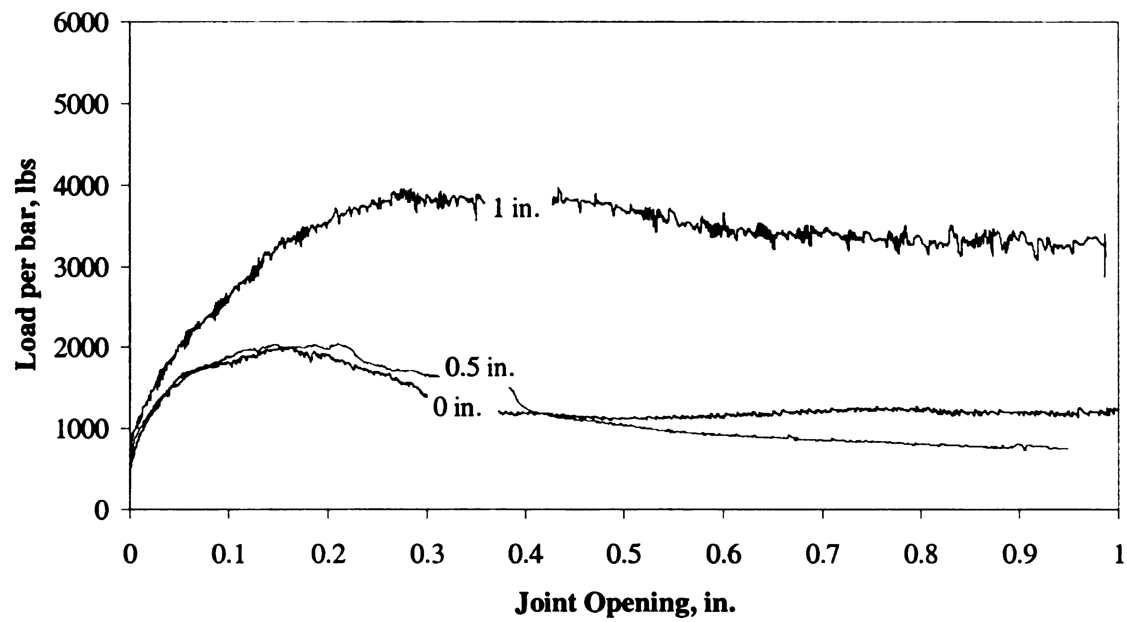

Figure 4.34. Comparison of load vs joint opening curves for 2-dowel Uniform Combined Misalignment tests

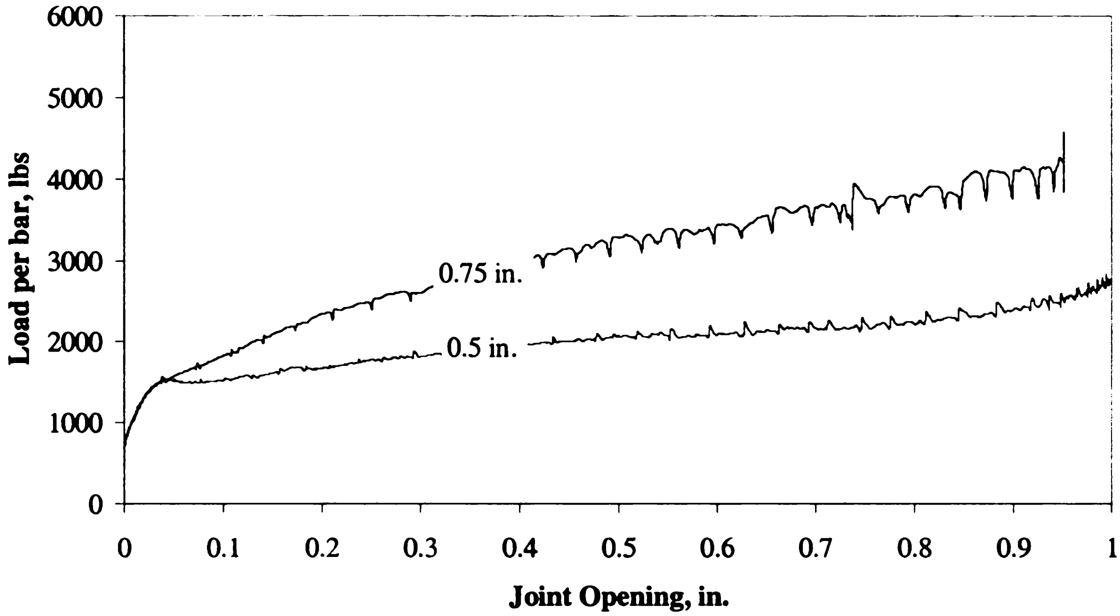

Figure 4.35. Comparison of load vs joint opening curves for 2-dowel Combined Misalignment (One dowel misaligned)

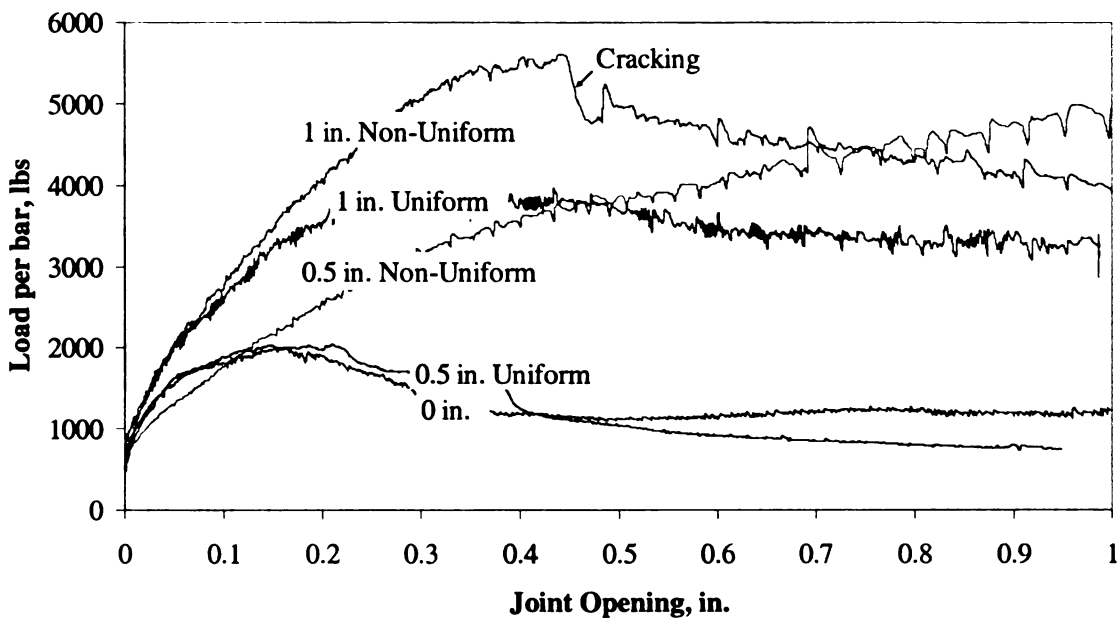

Figure 4.36. Comparison of load vs joint opening curves for 2-dowel Combined Misalignment (Non-uniform vs Uniform)

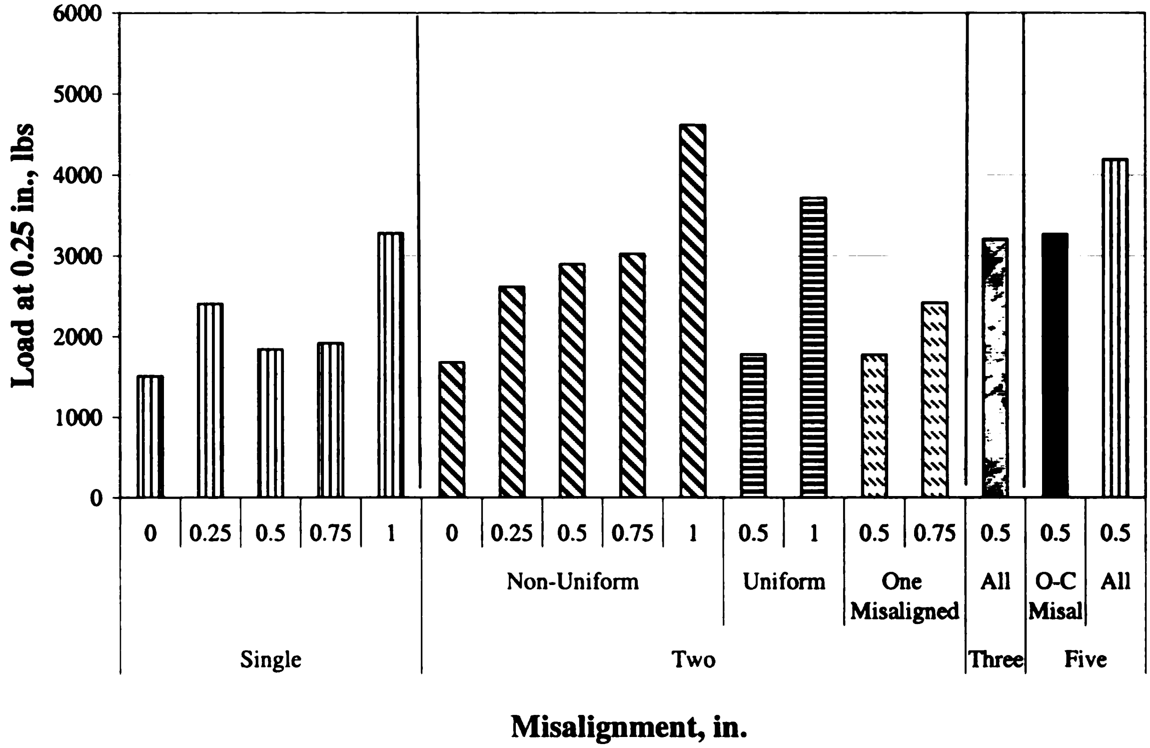

Figure 4.37. Comparison of loads at ¼ in. joint opening (Combined Misalignment)

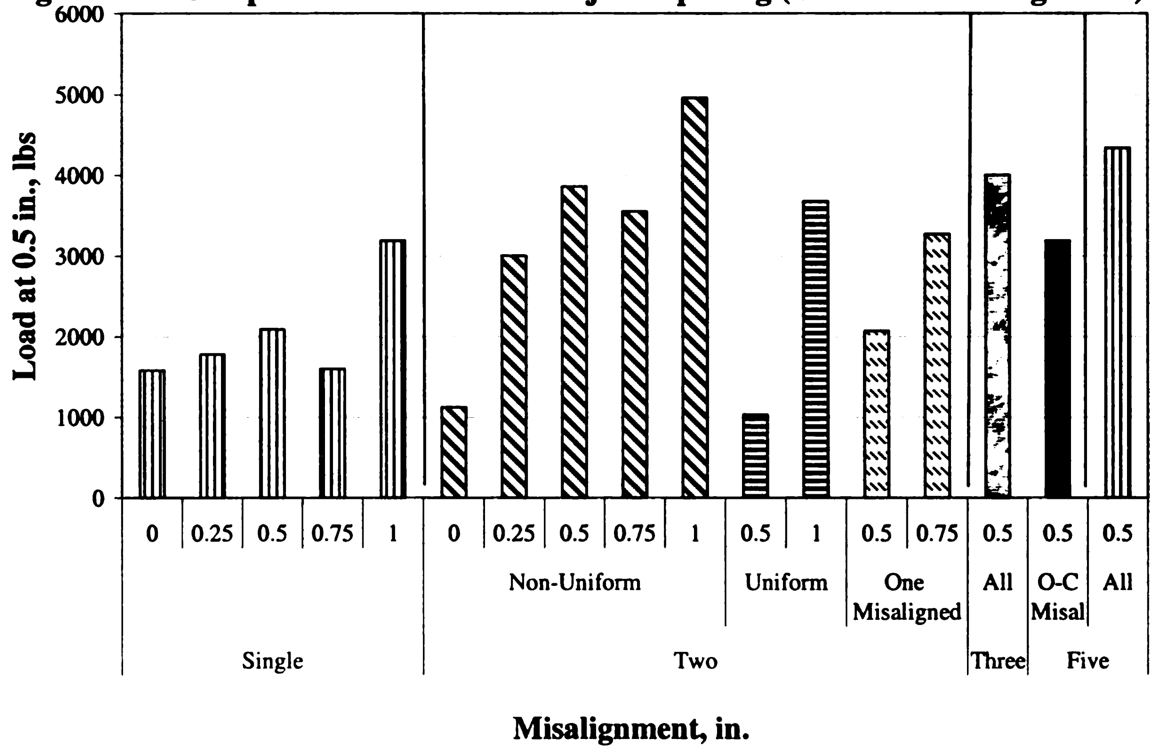

Figure 4.38. Comparison of loads at ½ in. joint opening (Combined Misalignment)

4.3.2 Comparison across different number of dowels misaligned

The comparisons covered in this subsection can be further categorized as (x = H, V, or C):

- Number of dowels misaligned is different but the total number of dowels remains the same (2xAM vs 2xNU/U and 5xAM vs 5xNU)
- Number of dowels in the setup are different (1x vs 2xNU/U and 3xNU vs 5xNU)

4.3.2.1 Comparisons within same setup with different number of dowels misaligned

The first comparison, illustrated in figures 4.39 through 4.44, compares the 2-dowel tests with one dowel misaligned (2xAM) against both misaligned (2xNU/U). In the ½ in. misalignment tests (horizontal, vertical, and combined), the 2AM tests lie below the 2NU tests, but above the 2U tests, with intersections in the lower joint openings due to experimental variability. In the ¾ in. misalignment tests, only the 2NU series tests were carried out and the 2AM tests lie below the 2NU tests (figures 4.42 through 4.44).

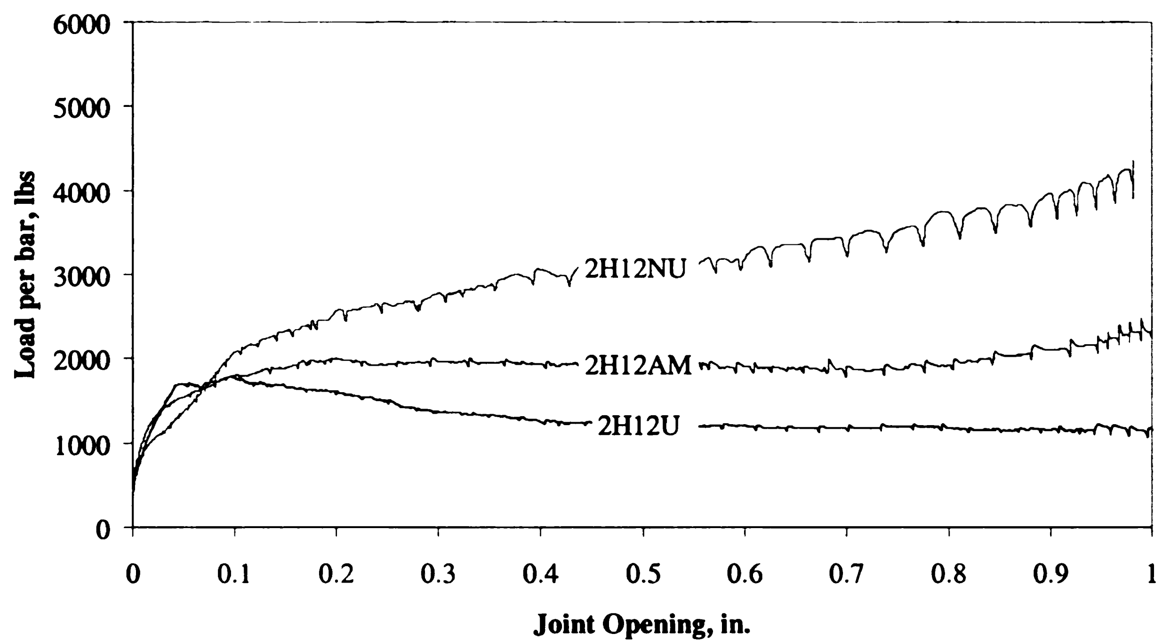

Figure 4.39. Comparison of load vs joint opening curves of 2-dowel ½ in. Horizontal Misalignment (2H12NU, 2H12U, and 2H12AM)

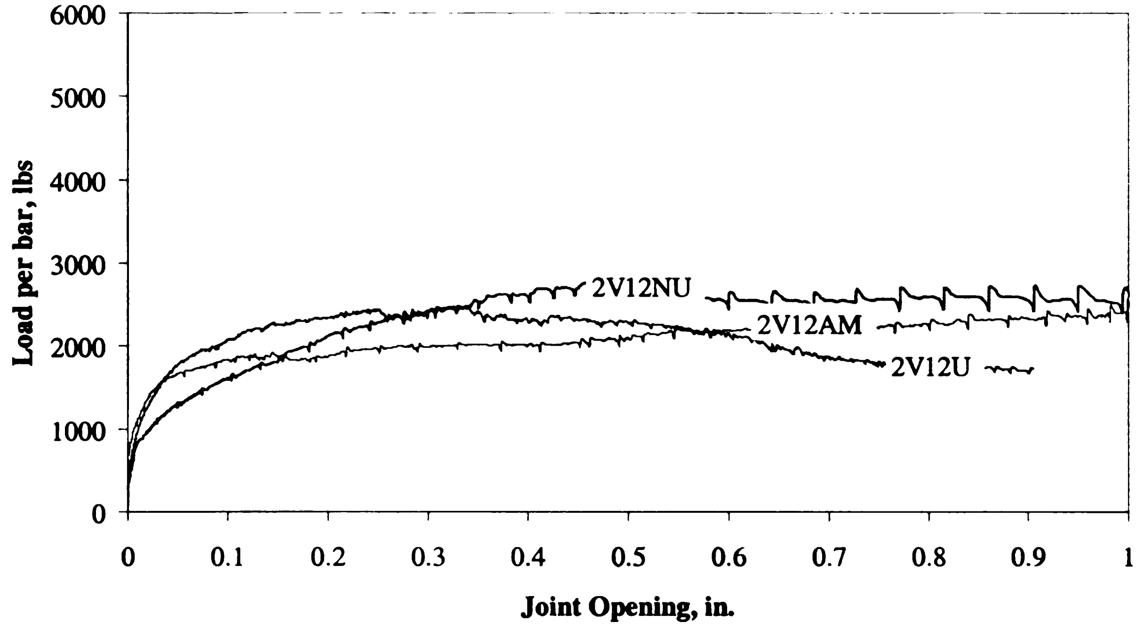

Figure 4.40. Comparison of load vs joint opening curves of 2-dowel ½ in. Vertical Misalignment (2V12NU, 2V12U, and 2V12AM)

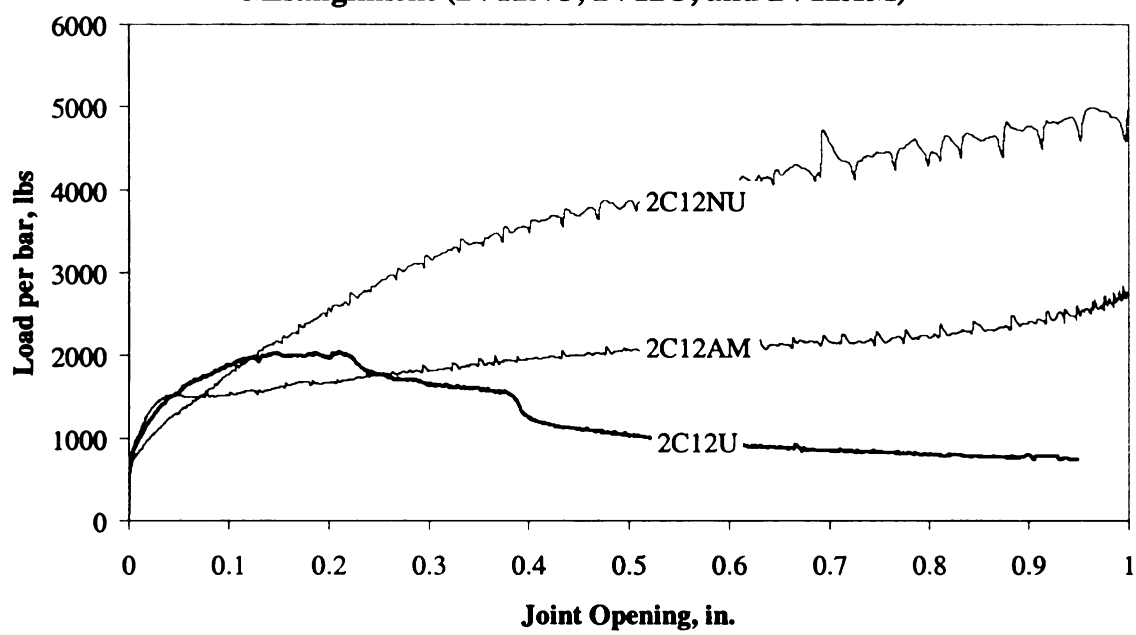

Figure 4.41. Comparison of load vs joint opening curves of 2-dowel ½ in. Combined Misalignment (2C12NU, 2C12U, and 2C12AM)

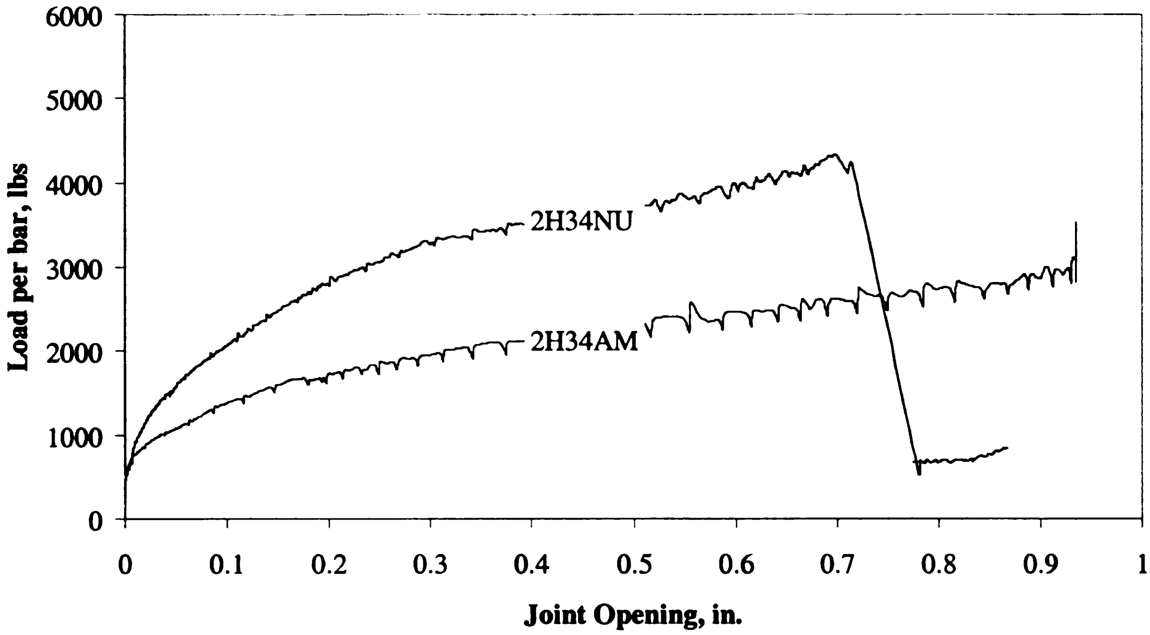

Figure 4.42. Comparison of load vs joint opening curves of 2-dowel ¾ in. Horizontal Misalignment (2H34NU and 2H34AM)

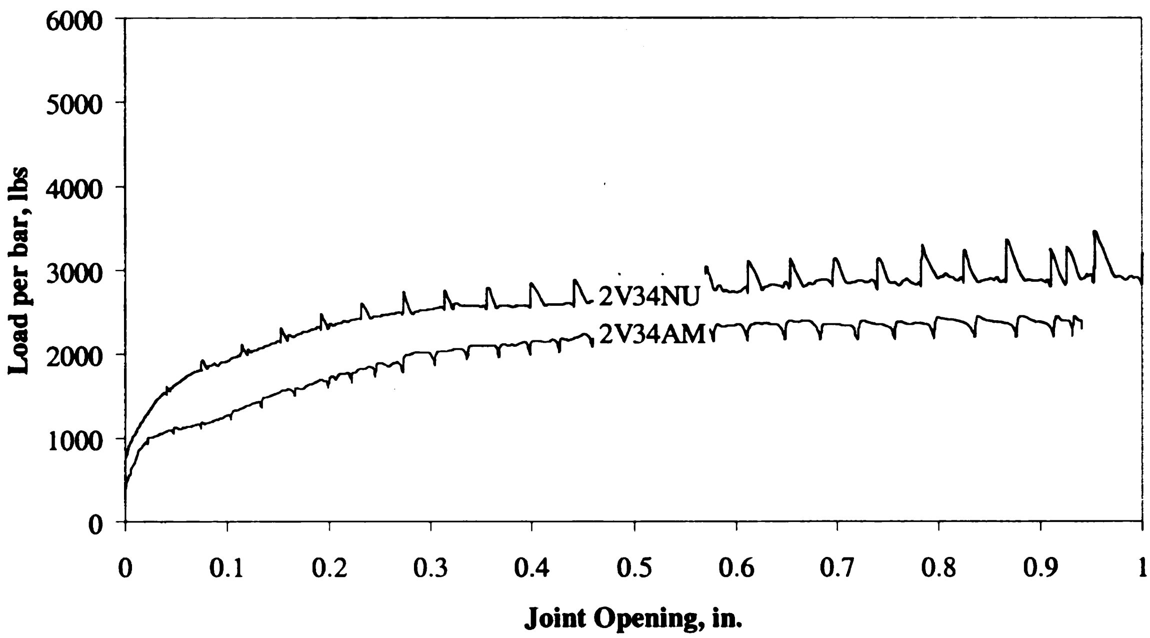

Figure 4.43. Comparison of load vs joint opening curves of 2-dowel ¾ in. Vertical Misalignment (2V34NU and 2V34AM)

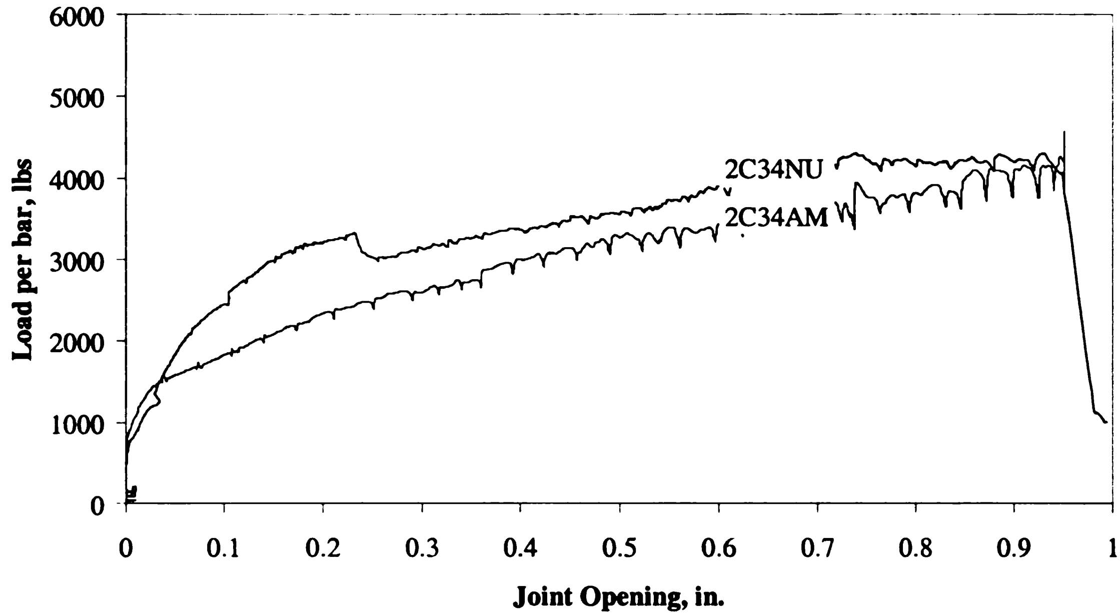

Figure 4.44. Comparison of load vs joint opening curves of 2-dowel ¾ in. Combined Misalignment (2C34NU and 2C34AM)

There is just one misalignment magnitude (½ in.) available for comparison of trends across different number of dowels misaligned in the 5-dowel tests (5x12NU vs 5x12AM) (figures 4.45 through 4.47). In the horizontal misalignment tests, the outer and center dowels misaligned (AM) test has higher loads at a given joint opening than the all dowels misaligned tests (Figure 4.45), but in the vertical and combined misalignment tests it is vice versa (figures 4.46 and 4.47). Also the 5NU tests were more destructive than the 5AM tests.

In general, it can be concluded that for a given misalignment magnitude, the load induced per dowel increases as the number of dowels misaligned increases.

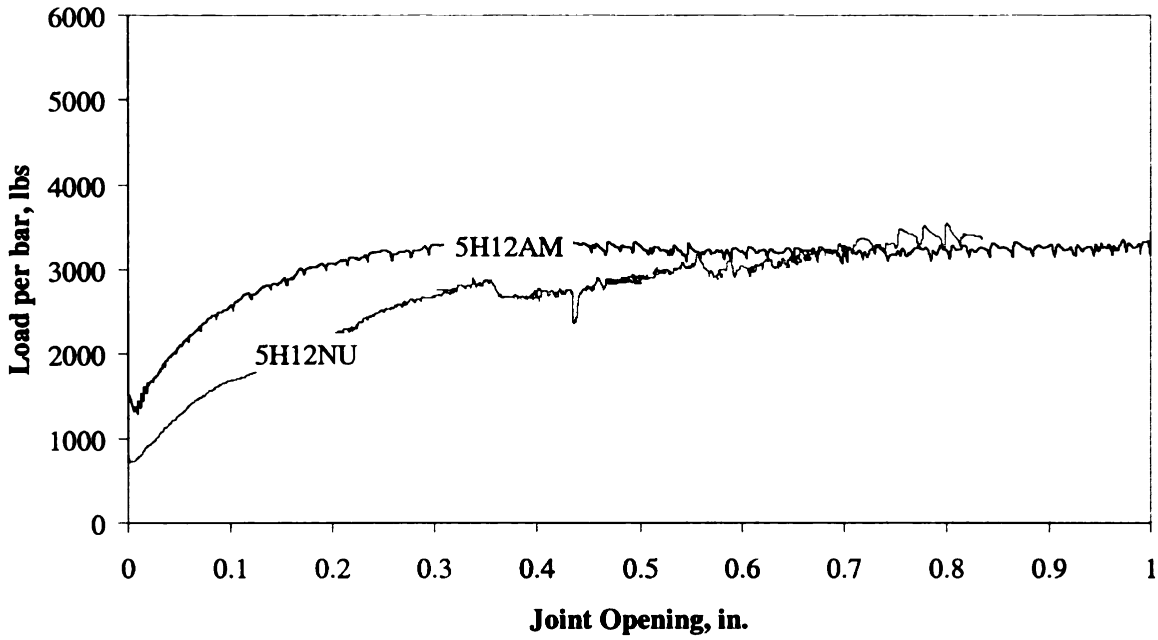

Figure 4.45. Comparison of load vs joint opening curves of 5H12NU and 5H12AM

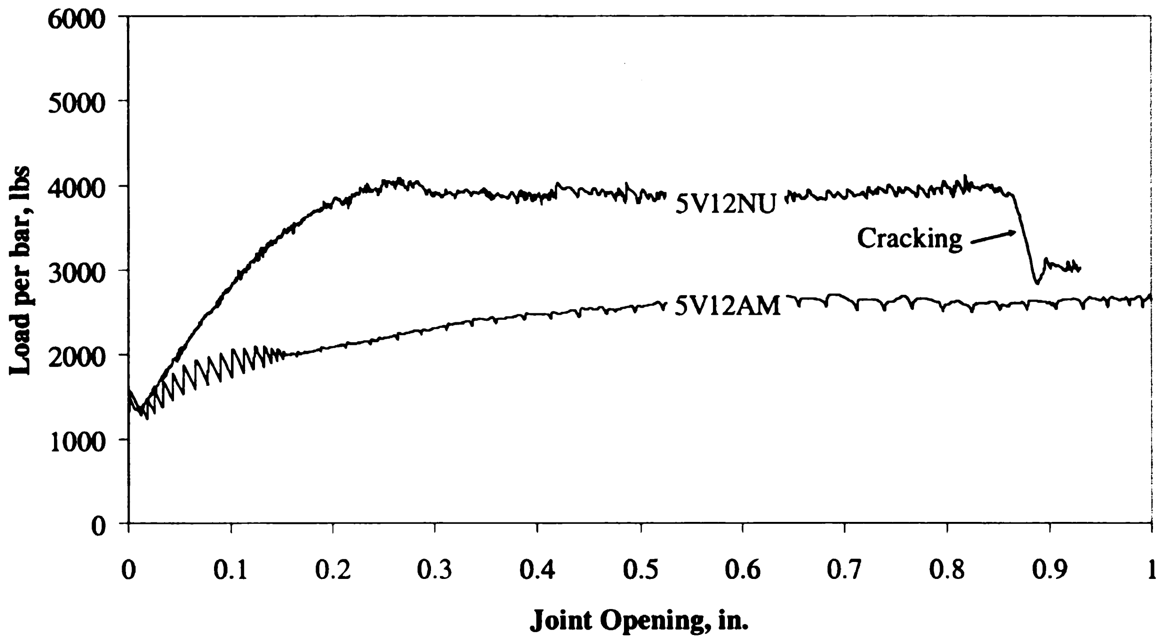

Figure 4.46. Comparison of load vs joint opening curves of 5V12NU and 5V12AM

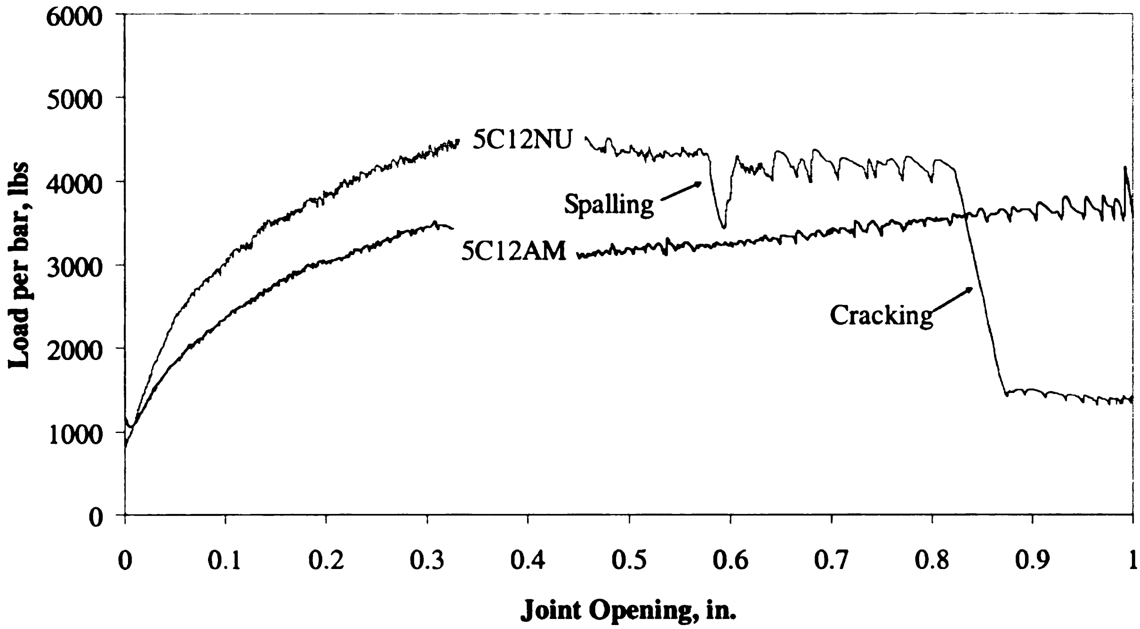

Figure 4.47. Comparison of load vs joint opening curves of 5C12NU and 5C12AM

4.3.2.2 Comparison across different number of dowels setups

This section presents a pair wise comparison of 1 vs 2-dowel tests and 3 vs 5-dowel tests. A comparison across the two pairs will not be valid because the specimen molds, and hence the volume of concrete in the two setups, is different. The 2-dowel (5-dowel) specimens underwent more significant distress than the 1-dowel (3-dowel) tests because the total applied load (load per dowel x number of dowels) is higher.

Horizontal Misalignment: In the ½ and 1 in. misalignment tests, the 1H lies between the 2HNU and 2HU tests, with the 2HNU lying above the 1H test (figures 4.48 and 4.49). As illustrated in Figure 4.50, the load per bar at a given joint opening increases with an increase in the number of bars from three to five.

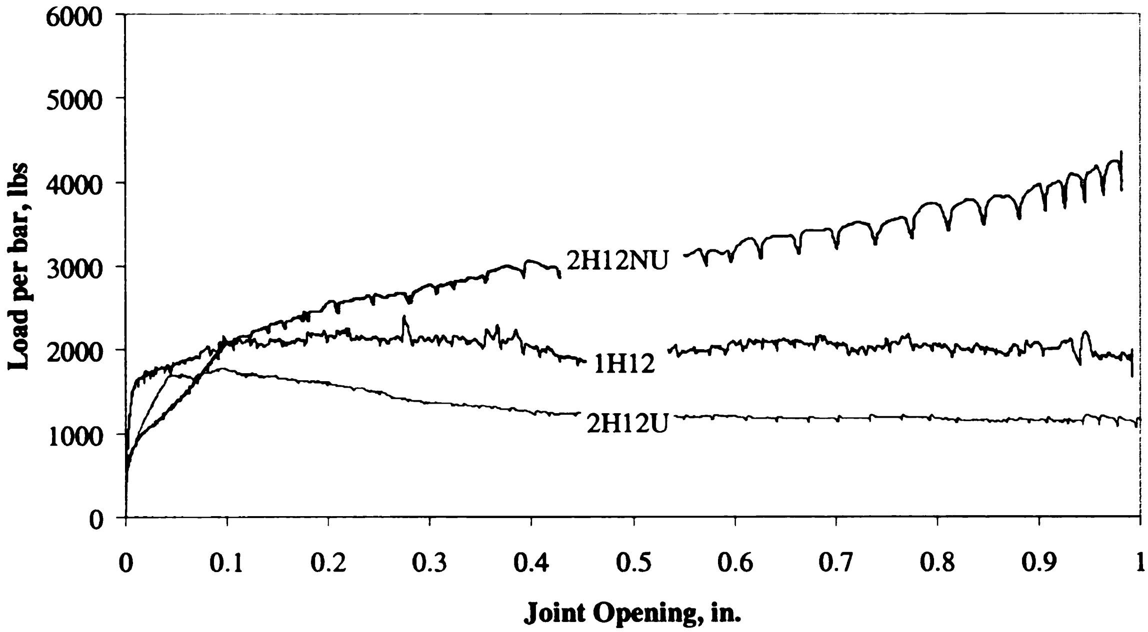

Figure 4.48. Comparison of load vs joint opening curves of 1H12 and 2-dowel ½ in. Horizontal Misalignment (2H12NU, 2H12U)

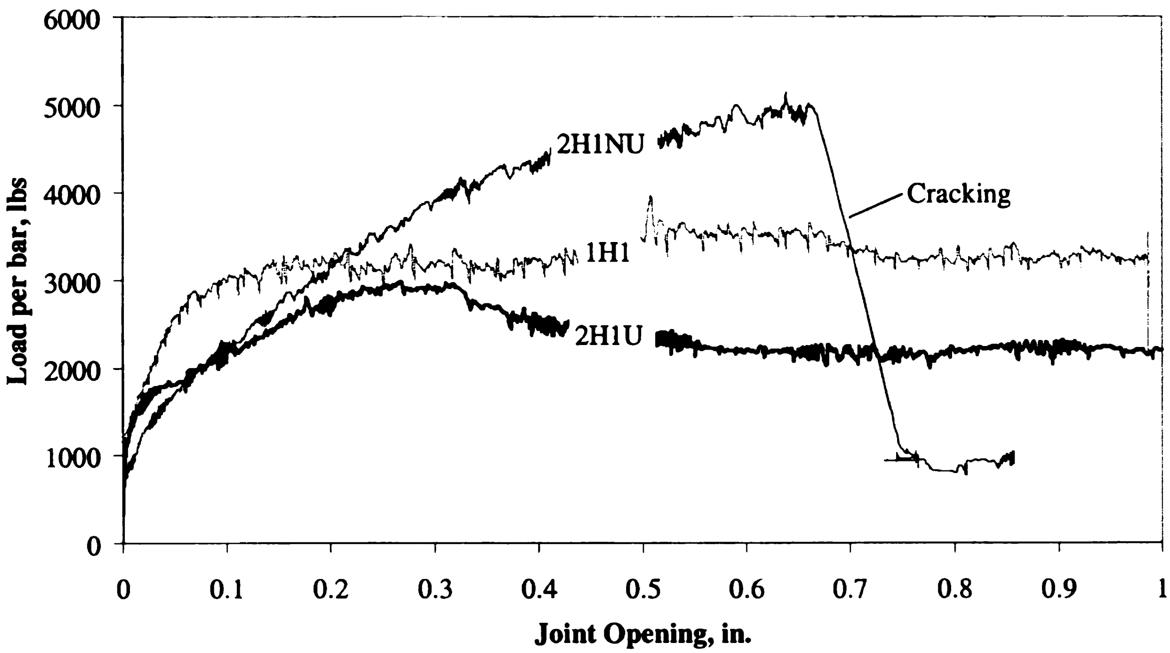

Figure 4.49. Comparison of load vs joint opening curves of 1H1 and 2-dowel 1 in. Horizontal Misalignment (2H1NU, 2H1U)

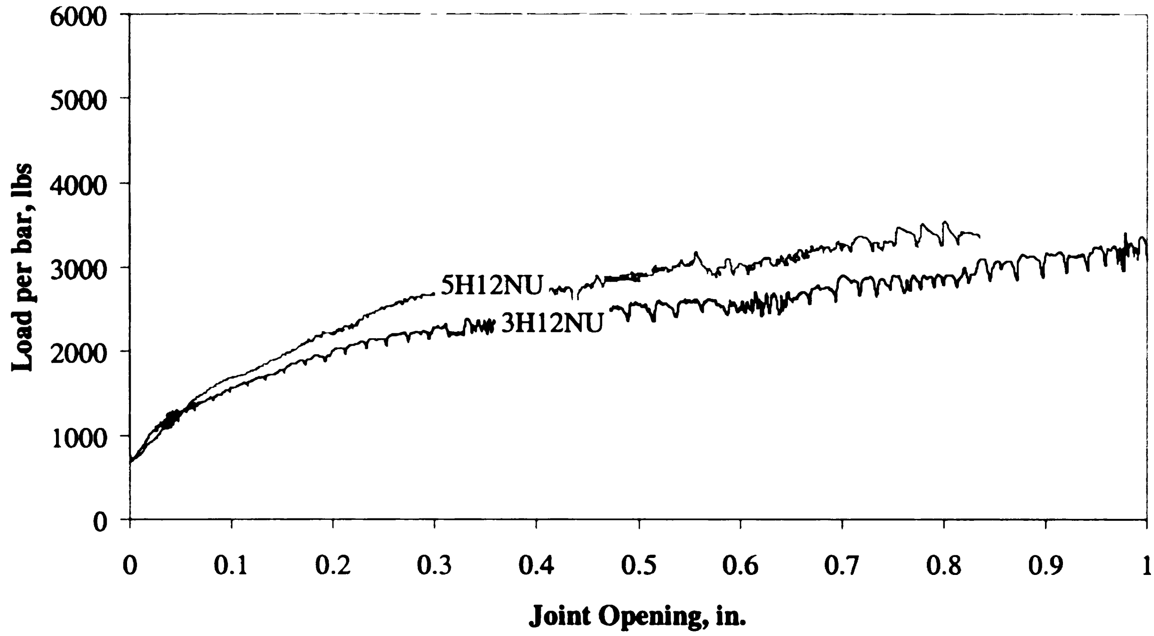

Figure 4.50. Comparison of load vs joint opening curves of 3H12NU and 5H12NU

Vertical Misalignment: In the ½ in. misalignment tests, the 1V12 test lies between the 2V12NU and 2V12U tests, with the 2V12NU test lying above the 1V12 test (Figure 4.51). However, in the 1 in. misalignment tests, the 1V1 test lies below both the 2V1Uand 2V1NU tests, with the 2V1U test lying above the 2V1NU test (Figure 4.52). As illustrated in Figure 4.53, the load per bar at a given joint opening increases with an increase in the number of bars from three to five.

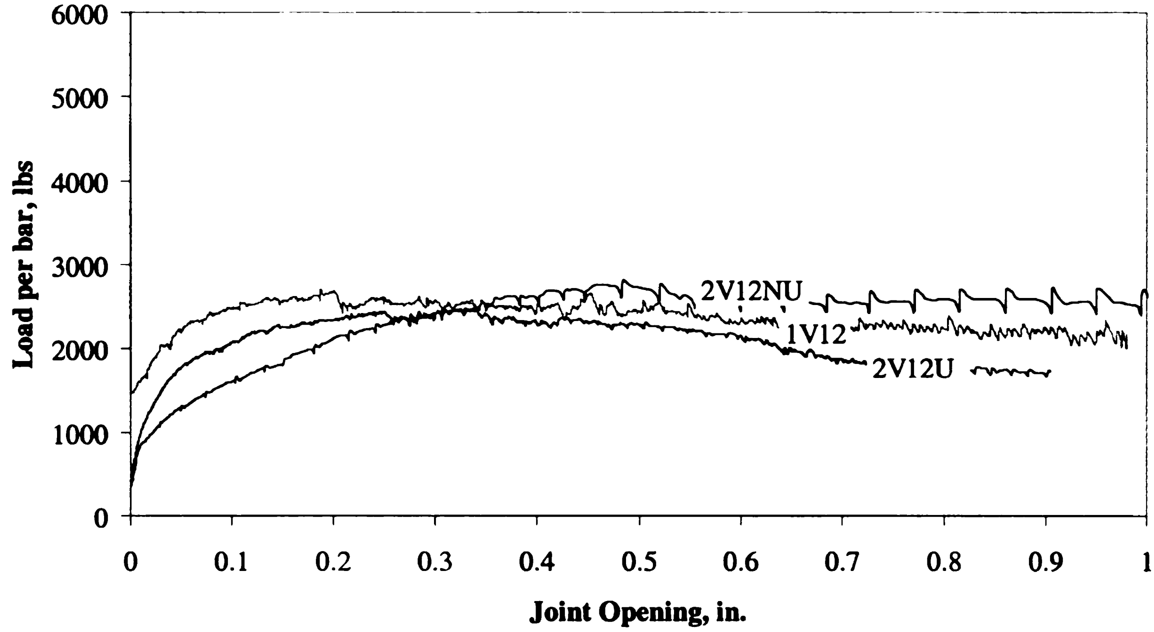

Figure 4.51. Comparison of load vs joint opening curves of 1V12 and 2-dowel ½ in. Vertical Misalignment (2V12NU, 2V12U)

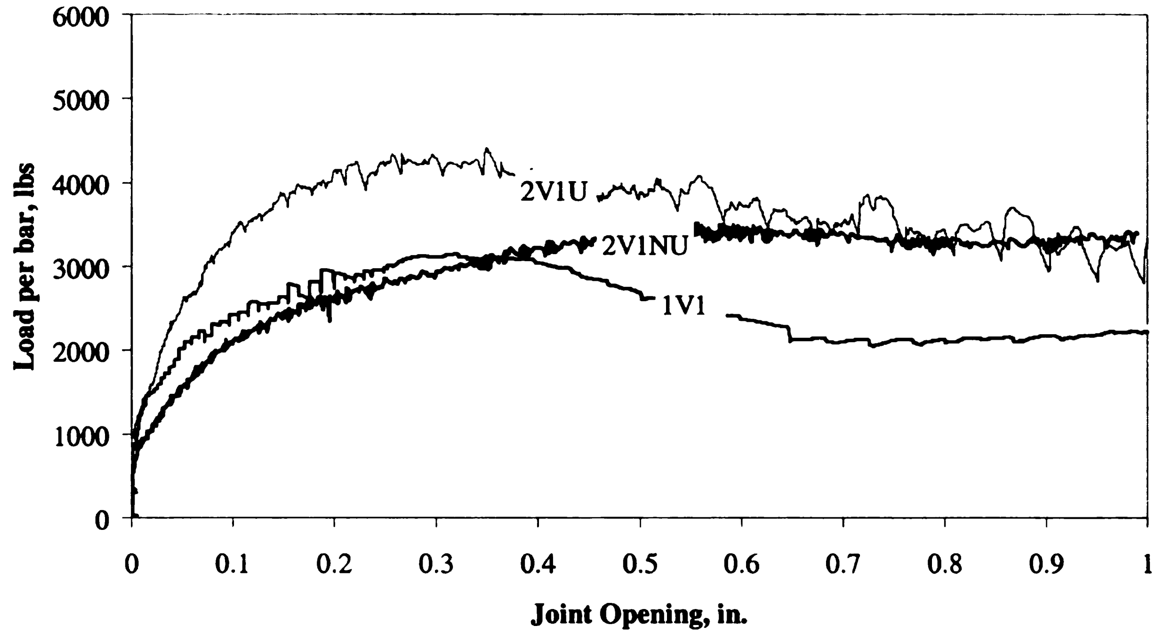

Figure 4.52. Comparison of load vs joint opening curves of 1V1 and 2-dowel 1 in. Vertical Misalignment (2V1NU, 2V1U)

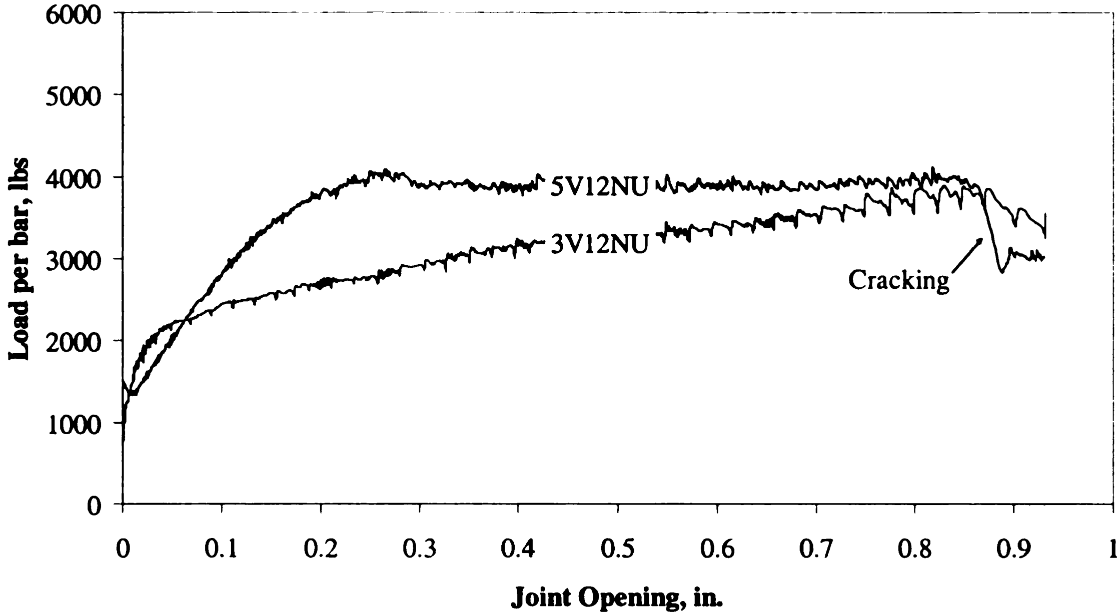

Figure 4.53. Comparison of load vs joint opening curves of 3V12NU and 5V12NU

Combined Misalignment: In the ½ in. misalignment tests, the 1C12 test lies between the 2C12NU and 2C12U tests, with the 2C12NU test lying above the 1C12 test (Figure 4.54). However, in the 1 in. misalignment tests, the 1C1 test lies below both the 2C1U and 2C1NU tests, with the 2C1NU test lying above the 2C1U test (Figure 4.55).

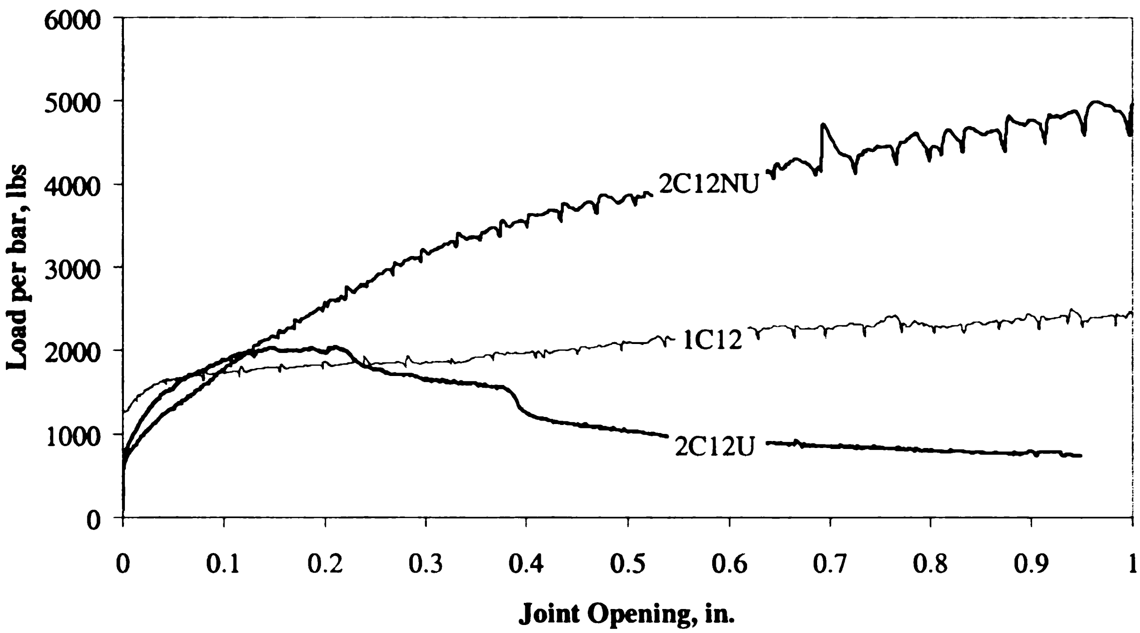

Figure 4.54. Comparison of load vs joint opening curves of 1C12 and 2-dowel ½ in. Combined Misalignment (2C12NU, 2C12U)

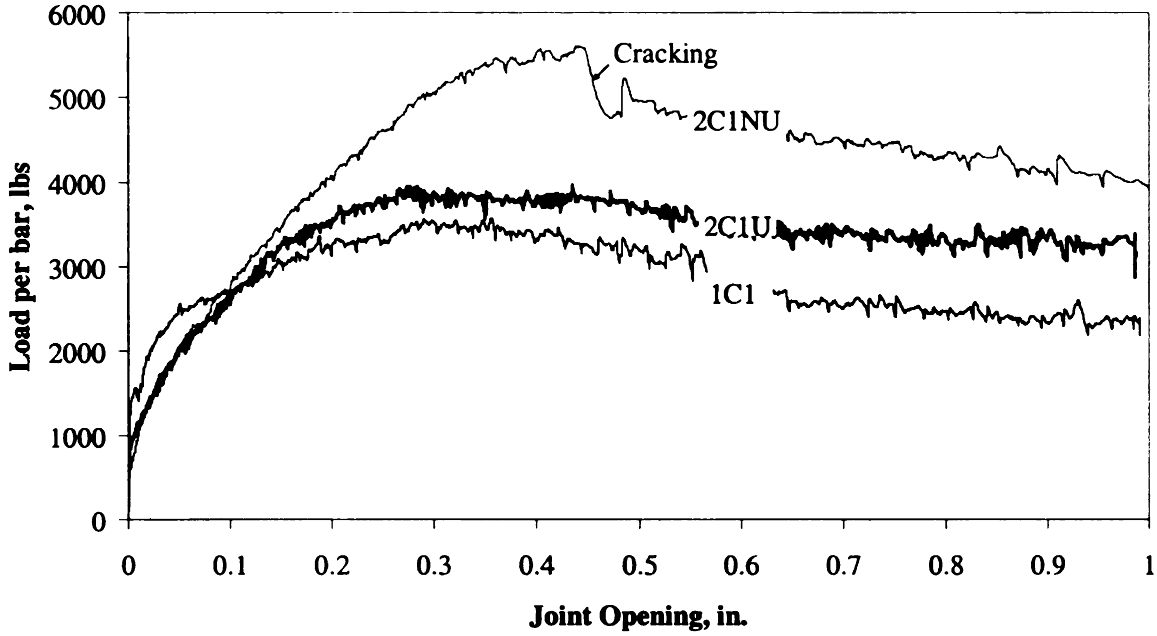

Figure 4.55. Comparison of load vs joint opening curves of 1C1 and 2-dowel 1 in. Combined Misalignment (2C1NU, 2C1U)

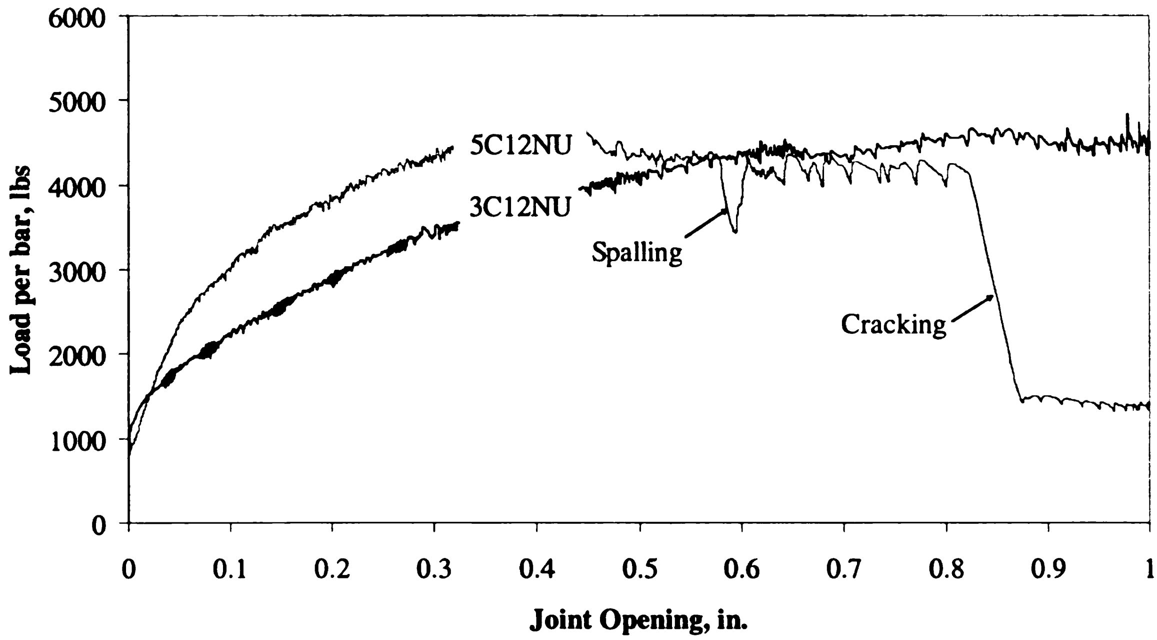

Figure 4.56. Comparison of load vs joint opening curves of 3C12NU and 5C12NU

A comparison of the loads at ¼ and ½ in. joint openings for different misalignment scenario has been presented in figures 4.57 and 4.58. In general, these graphs substantiate the fact that for a given misalignment magnitude, the trend of load versus misalignment type (horizontal, vertical and combined) is inconclusive. However, the following trends of loads at ¼ and ½ in. joint openings have been observed:

- 2-dowel non-uniform orientation: V < H < C
- 2-dowel uniform orientation: H < C < V
- 3 and 5-dowel non-uniform orientation (all misaligned): H << V< C

In the 1-dowel misalignment and the alternate dowels misalignment series, the trend is inconclusive. The trend of load vs misalignment type, for the 3 and 5-dowel non-uniform misalignment series presented before is further supported by figures 4.59 and 4.60.

It has to be to noted that two tests may have the same load at a ¼ in. joint opening but might exhibit totally different behavior at a later joint opening because the loads are equal but not the stress states at the dowel-concrete interface. For example, the 1H34 and 2H34NU curve have similar loads at ¼ in. joint opening but the load vs joint opening curve for the 1H34 test flattened and formed a plateau at later stages and no distress whatsoever was observed while in 2H34NU the stresses due to lockup caused the curve to follow an increasing trend and lead to a sudden drop at a joint opening of 0.72 in. as a result of cracking. Thus, these bar graphs are useful to get an overview of the trend of the load vs misalignment features but concluding purely based on these graphs is not warranted. Before making any conclusions, the trends have to be analyzed in conjunction of the corresponding load vs joint opening curves.

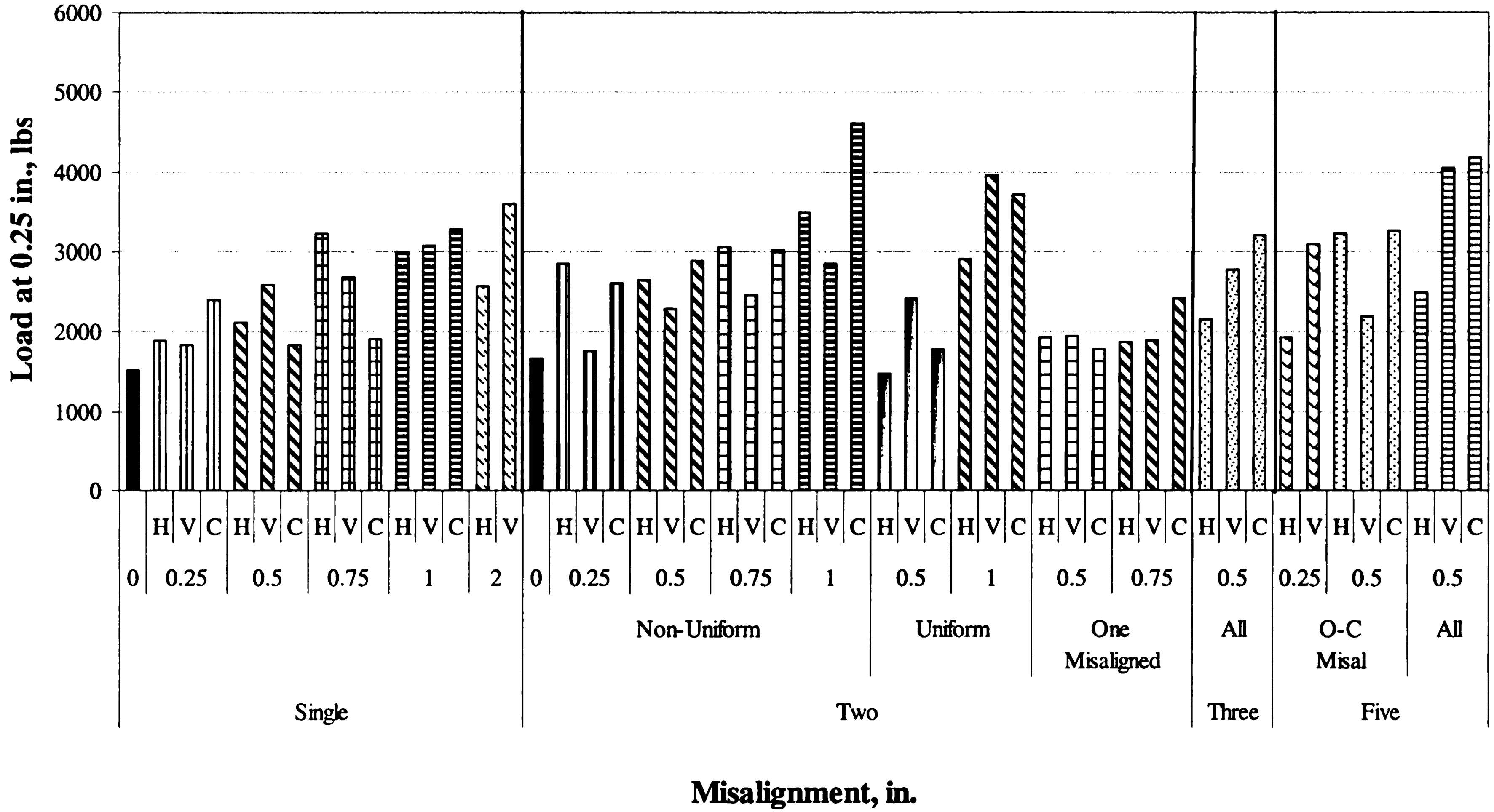

Figure 4.57. Comparison of loads at ¼ in. across different tests of misalignment

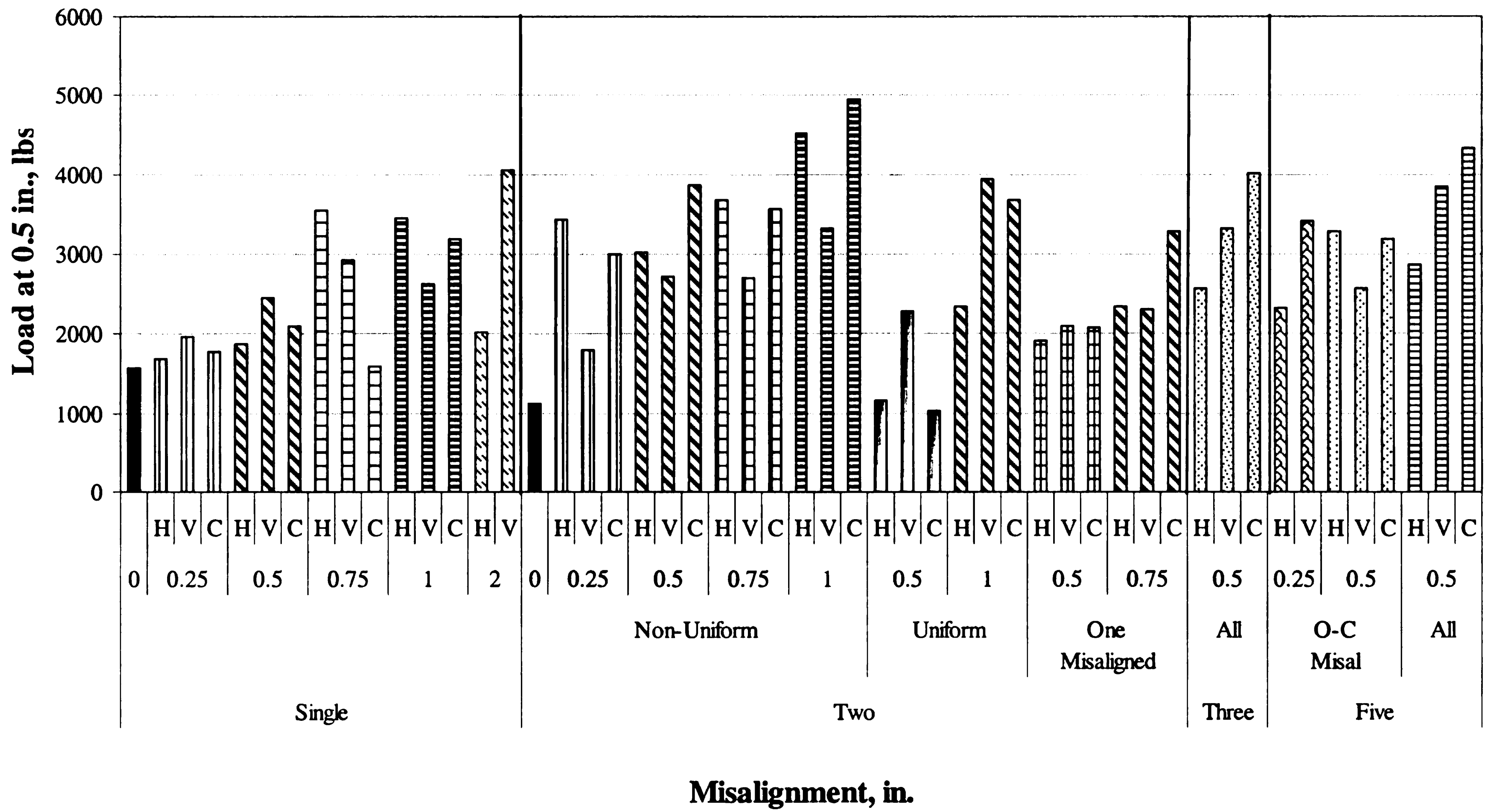

Figure 4.58. Comparison of loads at ½ in. across different tests of misalignment

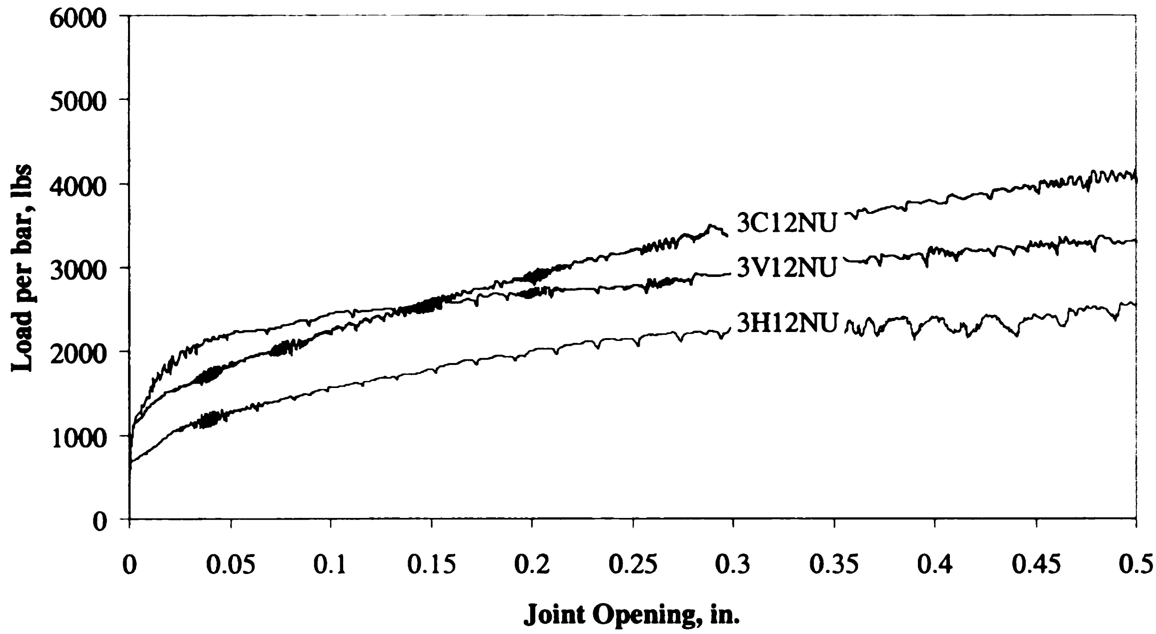

Figure 4.59. Comparison of load vs joint opening curves (3H12NU, 3V12NU, and 3C12NU)

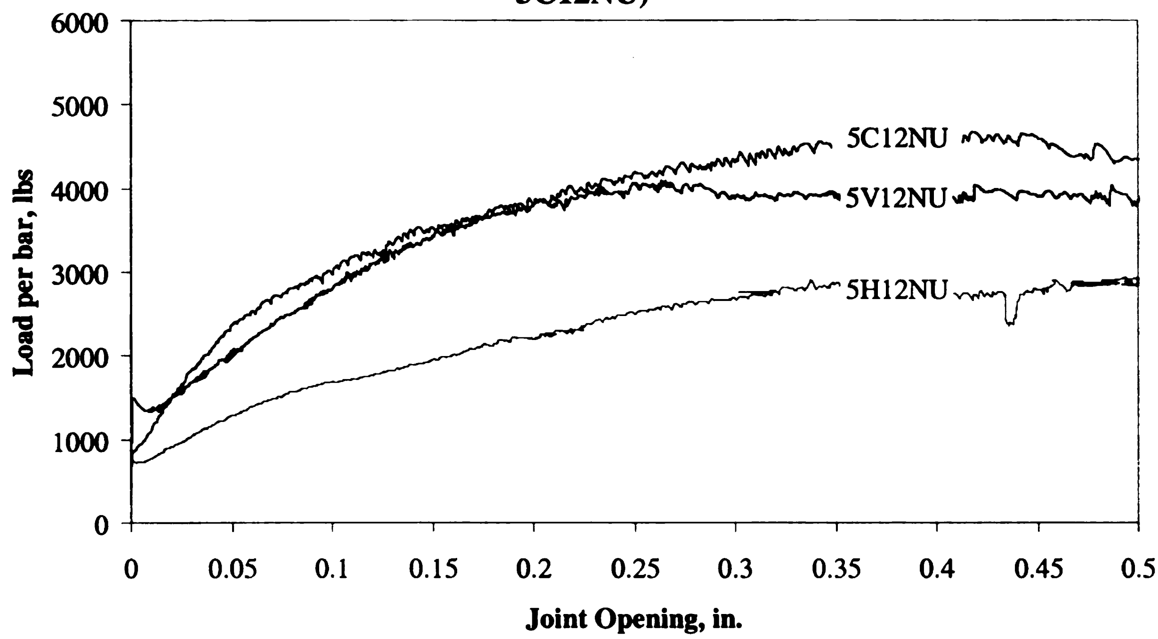

Figure 4.60. Comparison of load vs joint opening curves (5H12NU, 5V12NU, and 5C12NU)

4.4 LOAD ZONE PREDICTION

Based on the load vs joint opening behavior data from the 1-dowel and 2-dowel tests, regions were developed, where the load vs joint opening curve would be expected to lie, given the number of bars and misalignment orientation (figures 4.61 and 4.62). The misalignment magnitudes covered under the regions vary from 0 or aligned to 1 in. misalignment, over half length of the bar i.e. 9 in. Since the load per bar curves for different misalignment types lie close to each other the region has been generalized to all misalignment types. The range or extent of the load regions in the 1 and 2-dowel tests were used to develop similar regions for the 3 and 5-dowel tests. It has to be noted that Figure 4.61 has been developed for small slab specimens (2' X 4') and Figure 4.62 has been developed for big slab specimens (3' X 8'). However, it has to be noted that these regions are applicable to similar volumes of concrete as in the lab setup only.

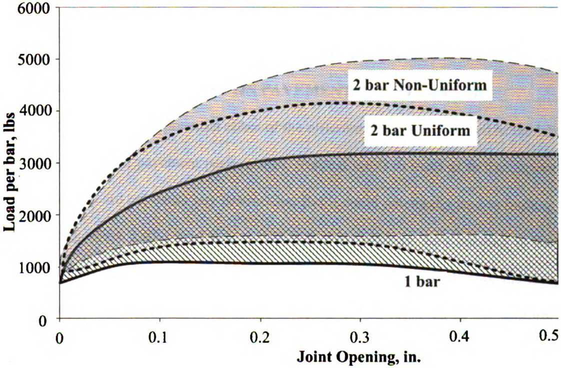

Figure 4.61. Regions for 1 and 2-dowel systems

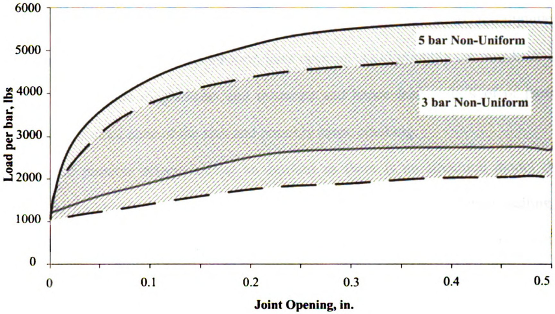

Figure 4.62. Regions for 3 and 5-dowel systems

4.5 EFFECT ON MISALIGNMENT ON PAVEMENT PERFORMANCE

The next step is to study the potential effect of the different distresses observed in the lab due to misalignment on pavement performance. Vertical uplift in itself as in the current experimental setup did not cause any destruction. But it could potentially lead to faulting and or cracking when traffic load acts on the slab. Non-uniform joint opening in the current setup did not lead to any destruction because the longitudinal edges of the slab had no restraint. In the lab, non-uniform joint opening was observed in the uniform (2H1U and 2C1U) as well as non-uniform orientation (2V1NU, 5H12NU, and 5V12NU) tests. In case of non-uniform orientation it was accompanied by other distresses also. However, in field conditions adjacent lanes and shoulder could cause increase in the concrete stresses and cause cracking. Poblete et.al. (1988) conducted a field study on thermal deformations of undoweled slabs and they found that in the presence of positive gradients higher than the "built-in curl", the slabs are normally expanded and since rotation at their transverse edges is restricted, a cylindrical shape around the longitudinal axis is imposed on the slab with its longitudinal edges supported. Thus, misalignment conditions that could lead to non-uniform joint opening could possibly cause cylindrical shape of the slab due to gradients and restraints and hence lead to lack of or partial support in the central zone of the slab and possibly cause cracking.

These possible effects cannot be verified as there is no structural model that accounts for the change in bearing stress due to dowel misalignment. Relating spalling at the dowel-concrete interface to pavement performance was attempted as described in the following paragraphs.

Spalling at the dowel-concrete interface could possibly lead to dowel looseness which is defined below. Dowel looseness is said to occur when voids develop underneath the dowel bar when the concrete near the dowel has got crushed and these crushed concrete particles are removed. Dowel looseness is also possible if the dowel-concrete bearing stress is very high (FHWA 2005). Dowel looseness can arise from poor construction techniques as well as damage to the surrounding concrete under cyclic loading (Davids 1998).

EverFE2.24 developed by Davids (1998) was used to study the theoretical effect of dowel looseness on different pavement responses. Dowel looseness as defined in EverFE2.24 is illustrated in Figure 4.63. The assumed gap γ tapers parabolically from a maximum value to zero over length L of the embedded dowel.

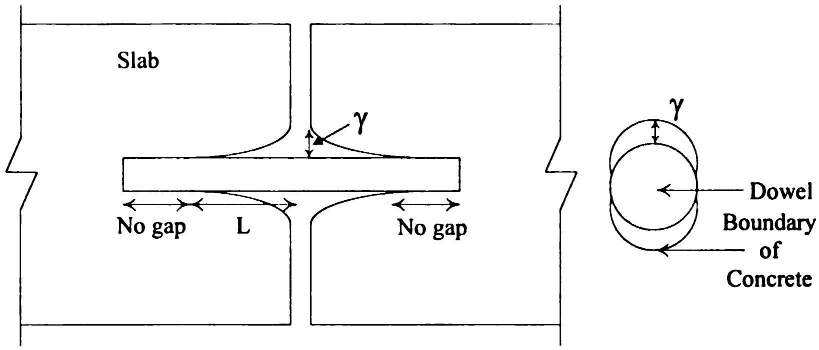

Figure 4.63. Dowel Looseness

A sensitivity analysis was performed on a 2-slab system with 15 ft joint spacing for different levels of looseness, the inputs of which are summarized in Table 4.7. L was maintained at 4 in. in all the cases. The loading configuration is shown in . The thermal gradients were based on the data for Detroit obtained using the Enhanced Integrated Climatic Model (EICM).

Table 4.7. Input Parameters for Sensitivity Analysis

Parameter	Values considered
Slab thickness and dowel diameter	10 in., 1.25 in. spaced 12 in. on center
System	• Slab on 6 in. granular base and 10 in. sand subbase (elastic foundation) • Slab on subgrade with effective k (dense liquid foundation)
γ	0, 0.0025, 0.005, 0.01, 0.02 in.
Thermal gradient (over 10 in.)	22.3 °F, 0.1 °F, -6 °F, -9.3 °F
Analysis parameters	• Vertical deflection • Load transfer efficiency

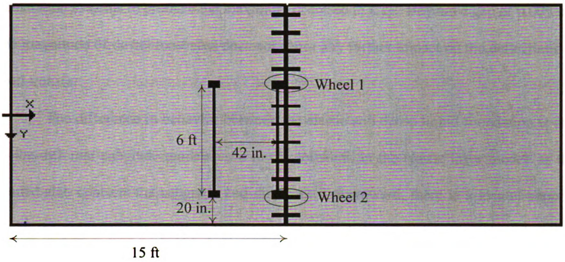

Figure 4.64. Screenshot of the Traffic loading location in EverFE

The relative vertical displacements of the two slabs grew with an increase in γ. The deflections on the loaded slab increased with an accompanying decrease in the unloaded slab deflections as the gap γ was increased. The load transfer efficiency (LTE) at the two wheel locations of the axle closer to the joint was studied and the effect of γ on loss of load transfer at these two locations is illustrated in figures 4.64 and 4.65. Figure 4.66 corresponds to the wheel location closer to the slab edge. In general, load transfer efficiency decreases with increasing dowel looseness up to a threshold value of the gap after which it tends to flatten out. The loss in LTE is more evident in the negative gradient cases. For a negative gradient of -9.3 °F, a dowel looseness of 0.0025 in. leads to a loss of LTE of nearly 30% when the slab is placed on an elastic foundation while the same gap leads to a loss of LTE of nearly 50% when the slab is placed directly on a dense liquid foundation. At points closer to the edge, the loss in LTE was higher and in some cases, there was no load transfer. For slabs on elastic foundation with positive gradient, there was just about 5% loss in load transfer. A smaller gap is required in dense liquid foundation systems to produce the maximum decrease in LTE. Beyond a gap of 0.005 in., the magnitude of dowel looseness does not cause any further impact on the deflections or load transfer.

The difference in behavior between the elastic and dense liquid foundation is due to the different subgrade models used in the software. In the elastic layer model, as the loaded slab contacts the subgrade and displaces it downward, there is a loss of support under the unloaded slab. With a dense liquid directly below the slab, the subgrade under the unloaded slab provides continuous support that is independent of the displacement of the loaded slab, tending to increase vertical displacements between the two slabs.

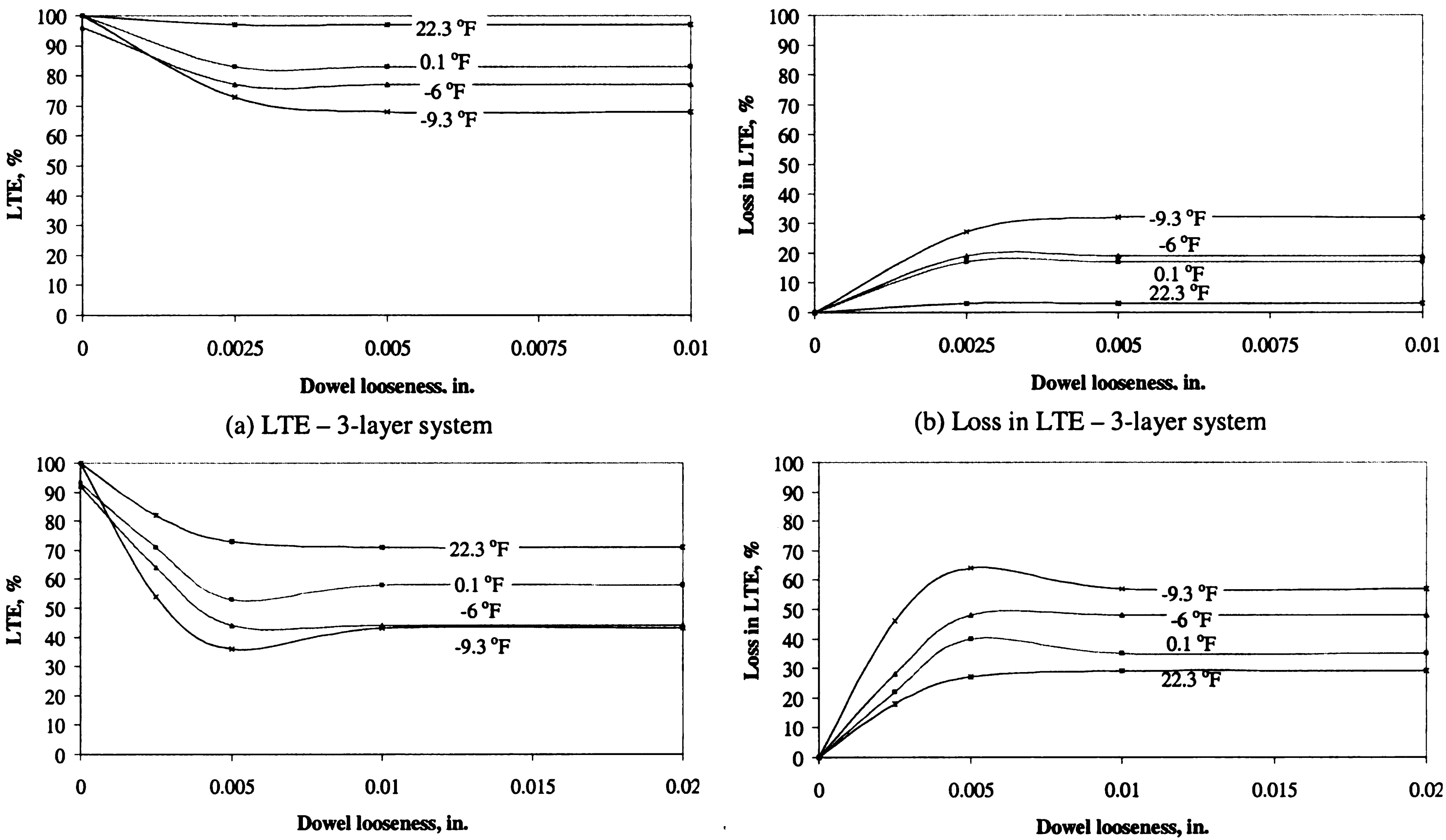

(a) LTE – 3-layer system

(b) Loss in LTE – 3-layer system

(c) LTE – Slab on subgrade with effective k

(d) Loss in LTE – Slab on subgrade with effective k

Figure 4.65. Effect of dowel looseness on LTE near Wheel 1 of tandem axle

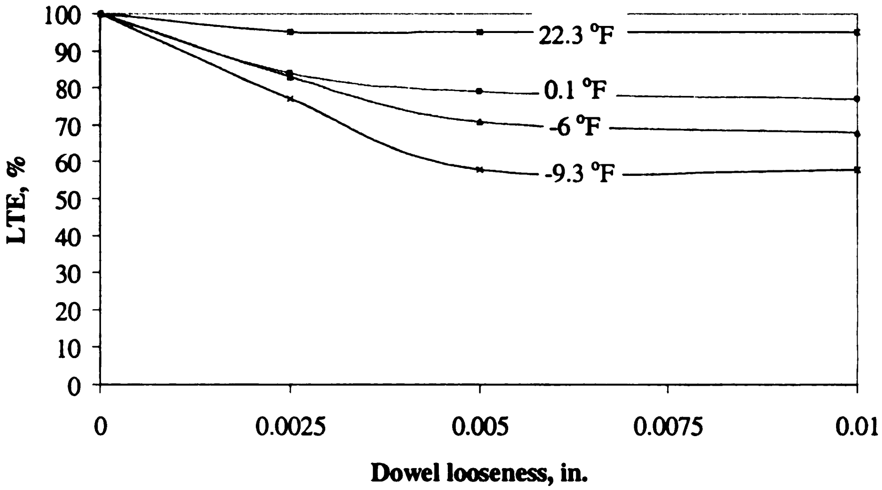

(a) LTE – 3-layer system

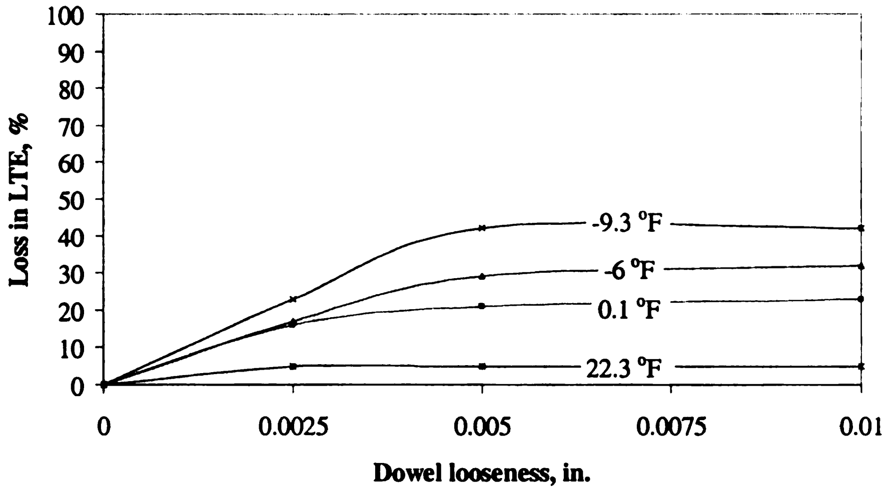

(b) Loss in LTE – 3-layer system

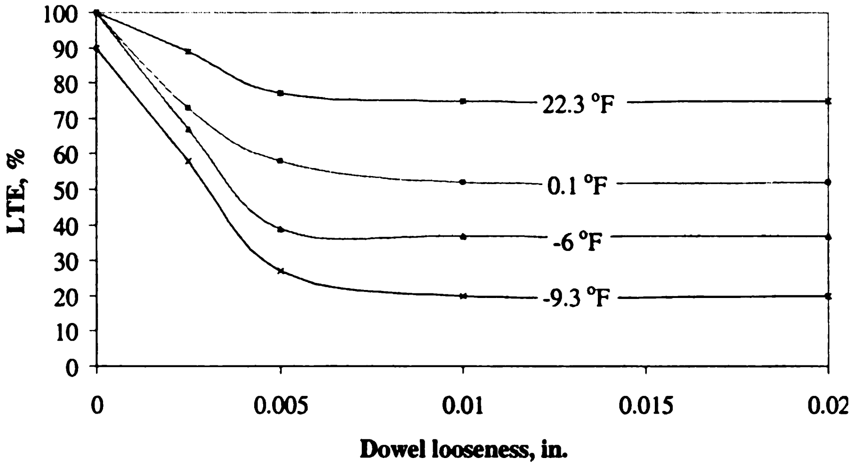

(c) LTE – Slab on subgrade with effective k

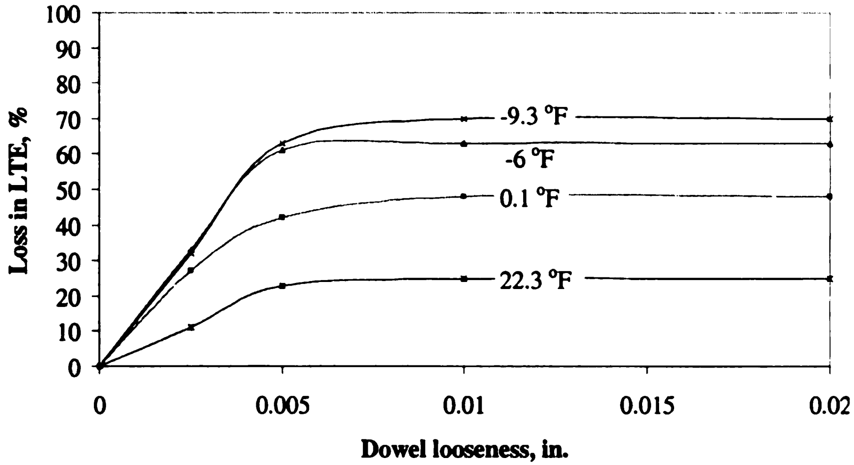

(d) Loss in LTE – Slab on subgrade with effective k

Figure 4.66. Effect of dowel looseness on LTE near Wheel 2 of tandem axle

CHAPTER 5 CONCLUSIONS AND RECOMMENDATIONS

5.1 CONCLUSIONS

To gain an insight into the effects of dowel misalignment on joint opening behavior, the objectives of this thesis were proposed as: to investigate experimentally the fundamental pullout behavior of misaligned dowel bars and gap-opening behavior of pavement joints with misaligned dowel bars in plain concrete pavements, under thermal expansion. It was initially hypothesized that the misalignment type and magnitude would affect the initial slip/debonding stress, type of joint and slab distresses observed, and post-slip behavior.

To systematically accomplish these objectives and test the hypotheses, an experimental plan was developed that focused on the following variables/misalignment features: number of dowel bars (1, 2, 3, or 5) and number misaligned (all or alternate), misalignment type (horizontal, vertical, or combined), orientation (uniform or non-uniform), and magnitude (0, ¼ , ½ , ¾ , 1, or 2 in.). Pullout tests simulating thermal expansion were carried out on all the tests listed in the experimental plan.

The experimental investigations were conducted on laboratory-scale pavement specimens with doweled contraction joints. Each pavement specimen consisted of (a) two 48 x 24 x 10 in. concrete slabs connected at the joint using 1 or 2 steel dowel bars or (b) two 96 x 36 x 10 in. concrete slabs connected at the joint using 3 or 5 steel dowel bars. Steel dowel bars that are 1.25 in. in diameter and 18 in. long were placed at the mid-depth at the joint, with equal lengths (9 in.) embedded in each concrete slab, and placed 12 in. on center. Each concrete slab was supported on smoothened rollers placed on hardened steel plates. The joint between the concrete slabs was formed using an ⅛ in. thick aluminum plate with circular holes of appropriate diameter to pass the dowel bars through it. After 7 days, the pavement specimen was tested by pushing apart the two concrete slabs using hydraulic actuators simulating thermal expansion at the approximate load rate of 20 lbs/min. followed by the opening displacement rate of approximately 0.02 in./min.

The concrete slabs were cast in-place directly in the molds. The concrete mixture was MDOT pavement mix grade P1 and the dowel bars were made of billet steel grade 40. After rough misalignment using a tape measure, each dowel was welded on one side and greased on the other half as per MDOT specification R-40-E. The dowel misalignments were adjusted and measured accurately (before placing the concrete), using total electronic stations (theodolites) and surveying techniques. The accuracy of the system was 0.005 rad.

Sliders and linear variable displacement transducers (LVDTs) were used to measure the transverse opening of the joint. The data from the different instrumentation was collected at the rate of 6 scans per second, using a data acquisition system.

The experimental setup/test procedure developed for the pullout of the slabs overcame most of the limitations of the previous dowel misalignment experimental studies. This thesis focused on the following additional details, in addition to, the basic pullout behavior studied in previous studies: bond stress behavior of dowel-concrete during pullout, relative effect of the misalignment orientation on load vs joint opening behavior, and tests on slabs accommodating five dowel bars. The high rate of data collection enabled better understanding of the pullout behavior, especially at smaller joint openings where debonding takes place between the dowel bar and concrete and the slope of the load vs joint opening curve is very high.

As a word of caution, all conclusions presented herewith have to be interpreted keeping in mind experimental variability and are valid for conditions of thermal expansion only.

Bond versus joint opening behavior: The bond stress versus joint opening curve has two distinct regions: (a) fully bonded region and (b) post-slip/debonded region. The first region is the high initial slope region where there is bond between the dowel bar and concrete. The applied pullout force which can be resolved in the axial and normal directions of the dowel bar is opposed only by the dowel-concrete bond force. Slip occurred after the bond stress per dowel increased beyond a certain threshold value which was found to be in the range 10-50 psi in the gamut of tests conducted. As further thermal expansion is induced, the forces induced in the dowel bar increase and depending on the misalignment, the induced force could form a plateau or increase causing failure of the test specimen due to cracking. Due to the presence of misalignment and joint opening, normal bearing stress in concrete is introduced and due to the frictional effect across the interface, shear stresses are developed.

Visual observations: The different joint and slab distresses observed during the tests include spalling of concrete near the dowel-concrete interface, cracking, non-uniform joint opening, and vertical uplift. The first three distresses are destructive even without traffic and/or restraints from the adjacent slabs and base while non-uniform joint opening and vertical uplift in the current setup of just thermal expansion are not destructive. Spalling was always observed only at the joint face of the slab containing the greased side of the dowel as this side slips out during the pullout test.

Load versus joint opening behavior: The key conclusions obtained in context of the load vs joint opening behavior are described below:

- Within a misalignment type, the load the load required per bar and the intensity of distresses increased with an increase in the misalignment magnitude.
- Degree of locking is higher in the non-uniform orientation of dowel bars and hence non-uniform misalignment tests were more destructive.
- For a given misalignment magnitude, the load required per bar and the intensity of distresses increased as the number of dowels misaligned increased.
- For a given misalignment magnitude, the overall trend of load versus type of misalignment (horizontal, vertical and combined) is unclear. However, the loads at ¼ and ½ in. joint openings followed typical trends in the 2, 3, and 5-dowel all misaligned tests. In the 2-dowel non-uniform and uniform orientation tests, the trend was V < H < C and H < C < V, respectively. In the 3 and 5-dowel non-uniform orientation series an H << V< C trend was observed. In the 1-dowel misalignment and the alternate dowels misalignment series, the trend is inconclusive.

The conclusions, visual observations as well as load versus joint opening behavior, are explained in context of the each misalignment type in the following paragraphs.

Horizontal Misalignment

- In the single dowel tests, spalling at the dowel-concrete interface was observed in the 2 in. test only. In the 2, 3, and 5-dowel tests, different combinations resulted in different distresses: spalling at the dowel-concrete interface, non-uniform joint opening, and cracking. Spalling was the predominant distress in these tests with spalls ranging from 2 in. by 2 in. to more than half-depth of the slab.

- Cracking occurred in tests with higher misalignment magnitudes and of the non-uniform orientation (2H34NU and 2H1NU) at high joint openings (equal to or greater than 0.5 in.).
- Non-uniform joint opening was observed in uniform (2H1U) as well as non-uniform misalignment (5H12NU) tests.
- In the 5-dowel all as well as alternate misalignment tests, spalling was found near the outer and center dowels.
- Non-uniform orientation of misalignment of two dowel bars required more load per dowel bar at a given joint opening as compared to the uniform orientation of dowels due to higher degree of locking.

Vertical Misalignment

- In the single dowel tests, no distresses were observed. In the 2, 3, and 5-dowel tests, different combinations resulted in different distresses: spalling at the dowel-concrete interface, non-uniform joint opening, vertical uplift, and cracking.
- Vertical uplift occurred in the tests with non-uniform orientation of dowels (2V12NU, 2V34NU, and 2V1NU).
- Non-uniform joint opening was observed in tests with non-uniform orientation (2V12NU and 5H12NU).
- In the 5-dowel all as well as alternate misalignment tests, spalling was found near the outer and center dowels.
- Uniform orientation of misalignment of two dowel bars required more load per dowel bar at a given joint opening as compared to the non-uniform orientation of dowels. In the test setup, there is more restraint against vertical uplift than horizontal rotation

and hence, in vertical misalignment tests the uniform orientation exhibited higher load vs joint opening behavior.

Combined Misalignment

- In the single dowel tests, spalling at the dowel-concrete interface was observed in the 1 in. test only. In the 2, 3, and 5-dowel tests, different combinations resulted in different distresses: spalling at the dowel-concrete interface, non-uniform joint opening, and cracking. Spalling was the predominant distress in these tests with spalls ranging from 2 in. by 2 in. to more than half-depth of the slab.
- Cracking occurred in tests with higher misalignment magnitudes and of the non-uniform orientation (2C34NU, 2C1NU, and 5C12NU) at high joint openings (equal to or greater than 0.5 in.).
- Non-uniform joint opening was observed in only one test (2C1U).
- In the 5-dowel all as well as alternate misalignment tests, spalling was found near the outer and center dowels.
- Non-uniform orientation of misalignment of two dowel bars required more load per dowel bar at a given joint opening as compared to the uniform orientation of dowels due to higher degree of locking.

Based on the load vs joint opening behavior data from the 1-dowel and 2-dowel tests, regions were developed, where the load vs joint opening curve would be expected to lie, given the number of bars and misalignment magnitude, under the lab conditions.

Spalling which was the main form of structural distress observed in the lab could possibly cause dowel looseness. A sensitivity analysis using EverFE2.24 revealed that looseness leads to higher relative vertical displacements between the loaded and the unloaded slabs and thus losses in load transfer efficiency. When subjected to a negative gradient of -9.3 °F, looseness of 0.0025 in. causes a loss of LTE of nearly 30%.

One of the significant contributions of this study apart from the conclusions stated above includes the load vs joint opening behavior from the single dowel bar tests. The bond shear stress-slip strain responses for the straight specimens (with zero misalignment) provide information regarding the overall longitudinal bond interaction between straight (aligned) dowels and the surrounding concrete and are critical in the analytical modeling of the dowel-concrete behavior. The bond shear stress-slip strain responses for the remaining specimens provide information regarding the longitudinal bond between the misaligned dowel and the surrounding concrete, while including the effects of friction and bearing stresses (from dowel misalignment).

5.2 RECOMMENDATIONS FOR FUTURE RESEARCH

To arrive at a definitive conclusion, tests with traffic as well as thermal loading have to be carried out and these were beyond the scope of this thesis. However, recommendations regarding the effects of different misalignment features on joint opening behavior are arrived at.

Each of the misalignment type, magnitude, and orientation would cause a specific certain stress state zone at the interface along the length of the bar and at the joint, which cannot be studied directly through lab observations/tests. The experimental results do not provide comprehensive knowledge of the mechanics of dowel-concrete interaction including: (a) the particular shear and normal stresses induced in the surrounding concrete by the dowel bar, (b) the effects of dowel misalignment on the stress-states induced in the concrete, and (c) the structural distresses produced by excessive stresses and stress concentrations. This knowledge is virtually impossible to obtain experimentally. Hence, analytical investigations based on the experimental results presented in this thesis, are needed to develop better understanding of the basic dowel-concrete interaction mechanics. Analytical studies on these lines have been initiated in the later phases of the MDOT project study.

APPENDIX A
DETAILS OF EXPERIMENTAL SETUP AND COMPONENTS

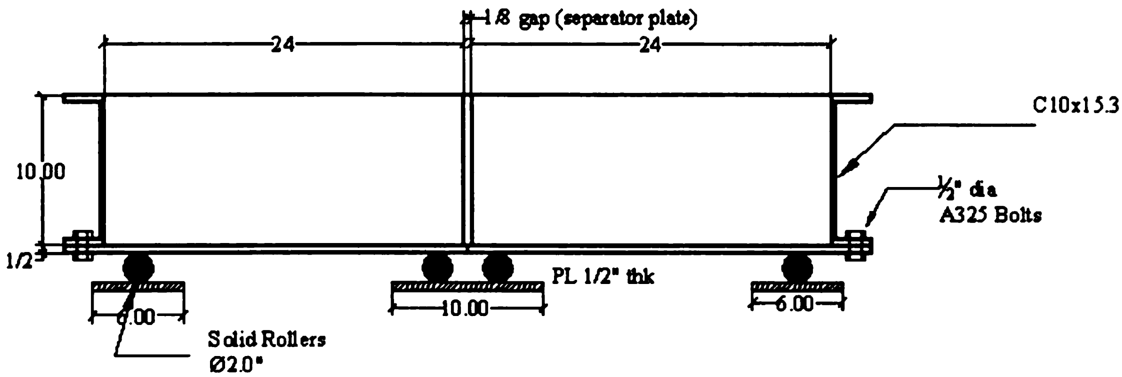

Figure A-1. Cross section of the small mold for pullout test

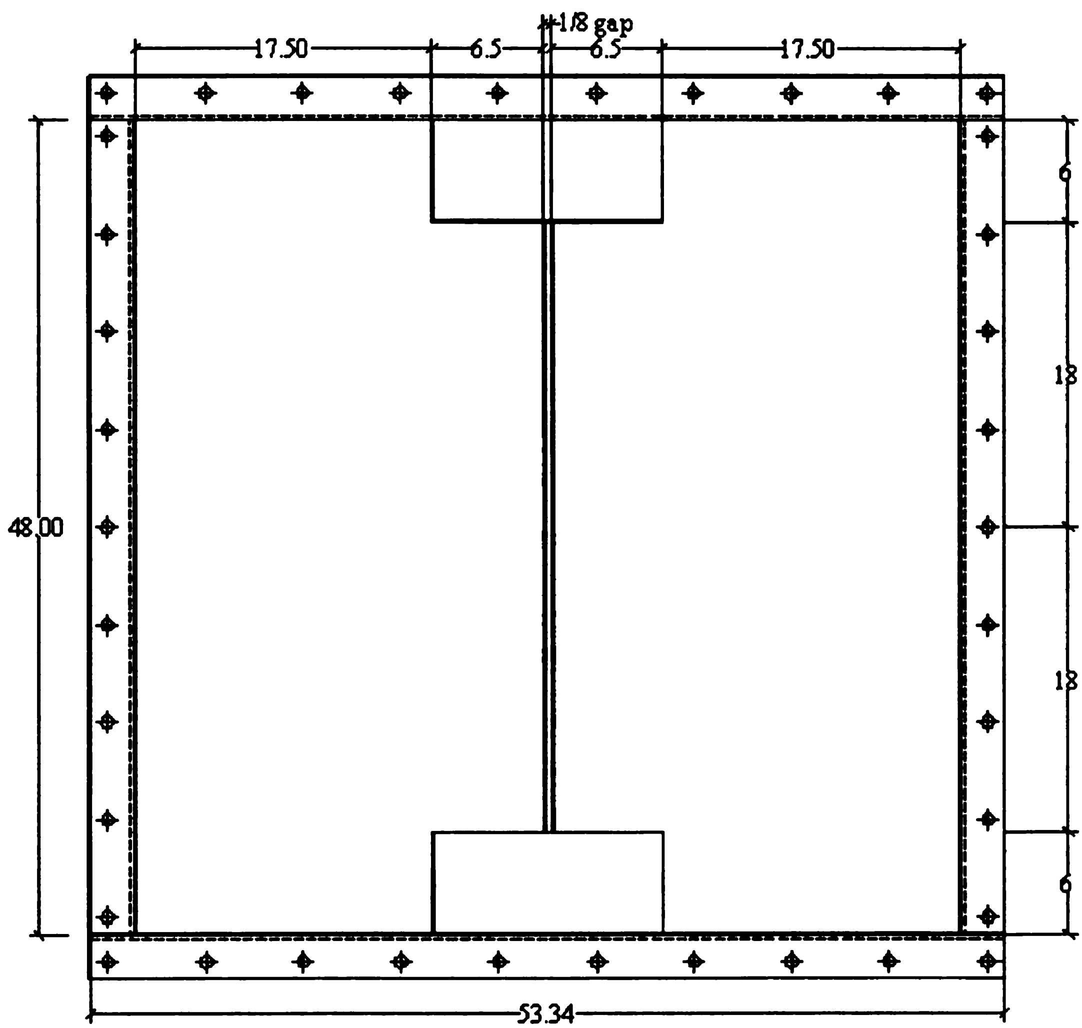

Figure A-2. Plan of the small mold with outside dimensions

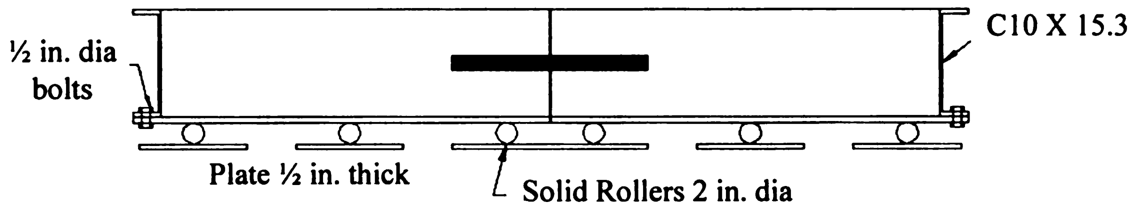

Figure A-3. Typical sectional view of the big mold

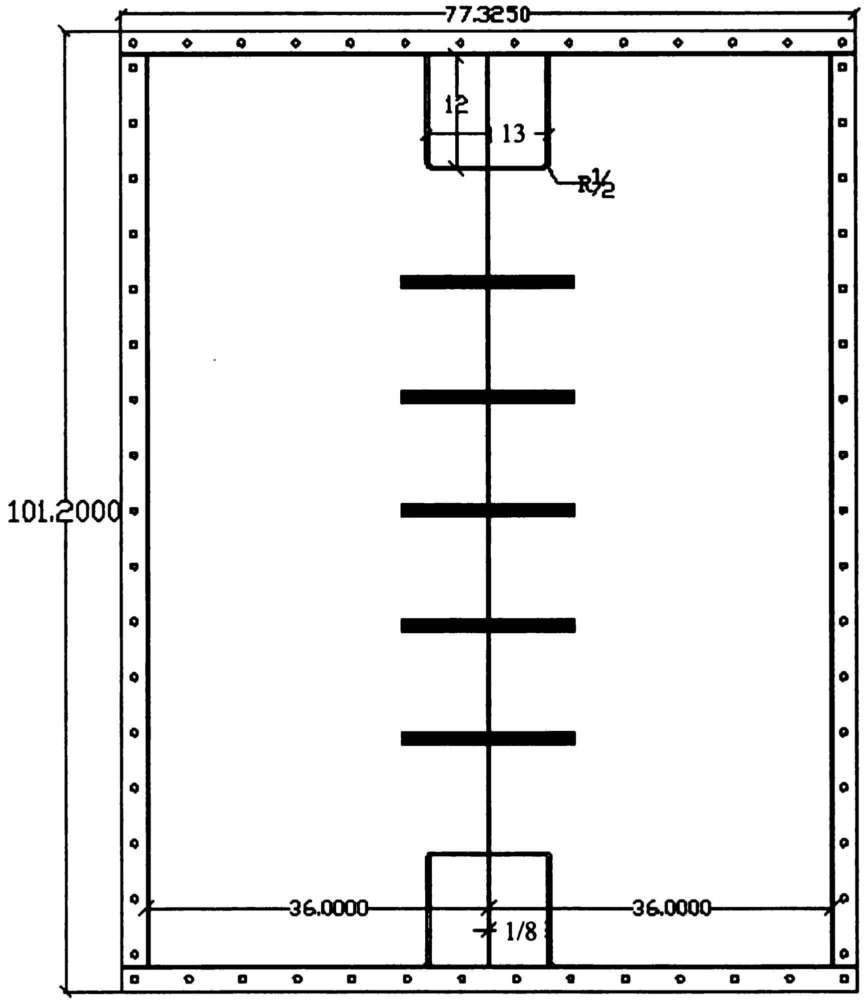

Figure A-4. Typical plan view of mold with 5 dowel bars

Table A-1. Mix Design Specifications

Specification: 2003 Standard Specifications
Grade of Concrete: P1
Intended Use of Concrete: Pavement Form

Material	Class	Specific Gravity	Absorption %
Cement	I/IA	3.13	
Fine Aggregate	2NS	2.61	1.47
Coarse Aggregate	6AA	2.66	1.50

Cement content	: 564 lb/yd^3	B/Bo	: 0.72
Air Content	(design): 6.5 % (specified): 6.5 %	Specification Tolerance	: 1.5 %
R.W.C	: 1.15	Theoretical Yield	: 100.00%
Fly Ash Content, lb/yd^3	: 0		

Weight of Coarse Aggregate (Dry/Loose) lb/ft^3	Aggregate and Water Proportions Quantities, lb/yd^3 of concrete		
	Fine Aggregate (Oven Dry)	Coarse Aggregate (Oven Dry)	Total Water
88	1330	1711	288
89	1313	1730	287
90	1297	1750	286
91	1280	1769	286
92	1264	1788	285
93	1247	1808	284
94	1231	1827	283
95	1214	1847	282
96	1198	1866	281
97	1181	1886	280
98	1164	1905	279

Typical Unit Weight (dry, loose) of coarse aggregate as described above is 93 lb/ft^3

Table A-2. Description of Linear Variable Differential Transducer

Model	LD610-15
Excitation Voltage	± 15 V@ 18 mA maximum
Output	± 10 V DC
Stroke	± 15 mm
Total Stroke	30 mm (1.18 in.)

Table A-3. Description of the Hydraulics (Actuators RC 156 and RC 256)

Name	Capacity (ton)	Stroke (in.)	Cylinder Effective Area (in.^{2})	Weight (lbs)
Actuator RC 156	15	6	3.14	15
Actuator RC 256	25	6	5.16	22

Calibration Procedure

A. Sliders and Linear Variable Differential Transducers

The calibration procedure of the LVDTs and sliders is described below:

- Precalibrated steel pieces of thicknesses 0.1 in. through 1.5 in. and 0.1 in. through 1.0 in. were used, for the 1.0 in. stroke and 1.5 in. stroke sliders, respectively.
- The sliders/LVDTs were excited at their respective excitation voltages (+5 V DC for sliders and ± 15 V DC for LVDTs) and the output voltage was recorded at every 0.1 in. increment using a multimeter.
- Graphs were plotted for the transducer stroke displacements (measured in inches) versus the output voltages.
- The calibration graphs for the sliders and LVDTs are presented in figures A-5 through A-13, respectively. The graphs were found to be linear in all cases.

B. Calibration of Hydraulics and Pressure Transducers

The calibration procedure of the actuators and pressure transducers are described below:

- For calibration of the actuators and pressure transducers, a MTS pre-calibrated machine in the lab was used to measure the load from the actuators.

- The actuators were placed one at a time between the two compression plates of the machine. A 10 V excitation DC voltage was applied to the pressure transducer to obtain the output between 0.5 V to 5 V.
- On application of pressure from the hand pump, the MTS machine readout gave the amount of load that the actuator was exerting on the plates.
- This readout at every 1000 psi load step was noted along with the voltage from the transducer.
- Graphs showing the load from the MTS vs. voltage were plotted and are shown in figures A-14 through A-17.
- A trendline superimposed on this graph showed that the relation of load vs. output voltage was linear and this calibrated curve was input in the data acquisition software.

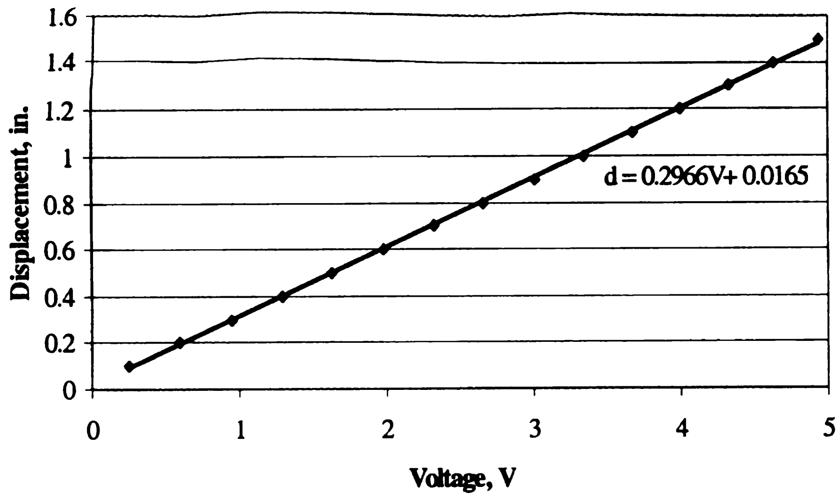

Figure A-5. Calibration of 1.5 in. slider-1

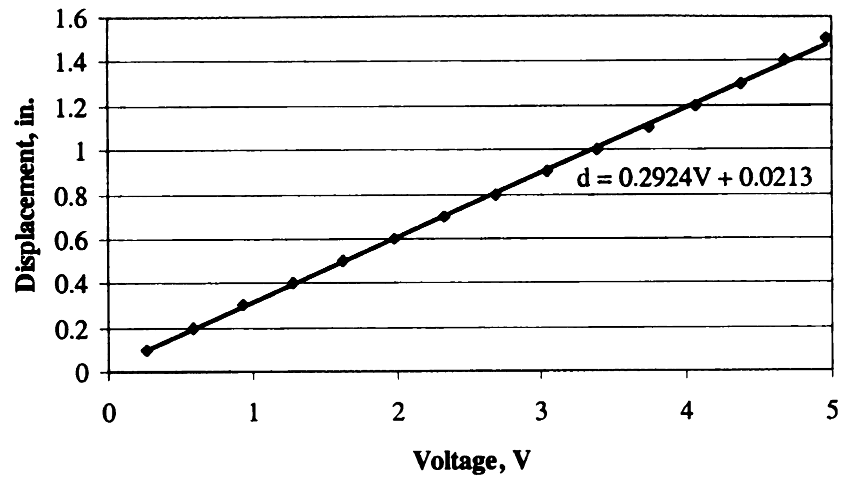

Figure A-6. Calibration of 1.5 in. slider-2

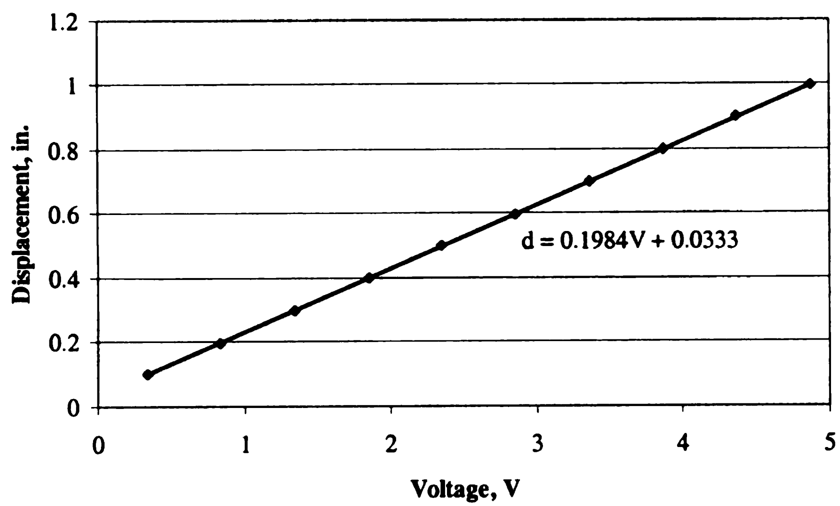

Figure A-7. Calibration of 1.0 in. slider-1

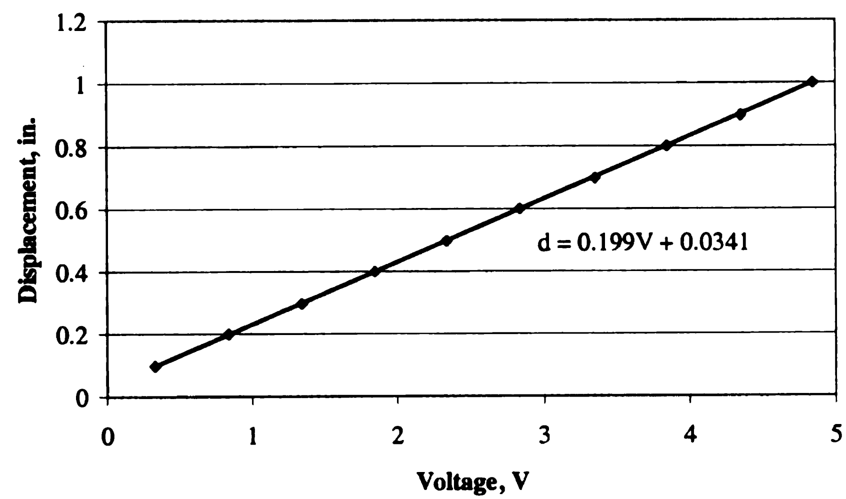

Figure A-8. Calibration of 1.0 in. slider-2

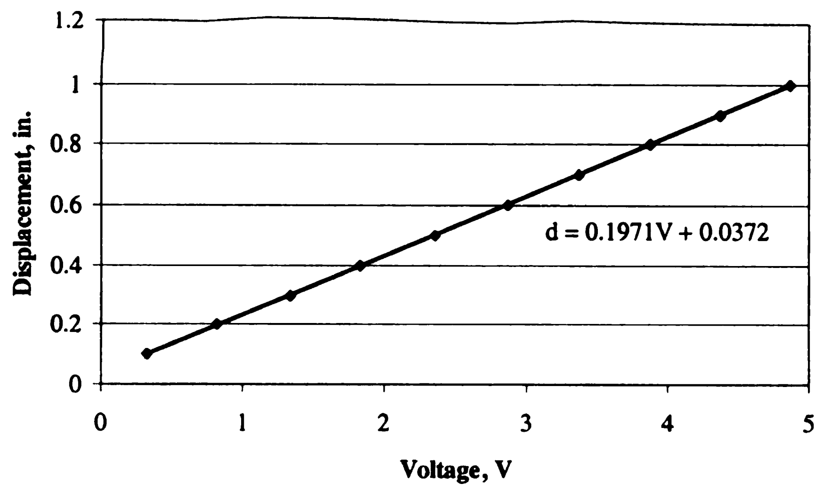

Figure A-9. Calibration of 1.0 in. slider-3

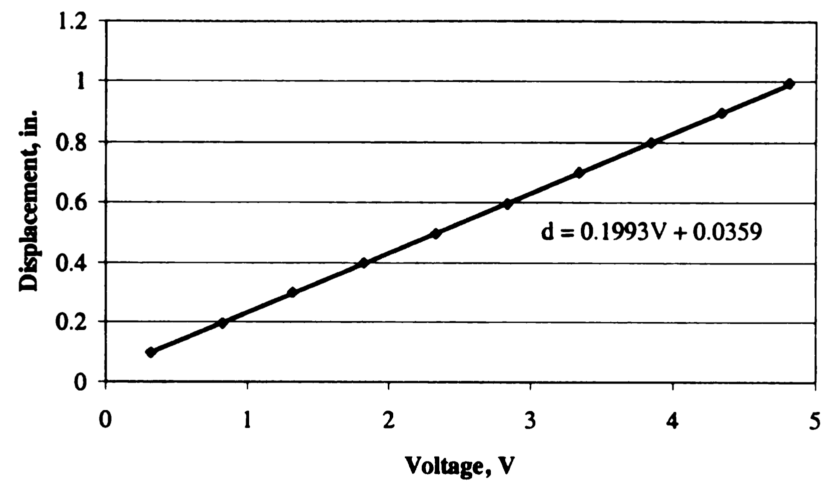

Figure A-10. Calibration of 1.0 in. slider-4

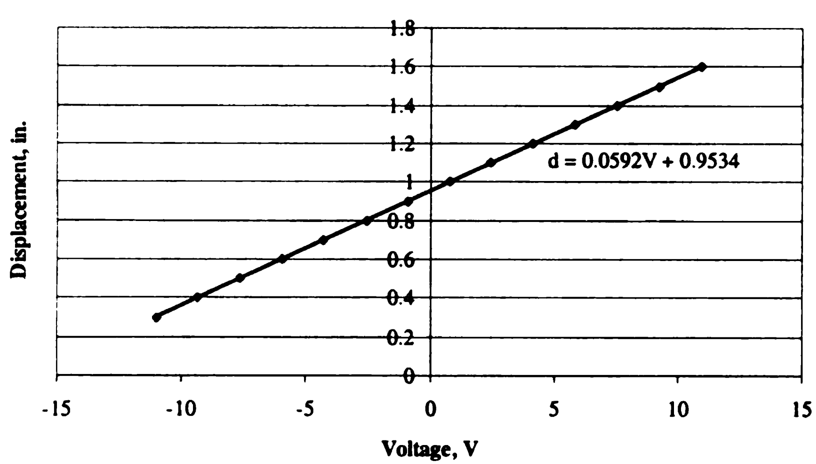

Figure A-11. Calibration of LVDT-1

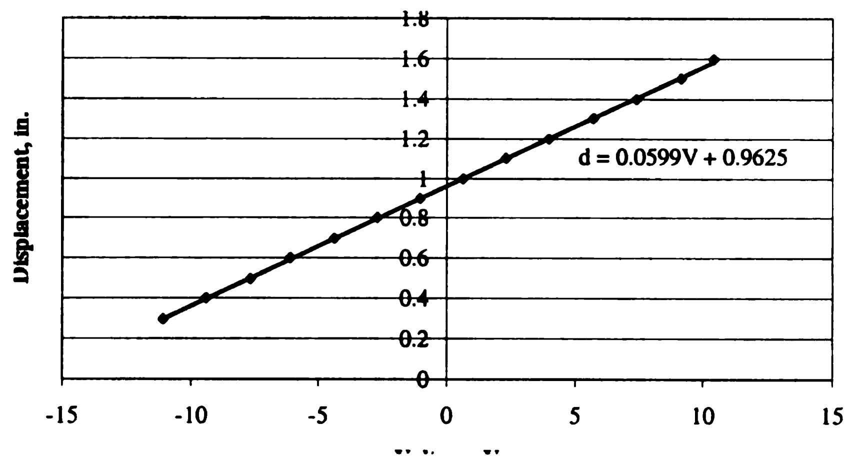

Figure A-12. Calibration of LVDT-2

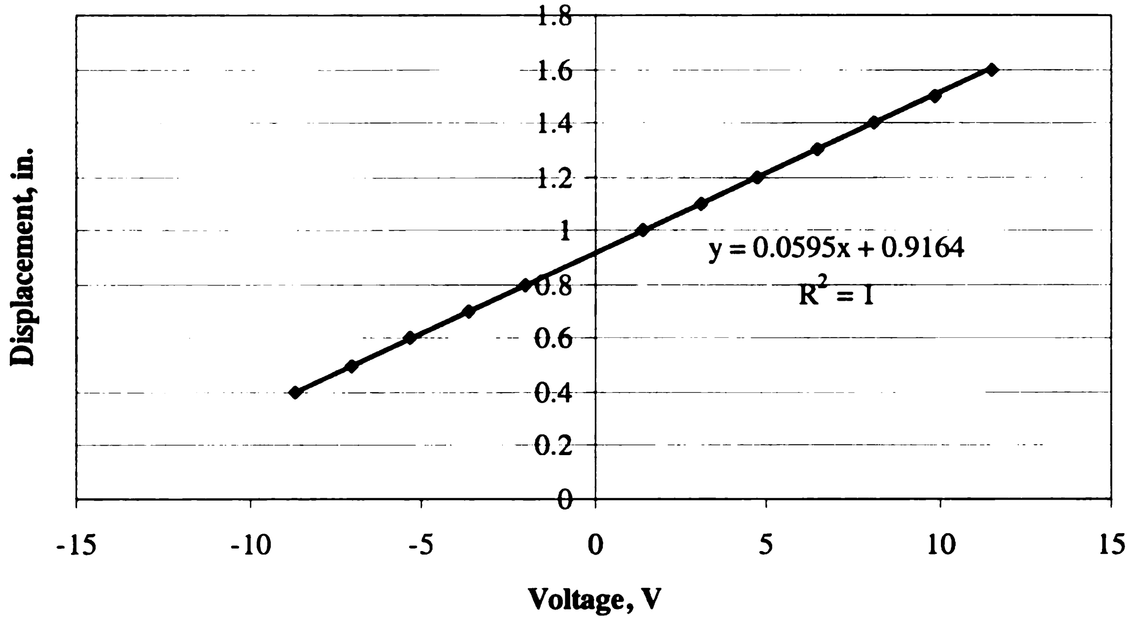

Figure A-13. Calibration of LVDT-3

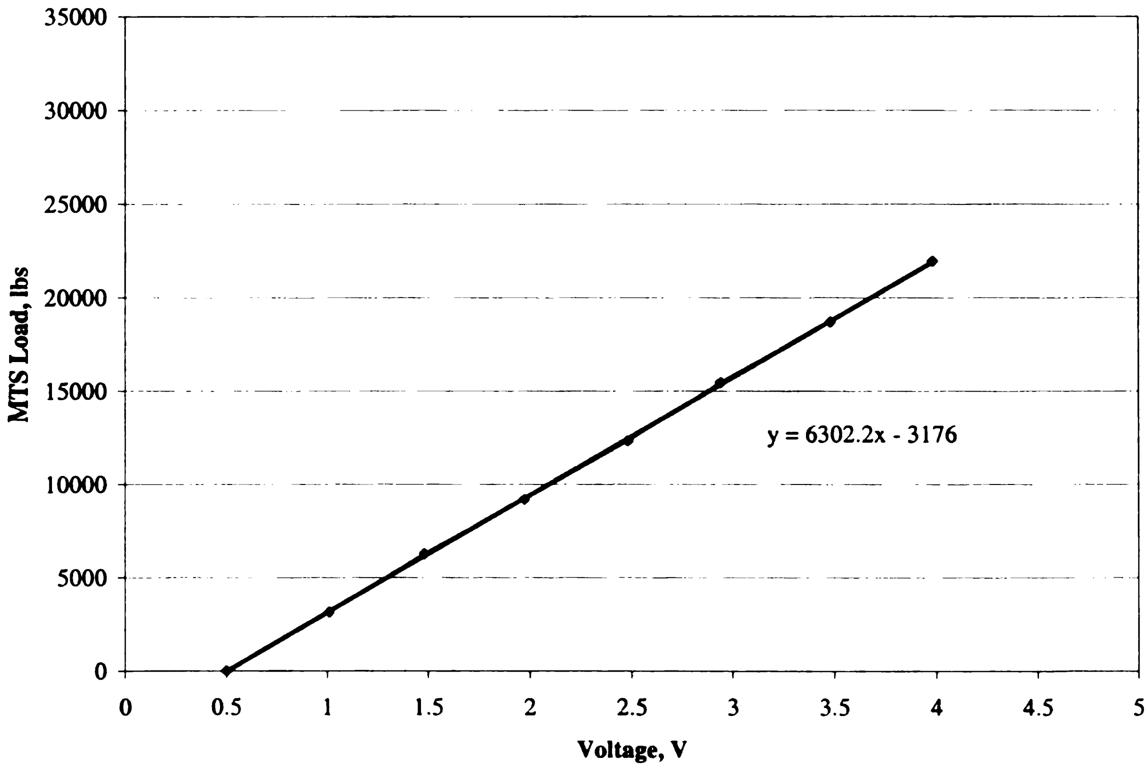

Figure A-14. Calibration of RC156 Actuator 1

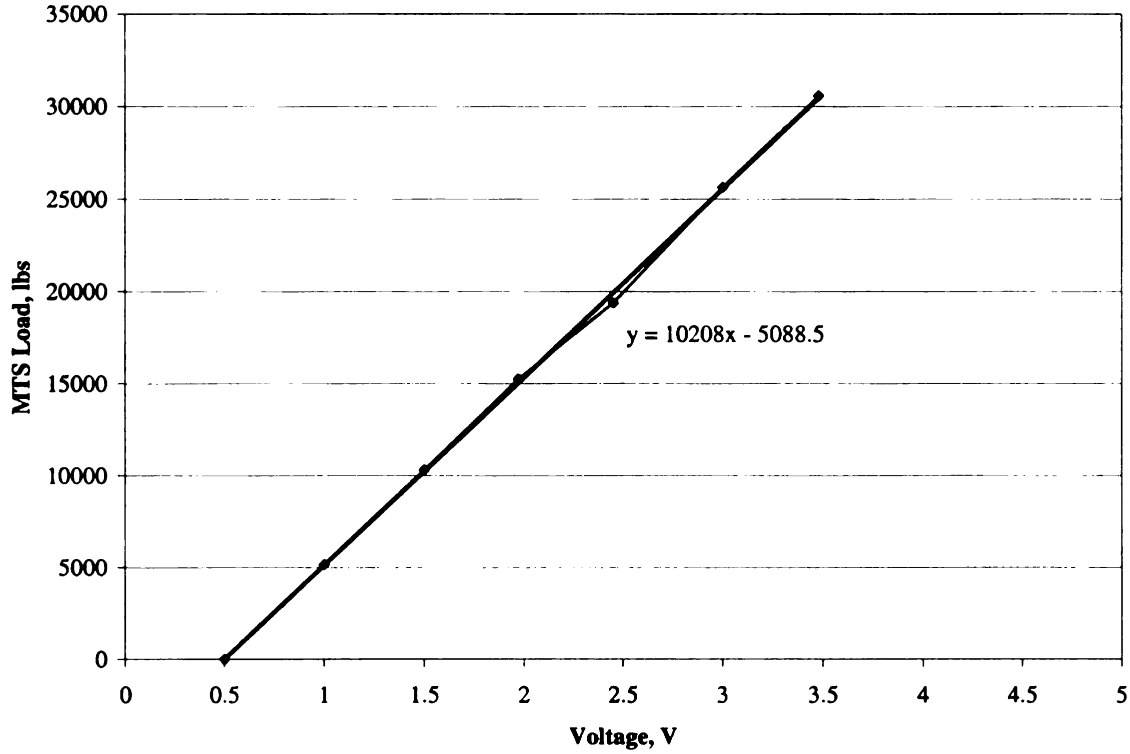

Figure A-15. Calibration of RC256 Actuator 1

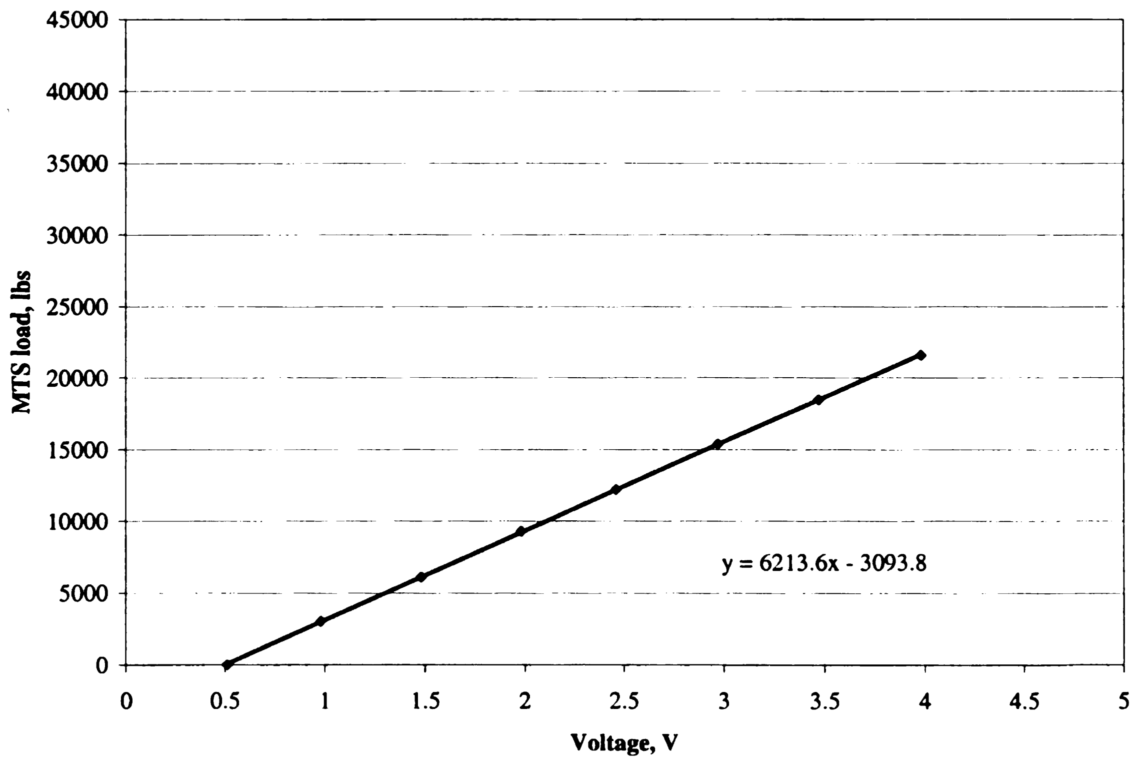

Figure A-16. Calibration of RC156 Actuator 2

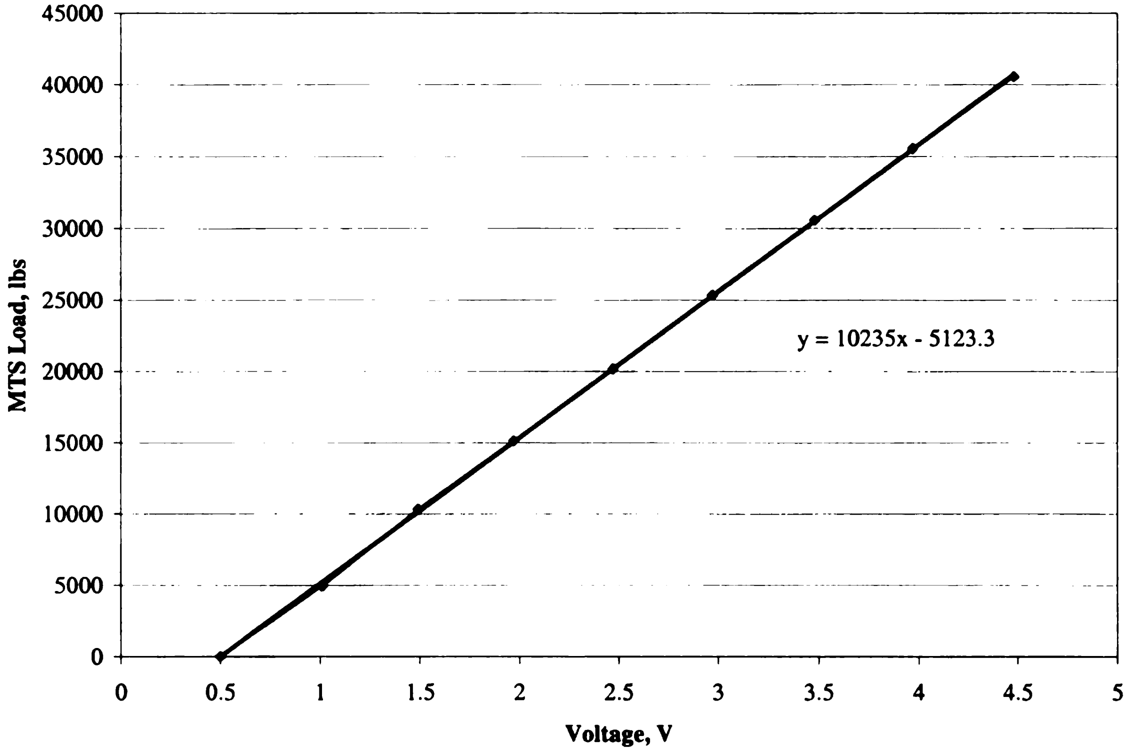

Figure A-17. Calibration of RC256 Actuator 2

Data Acquisition System

The data from the different instrumentation was collected at the rate of 6 scans per second, using a data acquisition system. The data acquisition system is capable of handling all the different instruments – sliders, LVDTs, and pressure transducers. The data flow is illustrated in Figure A-18.

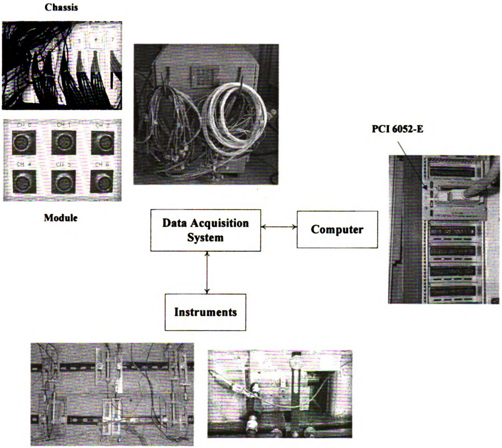

Figure A-18. Data Flow

The data acquisition system is designed to hold the chassis and provide access and power to each channel on the chassis. The chassis is the main unit which consists of all the channels of the data acquisition system. The chassis model is a SCXI-1001. The chassis consists of a series of modules connected together to form a unit. A module consists of a series of channels which are used for certain instrument types. For instance, module 1 consists of a series of modules connected together to form a unit. A module consists of a series of channels which are used for certain instrument types. For instance, module 1 consists of the first 32 channels and modules 2-7 all consist of eight strain gage channels. The modules are cards (SCXI-1102B or SCXI-1520) which can be individually removed from the chassis. Module 1 is a NI DAQ card termed SCXI-1102B and is the only module used in the pullout tests. Out of the 32 channels, channels 0-15 are three-wire connections, 16-25 are thermocouple connections, and channels 26-31 are four-wire connections. The three wire connections accommodate the sliders and the pressure transducers (Channels 0-15) while the four wire connections (Channels 26-31) accommodate the LVDTs. External power supplies are linked to the data acquisition system to provide the necessary excitation voltages for the different instruments.

The calibration files corresponding to the different instrumentation are fed into the computer. The instruments are connected to the different channels on the data acquisition system using connectors and wires. As shown in Figure A-18, the connection between the computer and the data acquisition system is established using a cable and the Analog-Digital card PCI 6052-E present in the computer. Measurement and automation explorer (MAX) is a DAQ program set up by National Instruments and is responsible for the configuring the computer to read the DAQ. This data is then converted to the corresponding measurement units by the software interface (Little General Version 6.1) using the calibration files mentioned earlier. Little General run off the configuration of MAX.

APPENDIX B
SURVEYING SUMMARY AND CALCULATIONS

Table B-1. Height Check Summary – One Dowel Tests

Type	Misalignment, in.	Height through surveying, in.		Actual Height, in.		Absolute Error, in.		Error, in.	
		West	East	West	East	West	East	West Side	East Side
Straight	0	5.074	5.028	5.00	5.00	0.074	0.028	>1/16 and <1/8	<1/16
		5.012	5.083	5.00	5.00	0.012	0.083	<1/16	>1/16 and <1/8
		5.028	5.022	5.00	5.00	0.028	0.022	<1/16	<1/16
V	0.25	5.168	4.804	5.25	4.75	0.082	0.054	>1/16 and <1/8	<1/16
	0.5	5.520	4.443	5.50	4.50	0.020	0.057	<1/16	<1/16
	0.75	5.816	4.312	5.75	4.25	0.066	0.062	>1/16 and <1/8	<1/16
	1_old	6.052	3.997	6.00	4.00	0.052	0.003	<1/16	<1/16
	1	5.922	4.099	6.00	4.00	0.078	0.099	>1/16 and <1/8	>1/16 and <1/8
	2	7.046	3.062	7.00	3.00	0.046	0.062	<1/16	<1/16
H	0.25	4.983	5.105	5.00	5.00	0.017	0.105	<1/16	>1/16 and <1/8
	0.5	5.069	5.095	5.00	5.00	0.069	0.095	>1/16 and <1/8	>1/16 and <1/8
	0.75	5.100	5.082	5.00	5.00	0.100	0.082	>1/16 and <1/8	>1/16 and <1/8
	1	4.926	5.122	5.00	5.00	0.074	0.122	>1/16 and <1/8	>1/16 and <1/8
	2	4.979	4.974	5.00	5.00	0.021	0.026	<1/16	<1/16
C	0.25	5.333	4.780	5.25	4.75	0.083	0.030	>1/16 and <1/8	<1/16
	0.5	5.593	4.549	5.50	4.50	0.093	0.049	>1/16 and <1/8	<1/16
	0.75_old	5.767	4.202	5.75	4.25	0.017	0.048	<1/16	<1/16
	0.75	5.821	4.237	5.75	4.25	0.071	0.013	>1/16 and <1/8	<1/16
	1	6.044	3.981	6.00	4.00	0.044	0.019	<1/16	<1/16

Table B-2. Height Check Summary – Two Dowel Tests (North Dowel)

Type	Misalign-ment, in.	Height through surveying, in.		Actual Height, in.		Absolute Error, in.		Error, in.	
		West	East	West	East	West	East	West	East
Straight	0	5.042	5.068	5.000	5.000	0.042	0.068	<1/16	>1/16 and <1/8
V	0.25	5.300	4.825	5.500	4.500	0.200	0.325	>1/16 and <1/8	>1/16 and <1/8
	0.5	5.599	4.580	5.500	4.500	0.099	0.080	>1/16 and <1/8	>1/16 and <1/8
	0.75	5.779	4.244	5.750	4.25	0.029	0.006	<1/16	<1/16
	1	6.027	4.042	6	4	0.027	0.042	<1/16	<1/16
	0.5_U	5.586	4.554	5.500	4.500	0.086	0.054	>1/16 and <1/8	<1/16
	1_U	6.070	4.217	6.0	4.0	0.070	0.217	>1/16 and <1/8	>1/16 and <1/8
H	0.25	5.080	4.972	5	5	0.080	0.028	>1/16 and <1/8	<1/16
	0.5	5.069	5.065	5.000	5.000	0.069	0.065	>1/16 and <1/8	>1/16 and <1/8
	0.75	5.045	5.049	5	5	0.045	0.049	<1/16	<1/16
	1	5.049	5.036	5	5	0.049	0.036	<1/16	<1/16
	0.5_U	5.030	5.037	5.000	5.000	0.030	0.037	<1/16	<1/16
	1_U	4.959	5.049	5.0	5.0	0.041	0.049	<1/16	<1/16
C	0.25	5.308	4.808	5.500	4.500	0.192	0.308	>1/16 and <1/8	>1/16 and <1/8
	0.5	5.567	4.552	5.500	4.500	0.067	0.052	>1/16 and <1/8	<1/16
	0.75	5.797	4.261	5.750	4.250	0.047	0.011	<1/16	<1/16
	1	6.057	3.959	6.0	4.0	0.057	0.041	<1/16	<1/16
	0.5_U	5.576	4.583	5.500	4.500	0.076	0.083	>1/16 and <1/8	>1/16 and <1/8
	1_U	5.930	4.066	6.0	4.0	0.070	0.066	>1/16 and <1/8	>1/16 and <1/8
V	0,0.5	5.115	5.055	5.000	5.000	0.115	0.055	>1/16 and <1/8	<1/16
	0,0.75	5.069	5.064	5.000	5.000	0.069	0.064	>1/16 and <1/8	>1/16 and <1/8
H	0,0.5	5.070	5.050	5	5	0.070	0.050	>1/16 and <1/8	<1/16
	0,0.75	5.021	5.063	5.000	5.000	0.021	0.063	<1/16	>1/16 and <1/8
C	0,0.5	4.997	5.043	5.000	5.000	0.003	0.043	<1/16	<1/16
	0,0.75	5.047	5.057	5.000	5.000	0.047	0.057	<1/16	<1/16

Table B-3. Height Check Summary – Two Dowel Tests (South Dowel)

Type	Misalign-ment, in.	Height through surveying, in.		Actual Height, in.		Absolute Error, in.		Error, in.	
		West	East	West	East	West	East	West	East
Straight	0	5.057	5.076	5.000	5.000	0.057	0.076	<1/16	>1/16 and <1/8
V	0.25	4.766	5.291	4.500	5.500	0.266	0.209	>1/16 and <1/8	>1/16 and <1/8
	0.5	4.430	5.547	4.500	5.500	0.070	0.047	>1/16 and <1/8	<1/16
	0.75	4.298	5.783	4.250	5.750	0.048	0.033	<1/16	<1/16
	1	4.074	6.066	4	6	0.074	0.066	>1/16 and <1/8	>1/16 and <1/8
	0.5_U	5.591	4.558	4.500	5.500	1.091	0.942	>1/16 and <1/8	>1/16 and <1/8
	1_U	6.078	4.208	6.0	4.0	0.078	0.208	>1/16 and <1/8	>1/16 and <1/8
H	0.25	5.031	4.903	5	5	0.031	0.097	<1/16	>1/16 and <1/8
	0.5	5.087	5.023	5.000	5.000	0.087	0.023	>1/16 and <1/8	<1/16
	0.75	5.095	5.025	5	5	0.095	0.025	>1/16 and <1/8	<1/16
	1	5.044	5.077	5	5	0.044	0.077	<1/16	>1/16 and <1/8
	0.5_U	5.084	5.111	4.500	5.500	0.584	0.389	>1/16 and <1/8	>1/16 and <1/8
	1_U	4.960	5.057	5.0	5.0	0.040	0.057	<1/16	<1/16
C	0.25	4.801	5.308	4.5	5.5	0.301	0.192	>1/16 and <1/8	>1/16 and <1/8
	0.5	4.600	5.534	4.500	5.500	0.100	0.034	>1/16 and <1/8	<1/16
	0.75	4.295	5.737	4.250	5.750	0.045	0.013	<1/16	<1/16
	1	4.030	5.964	4.0	6.0	0.030	0.036	<1/16	<1/16
	0.5_U	5.619	4.588	4.500	5.500	1.119	0.912	>1/16 and <1/8	>1/16 and <1/8
	1_U	5.961	3.999	6.0	4.0	0.039	0.001	<1/16	<1/16
V	0,0.5	4.581	5.548	4.500	5.500	0.081	0.048	>1/16 and <1/8	<1/16
	0,0.75	4.305	5.837	4.250	5.750	0.055	0.087	<1/16	>1/16 and <1/8
H	0,0.5	5.025	5.009	5	5	0.025	0.009	<1/16	<1/16
	0,0.75	4.935	4.959	5.000	5.000	0.065	0.041	>1/16 and <1/8	<1/16
C	0,0.5	4.589	5.472	4.500	5.500	0.089	0.028	>1/16 and <1/8	<1/16
	0,0.75	4.293	5.797	4.250	5.750	0.043	0.047	<1/16	<1/16

Table B-4. Height Check Summary – Three and Five Dowel Tests (Outer north dowel through outer south dowel)

Type	Dowels Misaligned	Misalignment, in.	Height through surveying, in.		Actual Height, in.		Absolute Error, in.		Error, in.	
			West	East	West	East	West	East	West	East
3C	All	0.5	5.491	4.575	5.5	4.5	0.009	0.075	<1/16	>1/16 and <1/8
			4.589	5.489	4.5	5.5	0.089	0.011	>1/16 and <1/8	<1/16
			5.509	4.585	5.5	4.5	0.009	0.085	<1/16	>1/16 and <1/8
3H	All		4.988	5.075	5	5	0.012	0.075	<1/16	>1/16 and <1/8
			5.056	5.063	5	5	0.056	0.063	<1/16	>1/16 and <1/8
			4.993	5.082	5	5	0.007	0.082	<1/16	>1/16 and <1/8
3V	All		5.591	4.577	5.5	4.5	0.091	0.077	>1/16 and <1/8	>1/16 and <1/8
			4.575	5.490	4.5	5.5	0.075	0.010	>1/16 and <1/8	<1/16
			5.559	4.569	5.5	4.5	0.059	0.069	<1/16	>1/16 and <1/8
5C	Outer & Center	0.5	5.391	4.596	5.5	4.5	0.109	0.096	>1/16 and <1/8	>1/16 and <1/8
		0	4.898	5.025	5	5	0.102	0.025	>1/16 and <1/8	<1/16
		0.5	4.416	5.574	4.5	5.5	0.084	0.074	>1/16 and <1/8	>1/16 and <1/8
		0	4.976	5.059	5	5	0.024	0.059	<1/16	<1/16
		0.5	5.393	4.568	5.5	4.5	0.107	0.068	>1/16 and <1/8	>1/16 and <1/8
5H	Outer & Center	0.5	5.079	-	5	-	0.079	-	>1/16 and <1/8	-
		0	5.045	-	5	-	0.045	-	<1/16	-
		0.5	4.926	-	5	-	0.074	-	>1/16 and <1/8	-
		0	5.106	-	5	-	0.106	-	>1/16 and <1/8	-
		0.5	4.959	-	5	-	0.041	-	<1/16	-
5H	All	0.5	5.153	5.033	5.000	5.000	0.153	0.033	>1/16 and <1/8	<1/16
		0.5	5.020	5.042	5.000	5.000	0.020	0.042	<1/16	<1/16
		0.5	4.949	5.110	5.000	5.000	0.051	0.110	<1/16	>1/16 and <1/8
		0.5	5.009	5.105	5.000	5.000	0.009	0.105	<1/16	>1/16 and <1/8
		0.5	5.047	5.106	5.000	5.000	0.047	0.106	<1/16	>1/16 and <1/8
5V	Outer & Center	0.5	5.447	4.596	5.5	4.5	0.053	0.096	<1/16	>1/16 and <1/8
		0	5.038	4.993	5	5	0.038	0.007	<1/16	<1/16
		0.5	4.549	5.465	4.5	5.5	0.049	0.035	<1/16	<1/16
		0	4.930	5.018	5	5	0.070	0.018	>1/16 and <1/8	<1/16
		0.5	5.561	4.503	5.5	4.5	0.061	0.003	<1/16	<1/16

Table B-5. Horizontal Misalignment Summary – One Dowel Tests

Type	Misalign-ment, in.	Distance through surveying, in.		Actual Distance, in.		Absolute Error, in.		Error, in.	
		West	East	West	East	West	East	West	East
H	0.25	0.270	0.244	0.250	0.250	0.020	0.006	<1/16	<1/16
	0.5	0.527	0.517	0.500	0.500	0.027	0.017	<1/16	<1/16
	0.75	0.778	0.783	0.750	0.750	0.028	0.033	<1/16	<1/16
	1	1.133	1.031	1.000	1.000	0.133	0.031	>1/16 and <1/8	<1/16
	2	2.083	2.032	2.000	2.000	0.083	0.032	>1/16 and <1/8	<1/16
C	0.25	0.252	0.316	0.250	0.250	0.002	0.066	<1/16	>1/16 and <1/8
	0.5	0.448	0.475	0.500	0.500	0.052	0.025	<1/16	<1/16
	0.75_old	0.839	0.739	0.750	0.750	0.089	0.011	>1/16 and <1/8	<1/16
	0.75	0.752	0.778	0.750	0.750	0.002	0.028	<1/16	<1/16
	1	0.955	1.041	1.000	1.000	0.045	0.041	<1/16	<1/16

Table B-6. Horizontal Misalignment Summary – Two Dowel Tests (North Dowel)

Type	Misalign-Ment, in.	Distance through surveying, in.		Actual Distance, in.		Absolute Error, in.		Error, in.	
		West	East	West	East	West	East	West	East
H	0.25	0.287	0.345	0.25	0.25	0.037	0.095	<1/16	>1/16 and <1/8
	0.5	0.520	0.500	0.500	0.500	0.020	0.000	<1/16	<1/16
	0.75	0.786	0.803	0.750	0.750	0.036	0.053	<1/16	<1/16
	1	0.998	0.976	1.000	1.000	0.002	0.024	<1/16	<1/16
	0.5_U	0.513	0.514	0.5	0.5	0.013	0.014	<1/16	<1/16
	1_U	1.093	1.031	1.000	1.000	0.093	0.031	>1/16 and <1/8	<1/16
C	0.25	0.276	0.276	0.250	0.250	0.026	0.026	<1/16	<1/16
	0.5	0.551	0.525	0.5	0.5	0.051	0.025	<1/16	<1/16
	0.75	0.754	0.763	0.750	0.750	0.004	0.013	<1/16	<1/16
	1	1.097	1.092	1.000	1.000	0.097	0.092	>1/16 and <1/8	>1/16 and <1/8
	0.5_U	0.552	0.479	0.5	0.5	0.052	0.021	<1/16	<1/16
	1_U	1.010	1.047	1.000	1.000	0.010	0.047	<1/16	<1/16

Table B-7. Horizontal Misalignment Summary – Two Dowel Tests (South Dowel)

Type	Misalign-ment, in.	Distance through surveying, in.		Actual Distance, in.		Absolute Error, in.		Error, in.	
		West	East	West	East	West	East	West	East
H	0.25	0.344	0.342	0.25	0.25	0.094	0.092	>1/16 and <1/8	>1/16 and <1/8
	0.5	0.486	0.505	0.500	0.500	0.014	0.005	<1/16	<1/16
	0.75	0.786	0.798	0.750	0.750	0.036	0.048	<1/16	<1/16
	1	0.983	0.961	1.000	1.000	0.017	0.039	<1/16	<1/16
	0.5_U	0.514	0.541	0.5	0.5	0.014	0.041	<1/16	<1/16
	1_U	1.021	1.021	1.000	1.000	0.021	0.021	<1/16	<1/16
C	0.25	0.259	0.277	0.250	0.250	0.009	0.027	<1/16	<1/16
	0.5	0.511	0.437	0.5	0.5	0.011	0.063	<1/16	>1/16 and <1/8
	0.75	0.762	0.736	0.750	0.750	0.012	0.014	<1/16	<1/16
	1	0.958	0.980	1.000	1.000	0.042	0.020	<1/16	<1/16
	0.5_U	0.513	0.514	0.5	0.5	0.013	0.014	<1/16	<1/16
	1_U	1.014	1.012	1.000	1.000	0.014	0.012	<1/16	<1/16
H	0.5	0.513	0.458	0.5	0.5	0.013	0.042	<1/16	<1/16
	0.75	0.693	0.762	0.750	0.750	0.057	0.012	<1/16	<1/16
C	0.5	0.473	0.477	0.5	0.5	0.027	0.023	<1/16	<1/16
	0.75	0.750	0.731	0.750	0.750	0.000	0.019	<1/16	<1/16

Table B-8. Horizontal Misalignment Summary – Three and Five Dowel Tests (Outer north dowel through outer south dowel)

Type	Dowels Misaligned	Misalign-ment, in.	Distance through surveying, in.		Actual Distance, in.		Absolute Error, in.		Error, in.	
			West	East	West	East	West	East	West	East
3C	All	0.5	0.517	0.526	0.5	0.5	0.017	0.026	<1/16	<1/16
		0.5	0.510	0.512	0.5	0.5	0.010	0.012	<1/16	<1/16
		0.5	0.515	0.416	0.5	0.5	0.015	0.084	<1/16	>1/16 and <1/8
3H	All	0.5	0.503	0.549	0.5	0.5	0.003	0.049	<1/16	<1/16
		0.5	0.501	0.510	0.5	0.5	0.001	0.010	<1/16	<1/16
		0.5	0.502	0.500	0.5	0.5	0.002	0.000	<1/16	<1/16
5C	Outer & Center	0.5	0.399	0.531	0.5	0.5	0.101	0.031	>1/16 and <1/8	<1/16
		0.5	-	-	-	-	-	-	-	-
		0.5	0.495	0.538	0.5	0.5	0.005	0.038	<1/16	<1/16
		0.5	-	-	-	-	-	-	-	-
		0.5	0.509	0.545	0.5	0.5	0.009	0.045	<1/16	<1/16
5H	All	0.5	0.513	0.482	0.5	0.5	0.013	0.018	<1/16	<1/16
		0.5	0.500	0.482	0.5	0.5	0.000	0.018	<1/16	<1/16
		0.5	0.499	0.540	0.5	0.5	0.001	0.040	<1/16	<1/16
		0.5	0.457	0.474	0.5	0.5	0.043	0.026	<1/16	<1/16
		0.5	0.515	0.514	0.5	0.5	0.015	0.014	<1/16	<1/16
5H	Outer & Center	0.5	0.473		0.5		0.027		<1/16	<1/16
		0.5	-	-	-	-	-	-	-	-
		0.5	0.489		0.5		0.011	0	<1/16	<1/16
		0.5	-	-	-	-	-	-	-	-
		0.5	0.507		0.5		0.007		<1/16	<1/16

Surveying Calculations

The algorithm used to compute the horizontal and vertical misalignments is explained here, along with examples to illustrate the procedure.

Measurement of Vertical Misalignment using Electronic Theodolite

Notations:

L = Distance between Station A and Station B

Horizontal Angles

θ_a= from Station A to the base plate (center of the base plate)

θ_b = from Station B to base plate (center of the base plate)

Vertical Angles

α_a = from Station A to the base plate (at the level of the base plate)

α_b = from Station B to base plate (at the level of the base plate)

β_a = from Station A to the dowel bar (at the level of the center of dowel bar)

β_b = from Station B to the dowel bar (at the level of the center of dowel bar)

A = Station A　　B = Station B

C = Base Plate (center)　　D = dowel bar (center)

E = height at eye level (center)

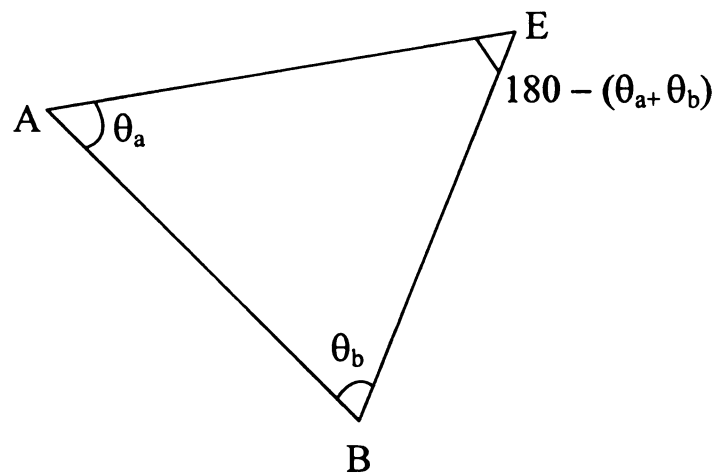

Figure B-1. Horizontal plane showing angles measured from center of base plate to misalignment

Referring to Figure B-1, in the horizontal plane,

For Δ ABE using sine rule: $AE = L\operatorname{cosec}(\theta_a + \theta_b)\sin(\theta_b)$

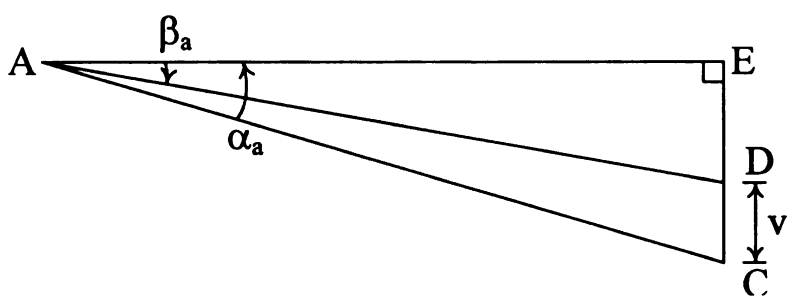

Figure B-2. Vertical plane in the center of the plate

Now with respect to the dowel at the center of the plate (Figure B-2):

The vertical height from the eye level to the base plate is $EC = AE\tan(\alpha_a)$.

The vertical height from the eye level to the center of the dowel bar is $ED = AE\tan(\beta_a)$.

The difference in the height taken from the eye level to the base plate and the center line of the dowel bar gives the vertical height, $V = EC - ED$

Therefore, vertical misalignment = V – 5 in. (mid height of the dowel)

Example Calculation for Vertical Misalignment of ½ in:

The sample calculations shown are for a vertical misalignment of ½ in on the east side of the test setup. Similar set of calculations are carried out on the west side.

Table B-9. Summary Table showing the various angles

Slab Designation	Location	EAST SIDE (L = 9.2')			
		Theodolite			Theoretical
		Degrees	Minutes	Seconds	Degrees
1V12 (½ in per half length)	θ_a	25	12	40	25.211
	θ_b	74	51	0	74.850
	α_a	333	44	20	333.739
	α_b	331	47	20	331.789
	β_a	335	39	40	335.661
	β_b	314	32	10	314.536

Referring to Figure B-1, for ΔABE using sine rule,

$$AE = L\operatorname{cosec}(\theta_a + \theta_b)\sin(\theta_b) = 108.227 \text{ in}$$

The vertical height from the eye level to the base plate is (Figure B-2):

$$EC = AE\tan(\alpha_a) = 53.397 \text{ in}$$

The vertical height from the eye level to the bottom edge of the dowel bar is:

$$ED = AE\tan(\beta_a) = 48.9549 \text{ in}$$

The difference in the height taken from the eye level to the base plate and dowel bar gives the distance from the base plate to the bottom edge of the dowel bar,

$$V = EC - ED = 4.4429 \text{ in}$$

Perfectly aligned bar will be at (base plate to center line of dowel bar) = 5 in.

Misalignment = 5 – 4.4429 = 0.557 in.

Error from desired misalignment = 0.557 – 0.5 = 0.057 in.

Measurement of Horizontal Misalignment using Electronic Theodolite

Notations:

L = Distance between Station A and Station B

Horizontal Angles

θ_a = from Station A to the base plate (center of the base plate)

θ_b = from Station B to base plate (center of the base plate)

γ_a = from Station A to the base plate (horizontal misalignment on the base plate)

γ_b = from Station B to base plate (horizontal misalignment on the base plate)

Vertical Angles

α_a = from Station A to the base plate (at the level of the base plate)

α_b = from Station B to base plate (at the level of the base plate)

δ_a = from Station A to the misaligned position on the base plate

δ_b = from Station B to the misaligned position on the base plate

ψ_a= from Station A to the dowel bar (at the level of the center of dowel bar)

ψ_b = from Station B to the dowel bar (at the level of the center of dowel bar)

A = Station A	B = Station B
C = Base Plate (center)	D = dowel bar (center)
E = height at eye level (center)	E = height at eye level (misaligned)
C' = Base Plate (misaligned)	D' = dowel bar (misaligned)

In the following surveying description the following are assumed:

1. The height of both the stations is equal
2. The two stations are parallel to the horizontal misalignment

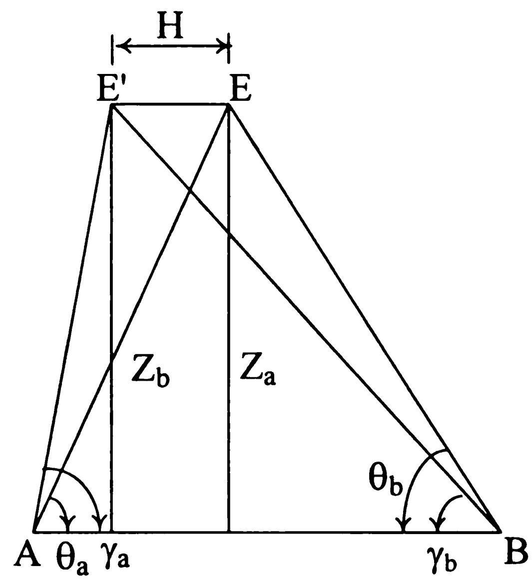

Figure B-3. Horizontal plane showing angles measured from center of base plate to misalignment

Referring to Figure B-3, in the horizontal plane,

For Δ ABE, using sine rule:

$$AE = L \operatorname{cosec}(\theta_a + \theta_b)\sin(\theta_b) \qquad BE' = L \operatorname{cosec}(\gamma_a + \gamma_b)\sin(\gamma_a)$$

To make sure that the two stations are parallel, the perpendicular distances (Z_a and Z_b) are compared:

$$Z_a = AE\sin(\theta_a) \qquad Z_b = BE'\sin(\gamma_b)$$

If, $Z_a \cong Z_b$, then the two stations are parallel to the horizontal misalignment.

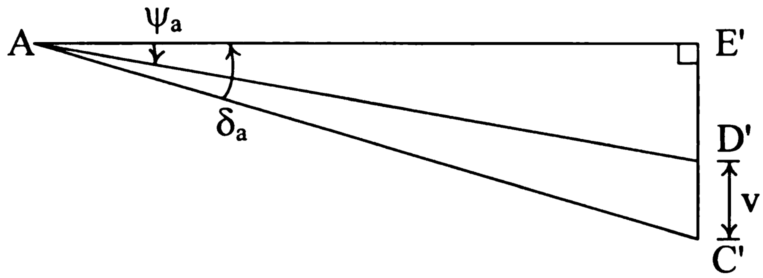

Figure B-4. Angles in the vertical plane, after forcing the misalignment of H

The vertical height from the eye level to the base plate is (Figure B-4):

$$E'C' = AE' \tan(\delta_a)$$

The vertical height from the eye level to the center of the dowel bar is

$$E'D' = AE' \tan(\psi_a)$$

The difference in the height taken from the eye level to the base plate and the center line of the dowel bar gives the vertical height: $V' = E'C' - E'D'$

Therefore, vertical misalignment = V' – 5 in. (mid height of the dowel)

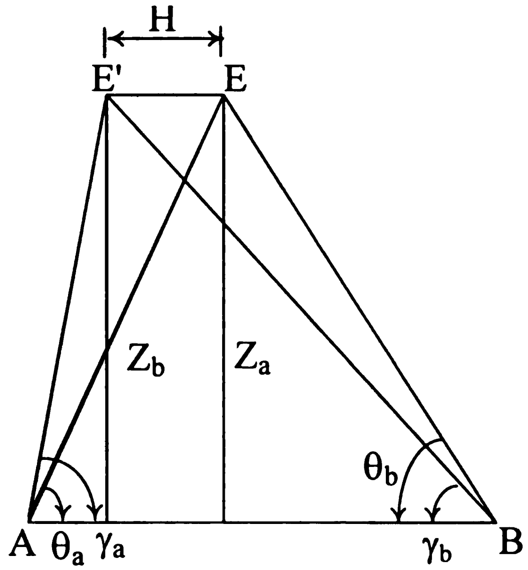

Figure B-5. Showing the final computation of the horizontal misalignment

For ΔABE', in horizontal plane, $AE' = Z\,\mathrm{cosec}(\gamma_a)$

Using cosine rule for $\Delta AEE'$ (Figure B-5):

$$H = \sqrt{AE^2 + \left(AE'\right)^2 - 2(AE)\left(AE'\right)\cos(\theta_a - \gamma_a)}$$

The H obtained is then compared with tape measure as a final check.

Example Calculation for Horizontal Misalignment of ½ in:

Table B-10. Summary Table showing all angles for horizontal misalignment

Slab Designation	Location	NORTH WEST SIDE (L = 5.7')				SOUTH EAST SIDE (L = 5.2')			
		Theodolite			Theoretical	Theodolite			Theoretical
		Deg	Min	Sec	Deg	Deg	Min	Sec	Deg
1H12 (½ in per half length)	θ_a	56	58	40	56.978	57	30	40	57.511
	θ_b	49	0	20	49.006	53	19	0	53.317
	γ_a	57	30	0	57.500	57	6	40	57.111
	γ_b	48	41	40	48.694	53	47	30	53.792
	α_a	317	58	30	317.975	319	53	20	319.889
	α_b	321	0	30	321.008	321	30	0	321.500
	β_a	321	6	40	321.111	323	13	40	323.228
	β_b	324	5	10	324.086	324	52	0	324.867
	δ_a	317	52	40	317.878	320	3	50	320.064
	δ_b	321	11	0	321.183	321	22	20	321.372
	ψ_a	321	0	30	321.008	323	24	0	323.400
	ψ_b	324	17	50	324.297	324	42	0	324.700

Referring to Figure B-3, in the horizontal plane,

For ΔABE, using sine rule,

$$AE = L\,\mathrm{cosec}(\theta_a + \theta_b)\sin(\theta_b) = 53.54 \text{ in.}$$

$$BE' = L\,\mathrm{cosec}(\gamma_a + \gamma_b)\sin(\gamma_a) = 56.09 \text{ in.}$$

To make sure that the two stations are parallel, the perpendicular distances, Z_a and Z_b are compared: $Z_a = AE\sin(\theta_a) = 45.16$ in. and $Z_b = BE'\sin(\gamma_b) = 45.27$ in.

If, $Z_a \cong Z_b$, then the two stations are parallel to the horizontal misalignment.

The vertical height from the eye level to the base plate is (from Figure B-4):

$$E'C' = AE' \tan(\delta_a) = 45.12 \text{ in.}$$

The vertical height from the eye level to the center of the dowel bar is

$$E'D' = AE' \tan(\psi_a) = 40.02 \text{ in.}$$

The difference in the height taken from the eye level to the base plate and the center line of the dowel bar gives the vertical height:

$$V' = E'C' - E'D' = 5.09 \text{ in.}$$

Therefore, vertical misalignment after forcing the misalignment in the horizontal plane should be = V' – 5 in. (mid height of the dowel) = 0.09 in

For Δ ABE', in horizontal plane,

$$AE' = Z \operatorname{cosec}(\gamma_a) = 53.89 \text{ in}$$

Using cosine rule for $\Delta AEE'$ (from Figure B-5):

$$H = \sqrt{AE^2 + (AE')^2 - 2(AE)(AE')\cos(\theta_a - \gamma_a)} = 0.5168 \text{ in}$$

The H obtained is then compared with tape measure as a final check.

APPENDIX C

BOND STRESS CURVES

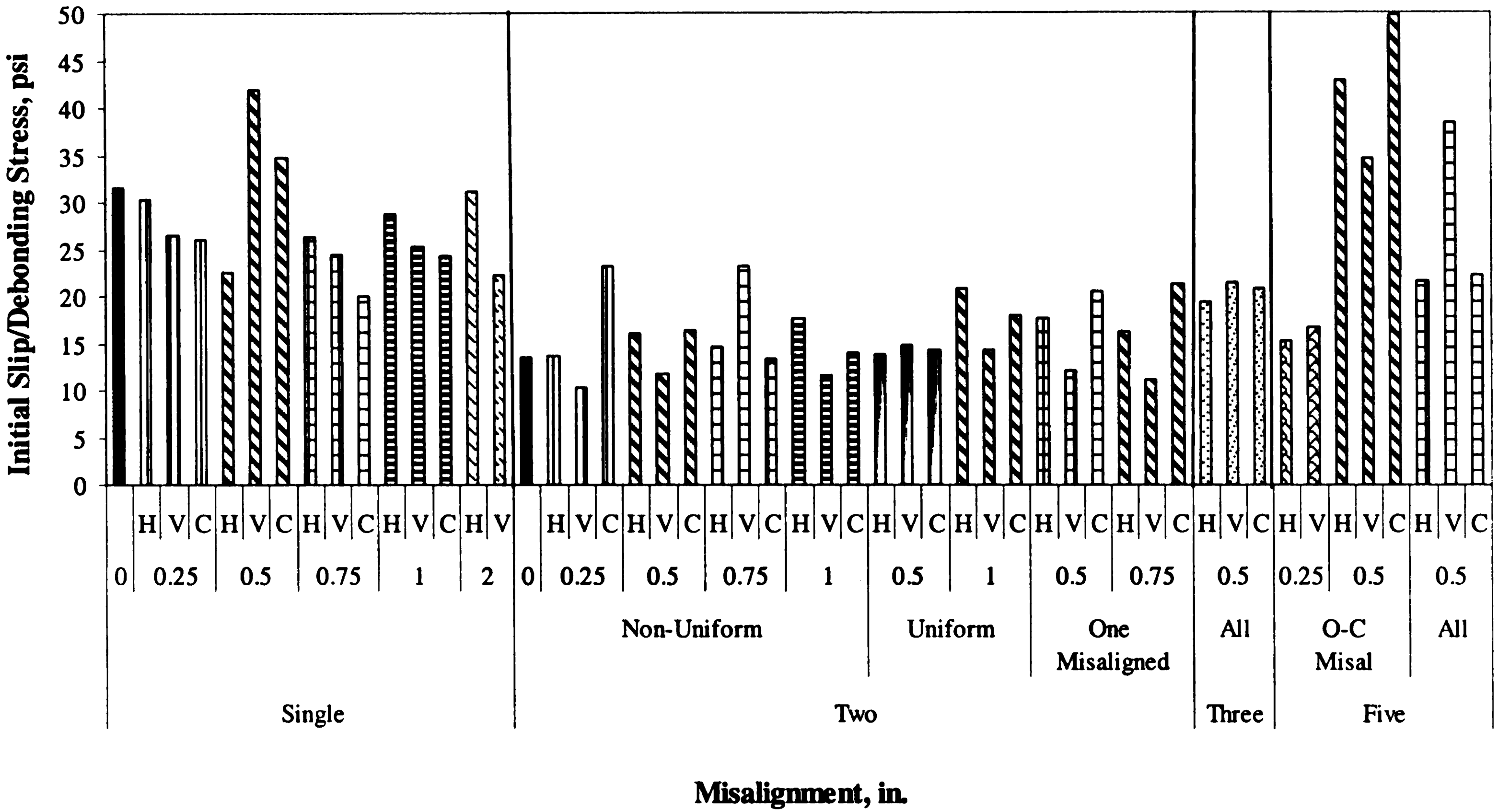

Figure C-1. Bond Stress vs Joint Opening curve

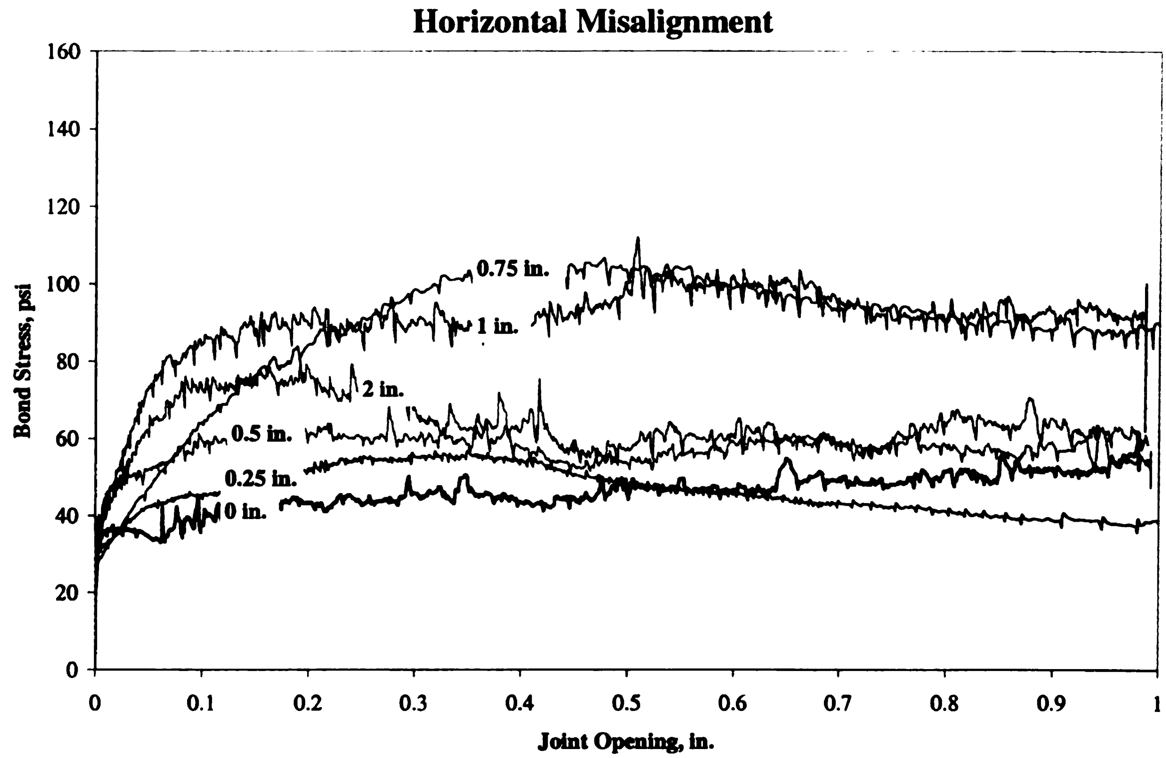

Figure C-2. Bond stress vs joint opening curves for 1-dowel Horizontal Misalignment cases

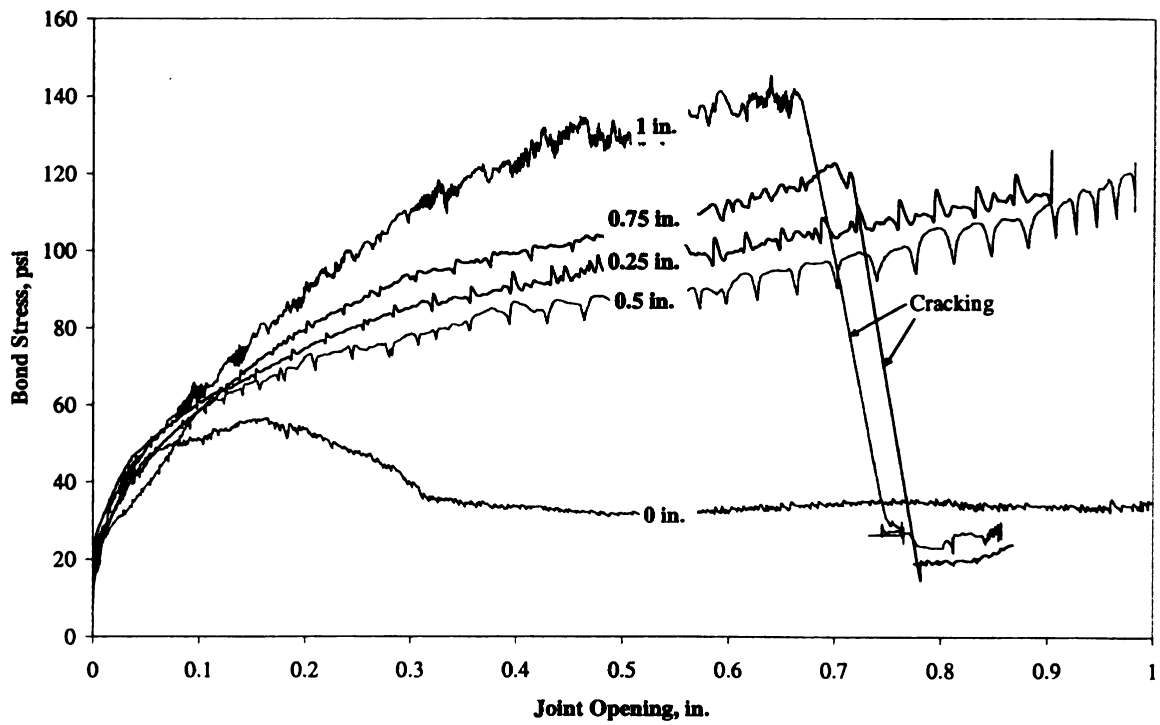

Figure C-3. Bond stress vs joint opening curves for 2-dowel Non-uniform Horizontal Misalignment cases

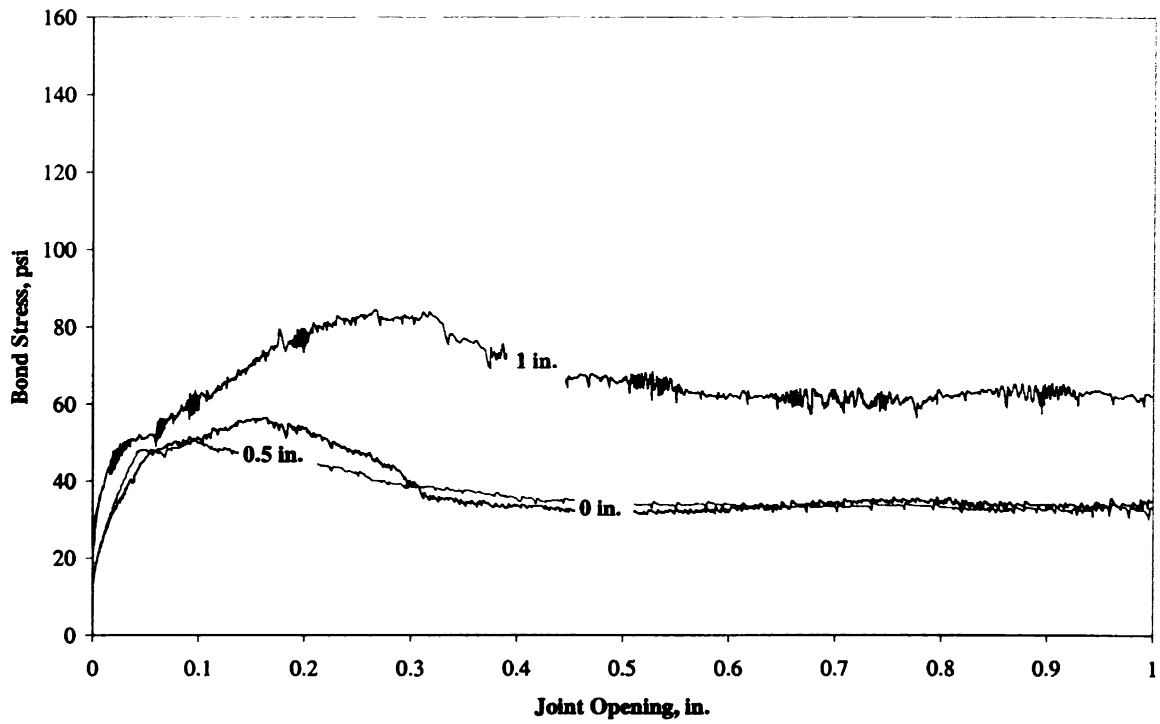

Figure C-4. Bond stress vs joint opening curves for 2-dowel Uniform Horizontal Misalignment cases

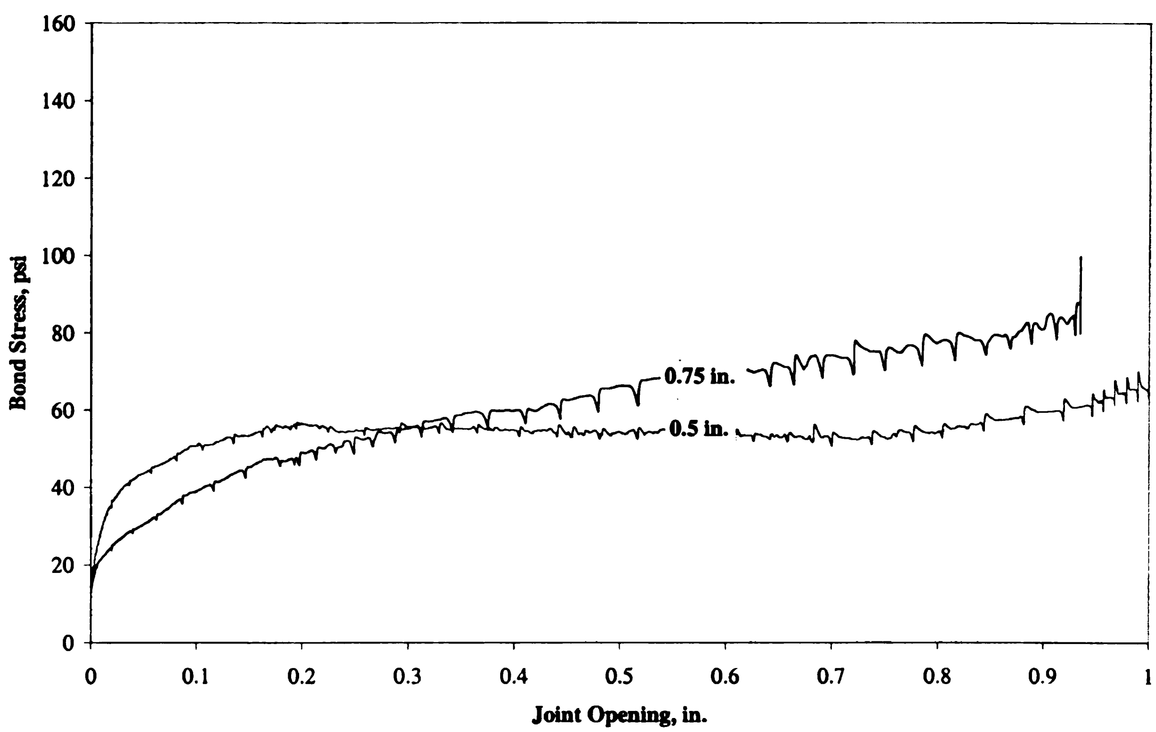

Figure C-5. Bond stress vs joint opening curves for 2-dowel Horizontal Misalignment cases (One dowel misaligned)

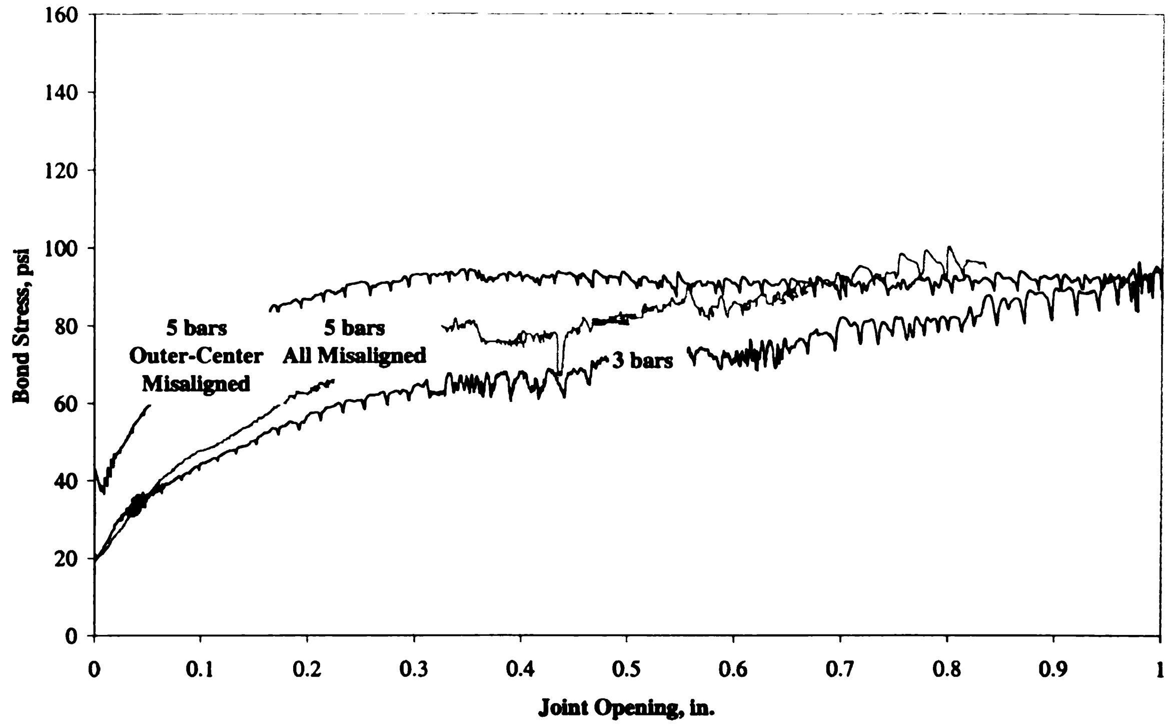

Figure C-6. Bond stress vs joint opening curves for 3 and 5-dowel Horizontal Misalignment cases

Vertical Misalignment

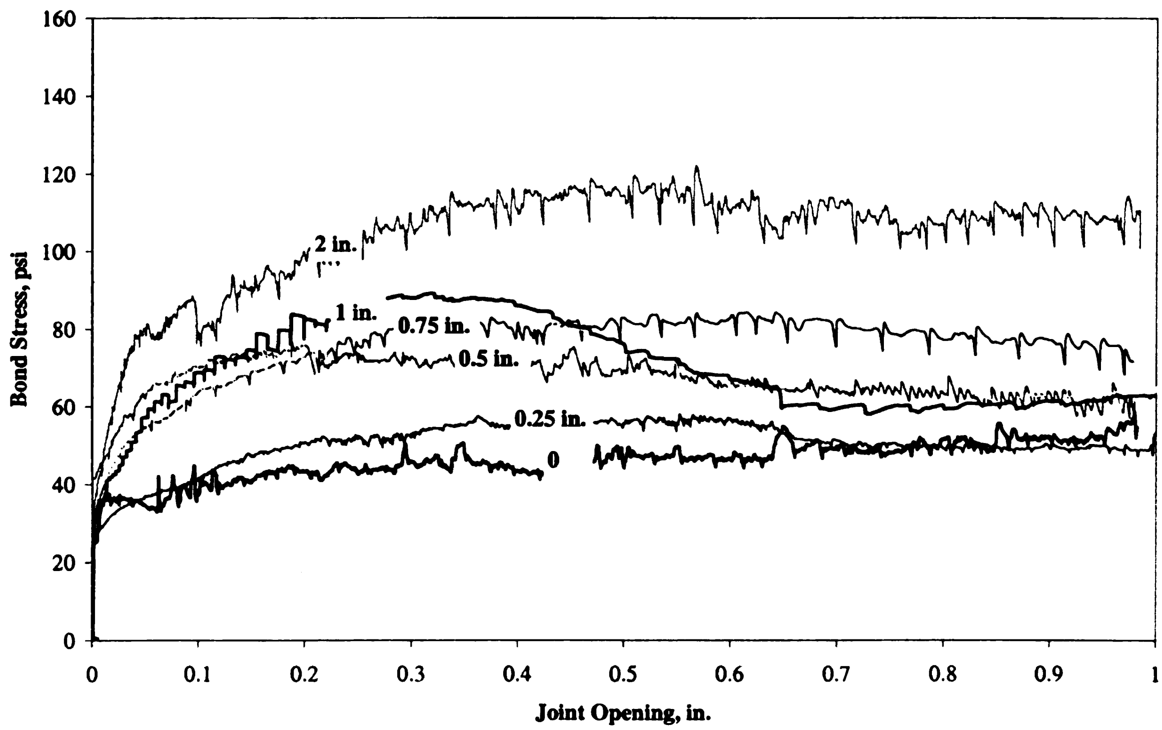

Figure C-7. Bond stress vs joint opening curves for 1-dowel Vertical Misalignment cases

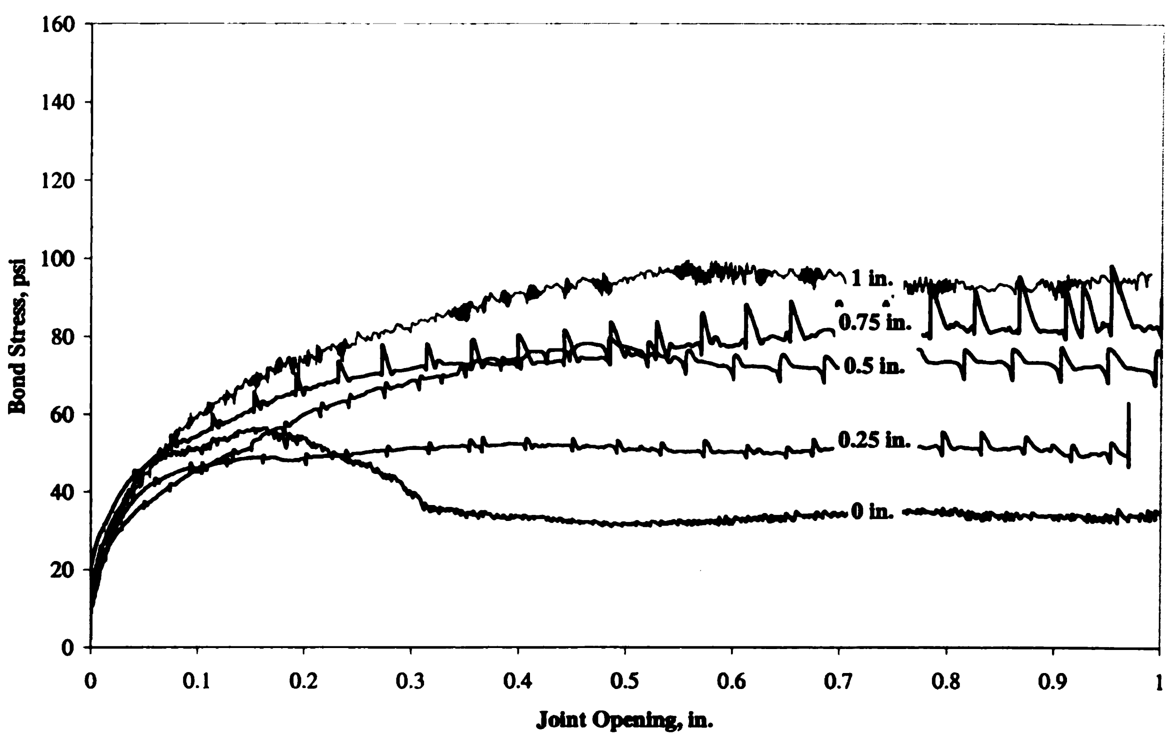

Figure C-8. Bond stress vs joint opening curves for 2-dowel Non-uniform Vertical Misalignment cases

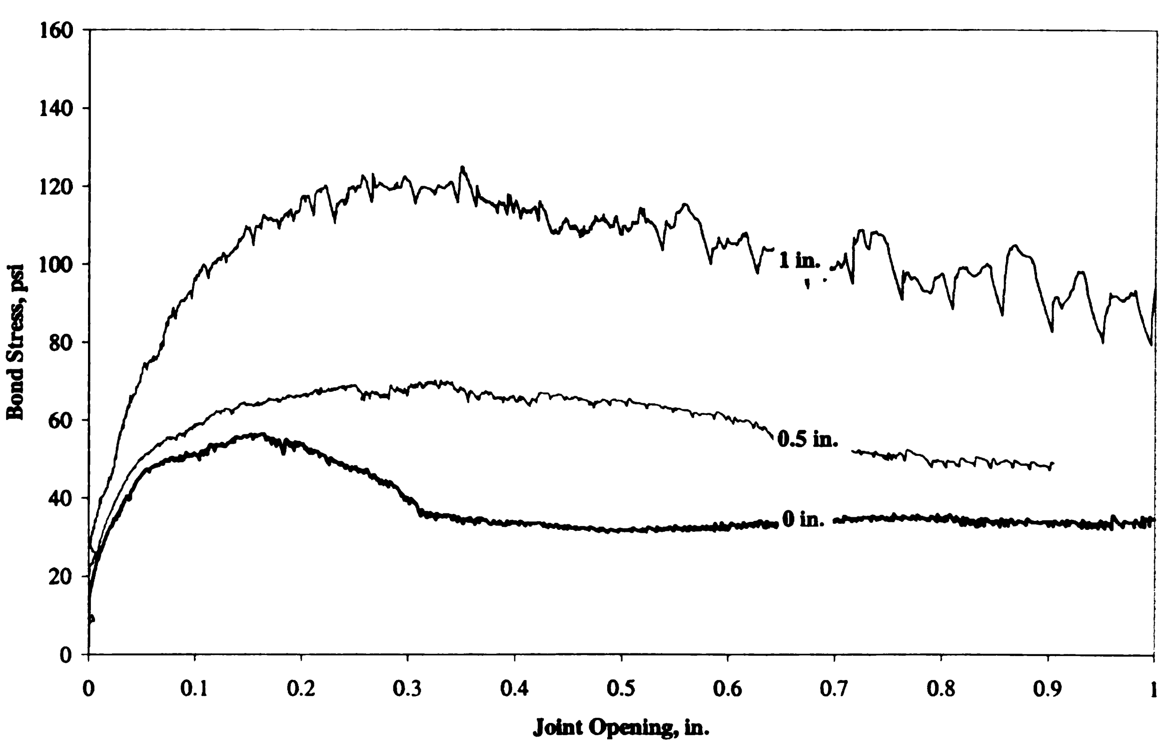

Figure C-9. Bond stress vs joint opening curves for 2-dowel Uniform Vertical Misalignment cases

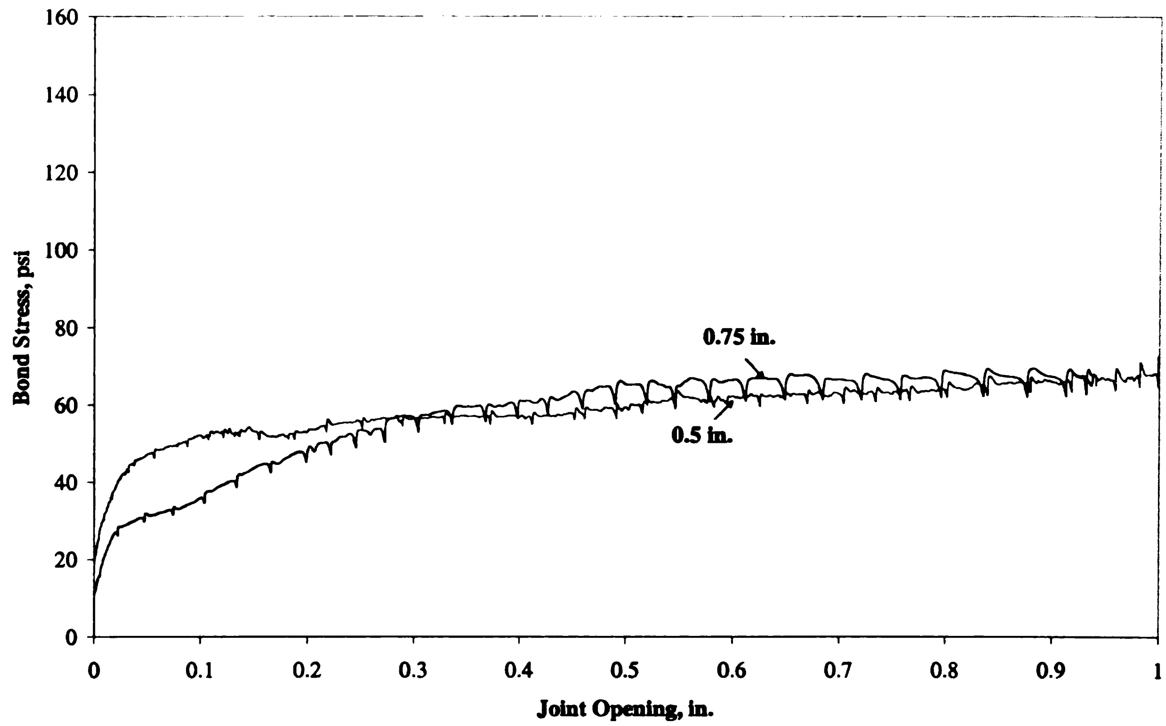

Figure C-10. Bond stress vs joint opening curves for 2-dowel Vertical Misalignment cases (One dowel misaligned)

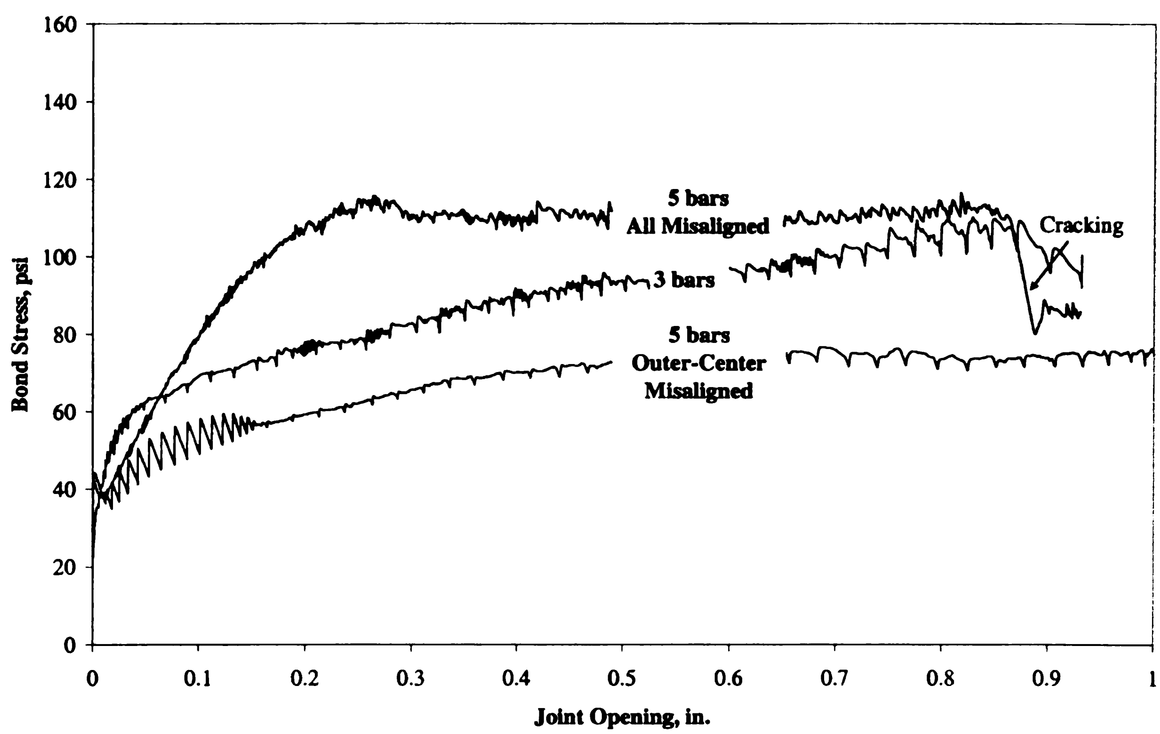

Figure C-11. Bond stress vs joint opening curves for 3 and 5-dowel Vertical Misalignment cases

Combined Misalignment

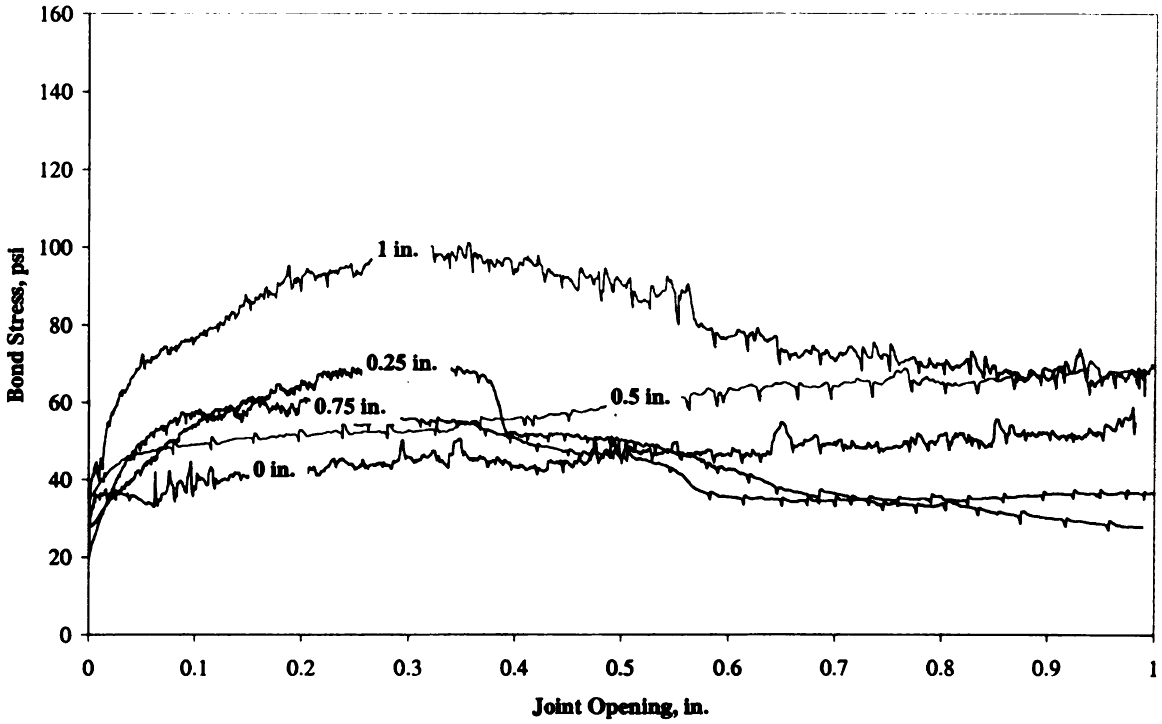

Figure C- 12. Bond stress vs joint opening curves for 1-dowel Combined Misalignment cases

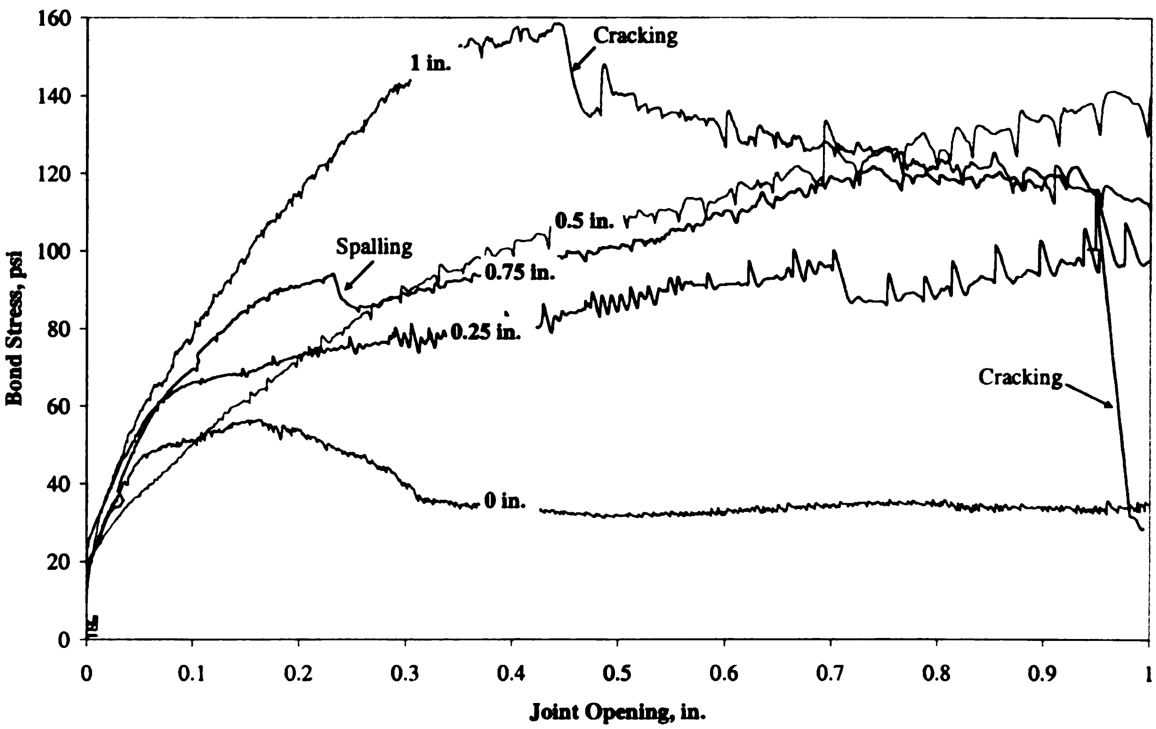

Figure C-13. Bond stress vs joint opening curves for 2-dowel Non-uniform Combined Misalignment cases

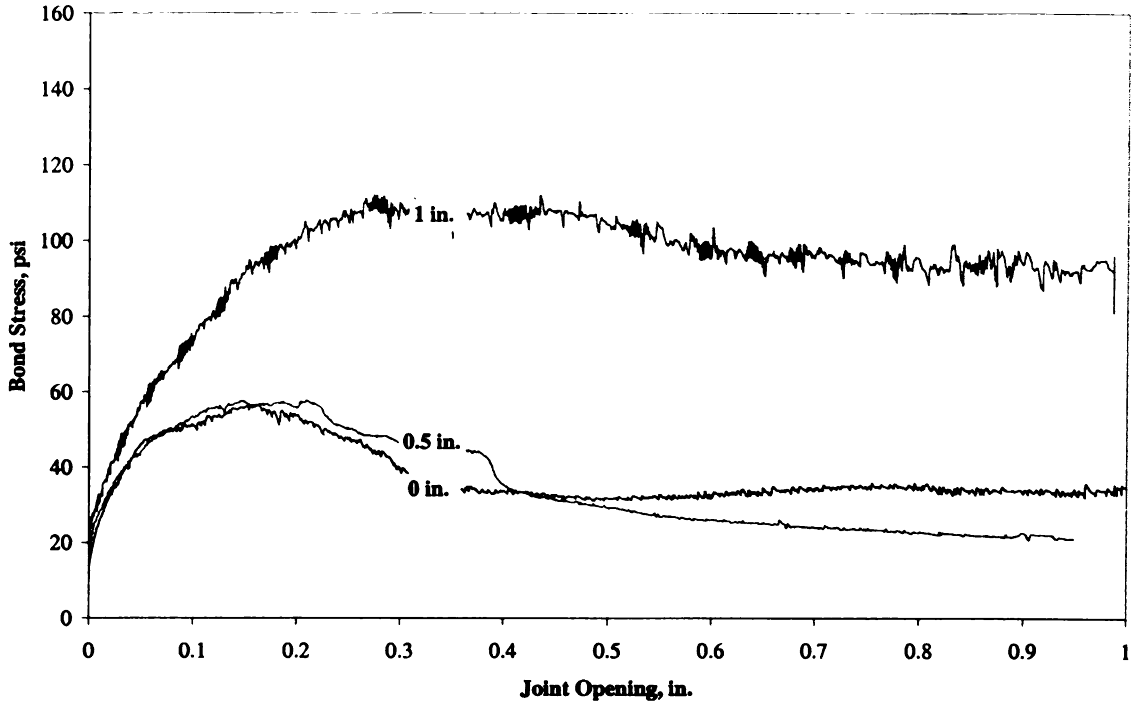

Figure C-14. Bond stress vs joint opening curves for 2-dowel Uniform Combined Misalignment cases

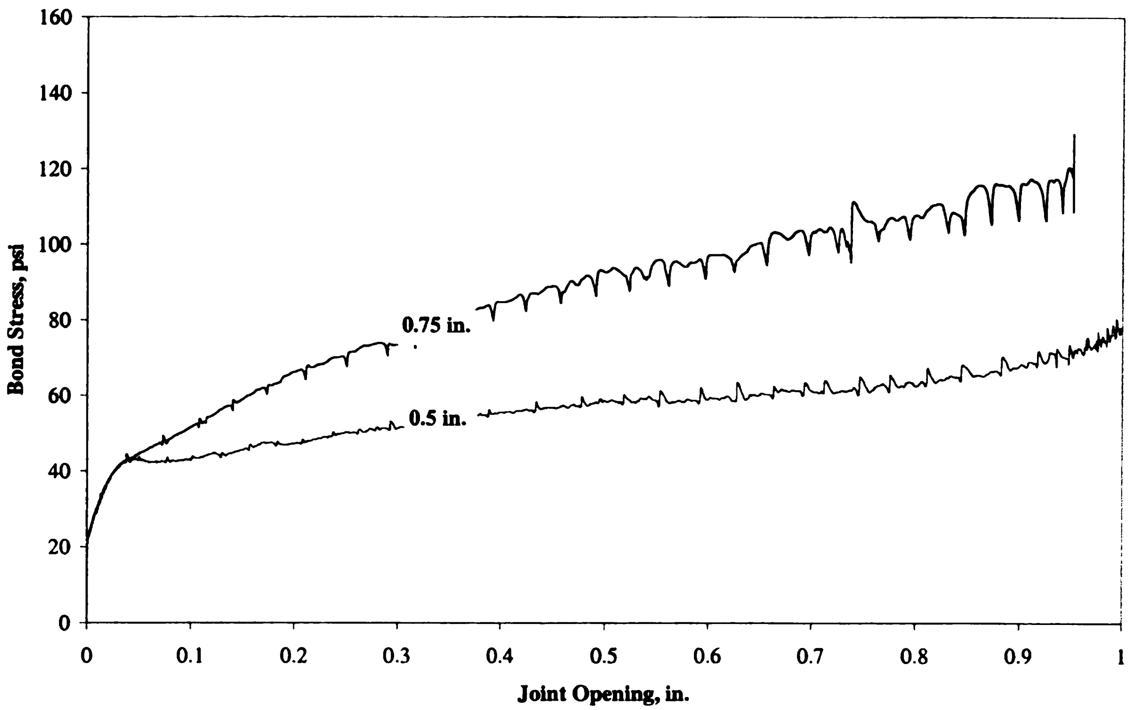

Figure C-15. Bond stress vs joint opening curves for 2-dowel Combined Misalignment cases (One dowel misaligned)

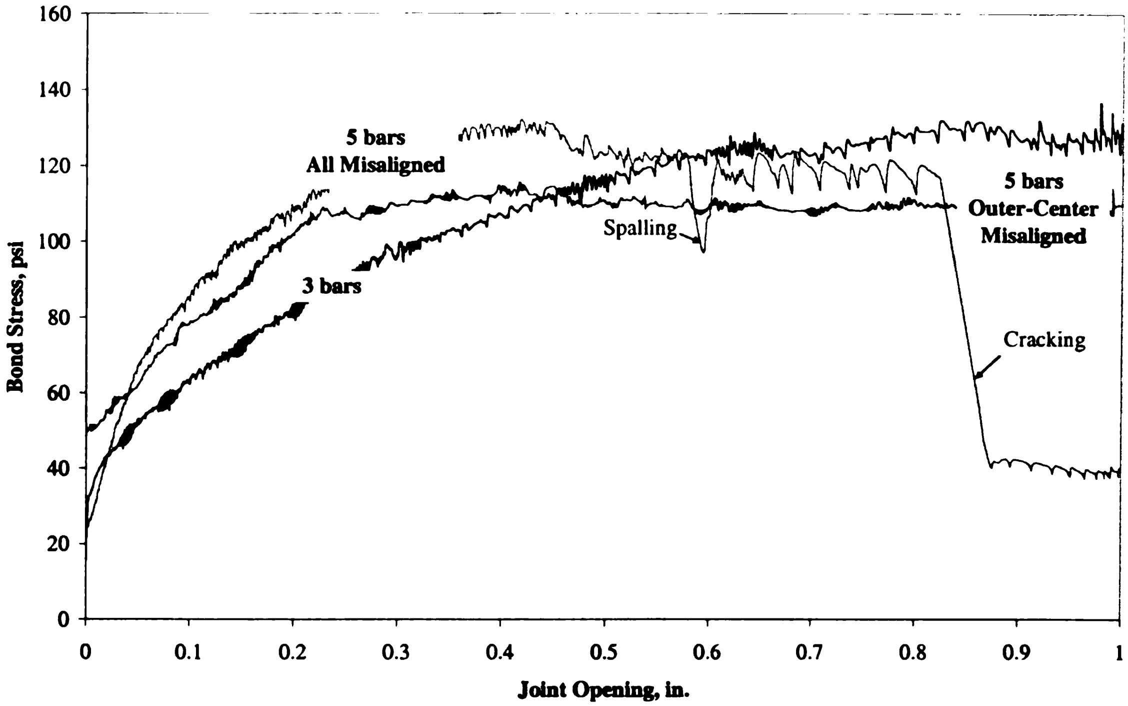

Figure C-16. Bond stress vs joint opening curves for 3 and 5-dowel Combined Misalignment cases

APPENDIX D
VISUAL OBSERVATIONS

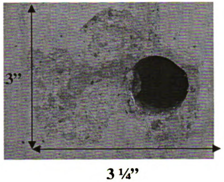

(a) West joint face (1H2)

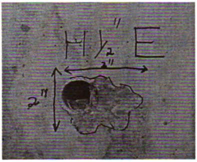

(b) East joint face (2H12NU)

(c) North outer dowel (5H12NU)

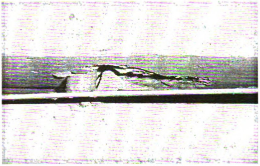

(d) South outer dowel (5H12NU)

Figure D-1. Spalling in the Horizontal Misalignment tests

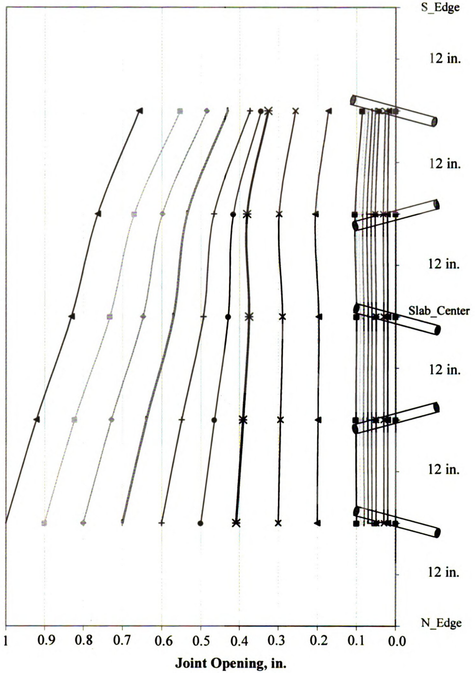

Figure D-2. Joint opening as a function of distance along the joint (5H12NU)

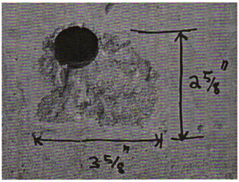

(a) East joint face (2V1NU)

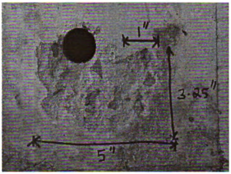

(b) West joint face (2V1NU)

(c) East joint face (2V1U)

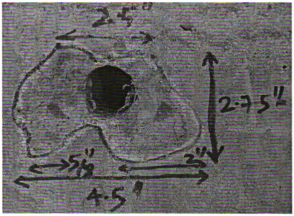

(d) West joint face (2V1U)

Figure D-3. Spalling in the Vertical Misalignment tests

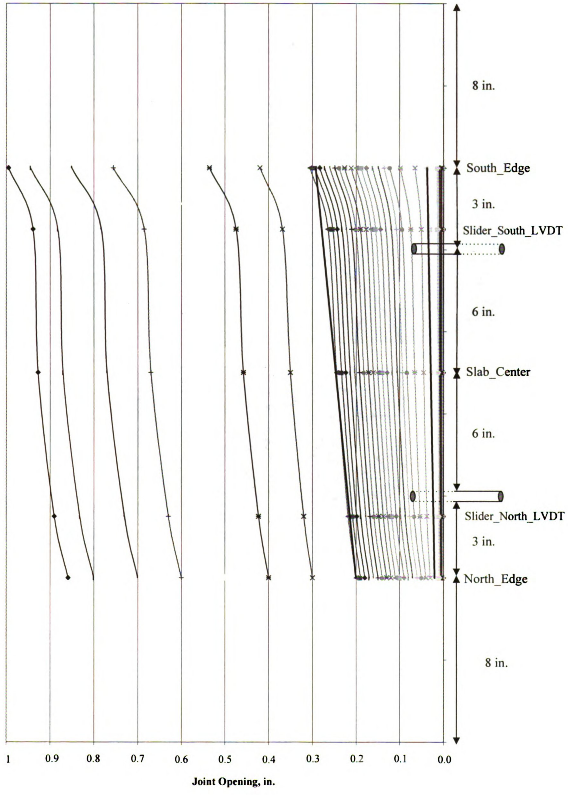

Figure D-4. Joint opening as a function of distance along the joint (2V1NU)

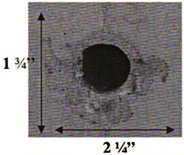

(a) East joint face (1C1)

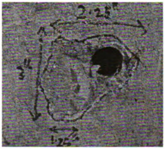

(b) East joint face (2C1U)

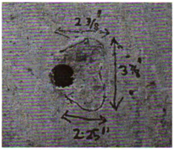

(c) West joint face (2C1U)

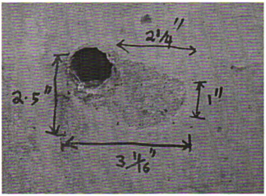

(d) East joint face (2C1NU)

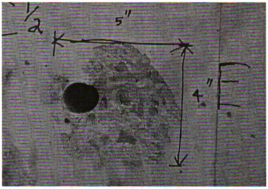

(e) East joint face (2C12NU)


(f) West joint face near the South dowel bar (2C34NU)

Figure D-5. Spalling in the Combined Misalignment tests

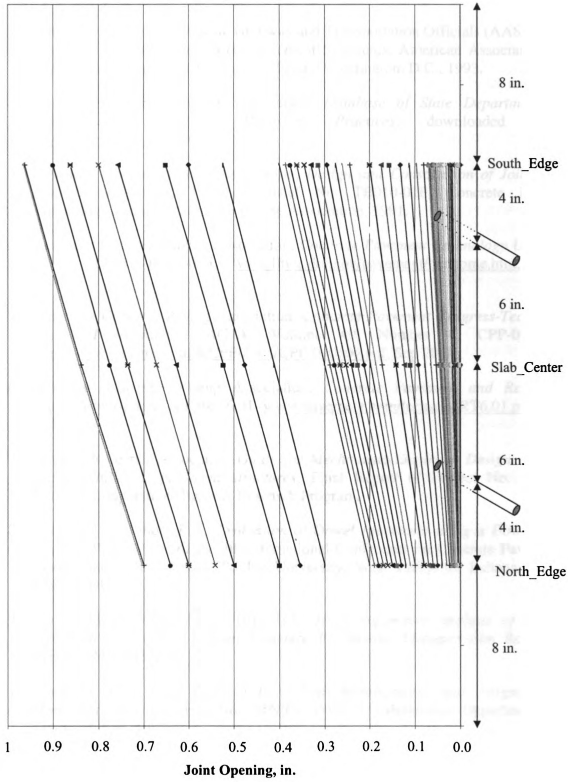

Figure D-6. Joint opening as a function of distance along the joint (2C1U)

REFERENCES

1. American Association of State Highway and Transportation Officials (AASHTO), AASHTO Guide for Design of Pavement Structures, American Association of State Highway and Transportation Officials, Washington, D.C., 1993.

2. American Concrete Paving Association, *Database of State Department of Transportation Concrete Pavement Practices*, downloaded from www.pavement.com, 2004a.

3. American Concrete Paving Association, *Design and Construction of Joints for Concrete Highways*, Technical Brief No. TB010-01P, Concrete Paving Technology, America Concrete Paving Association, 1991.

4. American Concrete Paving Association, *Concrete Pavement Technology Update*, ACPA, FHWA-IF-04-025, www.fhwa.dot.gov/pavement/conhome.htm, Aug 2004.

5. American Concrete Paving Association, *Concrete Pavement Progress-Technical tips and techniques*, ACPA, Volume 40, Number 4, CPP-090604, http://www.pavement.com/CPP/2004/CPP-090604.pdf, Sep 2004.

6. American Concrete Paving Association, *Concrete Pavement and Research Technology Update*, Number 6.01, www.pavement.com/techserv/RT6.01.pdf, Jan 2005.

7. Applied Research Associates, *Guide for Mechanistic-Empirical Design of new and rehabilitated pavement structures*, Final Report of Project No. I-37A, National Cooperative Highway Research Program.

8. Bock B.T., Okamoto P.A., *Evaluation of Dowel Placement using a Dowel Bar Inserter*, Proceedings of the 4th International Conference on Concrete Pavement Design and Rehabilitation, Purdue University, West Lafayette, Indiana, April 1989, p. 641-649.

9. Burati, J.L., Beeson, M.G., Hill, H.S. Jr., *Comparative analysis of dowel placement in Portland-Cement Concrete Pavements*, Transportation Research Record 924, 1983, p 19-27.

10. Burnham, T, *A Field study of PCC Joint Misalignment near Fergus Fall, Minnesota*, Final Report No. MN/RC-1999-29, Minnesota Department of Transportation, 1999.

11. California Department of Transportation, *Standard Specifications for construction of local streets and roads*, http://www.dot.ca.gov/hq/esc/oe/project_plans/HTM/stdplns-dual-new02.htm, 2002.

12. Cashell, Harry D., *Performance of Doweled Joints under repetitive loading*, Public Roads, Volume 30, Number 1, April 1958.

13. Darter,M.I., *Design of zero-maintenance plain jointed concrete pavement*, Report No. FHWA-RD-7-111, Federal Highway Administration, 1977.

14. Darter et.al., *Concrete Pavement Evaluation Systems*, NCHRP Report 277, Washington, D.C., 1985.

15. Davids, W.G., *Modeling of Rigid Pavements: Joint Shear Transfer Mechanisms and Finite Element Solution Strategies*, PhD thesis, University of Washington, 1998.

16. Donahue, J.P, *Investigation of Dowel Bar Placement Accuracy with a Dowel Bar Inserter*, Research Investigation RI01-049, Missouri Department of Transportation, April 2003.

17. Federal Highway Administration (FHWA), *The Benefits of using dowel bars*, Technical Paper No.89-03, Washington, 1989.

18. Federal Highway Administration (FHWA), *Computer-Based Guidelines For Concrete Pavements Volume II—Design and Construction Guidelines and HIPERPAV II User's Manual*, FHWA-HRT-04-122, Feb 2005.

19. Fowler, G. and Gulden,W., *Investigation of Location of Dowel Bars Placed by Mechanical Implantation*, FHWA/RD-82/153, Georgia Department of Transportation, Office of Materials and Research, May 1983.

20. Friberg, B.F, *Design of dowels in transverse joints of concrete pavements*, ASCE Transactions 105, 1940, p. 1076-1095.

21. Highway Research Board, *The AASHO road test – Report 5, Special Report 61E about Pavement Research*, Publication No. 954, Division of Engineering and Industrial Research, Washington, D.C, 1962.

22. Huang, Yang H., *Pavement Analysis and Design*, Prentice-Hall, 1993, p.192-200.

23. Illinois Department of Transportation, *Standard Specifications for Road and Bridge Construction*, http://www.dot.state.il.us/desenv/pdfspec2002/sec400.pdf, 2002.

24. Ioannides, A. M., Korovesis, G. T., *Analysis and design of doweled slab-on-grade pavement systems*, Journal of Transportation Engineering, v 118, n 6, Nov-Dec, 1992, p 745-768.

25. Ioannides, Anastasios M et.al., *Control of faulting through joint load transfer design*, Transportation Research Record No. 1286, 1990, p. 49-56.

26. Iowa Department of Transportation, *Standard Specifications for Road and Bridge Construction*, http://www.erl.dot.state.ia.us/Oct_2004/GS/frames.htm, 2004.

27. Khazanovich, L and Gotlif, A, *Evaluation of joint and crack load transfer – Final Report*, Report No. FHWA-RD-02-088, Federal Highway Administration, 2003.

28. Michigan Department of Transportation, *Standard Specifications for Construction*, http://mdotwas1.mdot.state.mi.us/public/specbook/, 2003.

29. Michigan Department of Transportation, *Office Memorandum on Surface Condition Survey and Dowel Bar Restraint – Recycled Concrete Pavement Research Project 78B-99*, Dec 1989.

30. Nichols, T.H. and Hoffman, G.L., *Machine Insertion of Plastic-Coated Dowel Bars in PCCP*, Research Project 78-8, Materials and Testing Division, Pennsylvania Department of Transportation, Harrisburg, May 1980.

31. Ohio Department of Transportation, *Construction and Material Specifications*, http://www.dot.state.oh.us/construction/OCA/Specs/Rewrite2005/2005SpecBook/2005_Whole_3-17-2005%20to%20Printer.pdf, 2005.

32. Okamoto, P.A., *Field Evaluation of Dowel Placement along a Section of I-45 in Texas*, Transportation Research Record No. 1186, Transportation Research Board, 1988, p 16-34.

33. Okamoto, P.A., *Field Evaluation of Dowel Placement along a Section of I-90 near Janesville, Wisconsin*, Report to Wisconsin Department of Transportation, District 1, Madison, Wisconsin, August, 1988.

34. Packard and Tayabji, *Mechanistic design of concrete pavements to control joint faulting and subbase erosion*, International Seminar on Drainage and Erodibility at the Concrete Slab-Subbase-Shoulder Interfaces, Mar 1983, Paris.

35. Parry, J, *Dowel Bar Placement: Mechanical Insertion versus Basket Assemblies*, Final Report, Study No. 88-10, Wisconsin Department of Transportation, 1989.

36. Poblete et.al., *Field Evaluation of Thermal deformations in Undoweled PCC Pavement slabs*, Transportation Research Record No. 1207, Transportation Research Board, 1988, p 217-228.

37. Ross, Rutkowski, *A Designed system of Load transfer dowels for Joints in PCC pavement*, Final Report WI 89-05, Jan. 1989.

38. Rufino, Mallela, and Darter, *Dowel bar and slab size recommendations based on the Mechanistic-Empirical pavement design guide*, 8th International Conference on Concrete Pavements, Aug 2005.

39. Schierer, D.L, *Paper on dowel bars*, prepared for FHWA, Washington, D.C. (unpublished), 1985.

40. Segner, E.P., Jr. and Cobb, J.R., *A Study of Misaligned Dowels in Concrete Pavements*, HPR Report 32, Alabama Highway Department, Aug 1967.

41. Smith, A.R. and Benham, S.W., *Effect of Dowel-Bar Misalignment across Concrete Pavement Joints*, ASCE Transactions, Paper No.2002, 1938, p.1133-1162.

42. Smith, K.D. et.al., *Performance of Jointed Pavements, Vol. I, Evaluation of Concrete Pavement Performance and Design Features*, Federal Highway Administration, FHWA, 1990.

43. Snyder, M.B., *Dowel load transfer systems for full-depth repairs of jointed Portland cement concrete pavements*, PhD thesis, University of Illinois, Urbana, 1989.

44. Soriano, A., *Dowel Bar Placement and Displacement*, Publication No.SK91-09-X, South Dakota Department of Transportation, Mar 1995.

45. Tabatabaie, A.M. et.al., *Longitudinal joint systems in slip-formed rigid pavements: Vol. II – Analysis of load transfer systems for concrete pavement*, Report No. DOT/FAA/RD-79/4, U.S. Department of Transportation, Federal Aviation Administration, Washington, D.C., 1979.

46. Tayabji, S.D., *Dowel Placement Tolerances for Concrete Pavements*, Transportation Research Record 1062, Transportation Research Board, 1986, p.47-54.

47. Tayabji, S.D., Okamoto, A.P., *Field Evaluation of Dowel Placement in Concrete Pavements*, Transportation Research Record 1110, Transportation Research Board, 1987, p.101-109.

48. Teller, L.W., and Cashell, H.D, *Performance of dowels under repetitive loading*, Public roads, 30 (1), 1958, p. 1-24.

49. Wisconsin Department of Transportation, *Standard Specifications*, http://www.dot.wisconsin.gov/business/engrserv/construction-library.htm, 2004.

50. Darter,M.I., *Design of zero-maintenance plain jointed concrete pavement*, Report No. FHWA-RD-7-111, Federal Highway Administration, 1977.

51. Yu, H.T and Khazanovich, L, Applied Research Associates, Final Report of *Use of Magnetic Tomography Technology to evaluate Dowel Placement*, Federal Highway Administration Contract No. DTFH61-03-C-00120, Feb 2005.

52. Yu, H.T, Kim, H.B, *Use of MIT Scan-2 in Dowel Alignment Evaluation*, 5th International Conference on Pavement Technologies Proceedings Vol. II, May 2005.